The Dissertation Committee for Aja Lynne Gore Certifies that this is the approved version of the following dissertation:

Carbon Metabolism Influences *Shigella flexneri* Pathogenesis

Committee:

Shelley M. Payne, Supervisor

Dean Appling

Arturo DeLozanne

M. Stephen Trent

Marvin Whiteley

Carbon Metabolism Influences *Shigella flexneri* Pathogenesis

by

AJA LYNNE GORE, B.S.

DISSERTATION

Presented to the Faculty of the Graduate School of

The University of Texas at Austin

in Partial Fulfillment

of the Requirements

for the Degree of

DOCTOR OF PHILOSOPHY

THE UNIVERSITY OF TEXAS AT AUSTIN

MAY, 2010

Dedication

This work is dedicated to my family. To my mother, for her unwavering faith in me. To my sister, for always being a friend. To my father, for inspiring me to always question the world around me. To my husband, for sharing this journey with me. Thank you for your support and encouragement.

Love always

A

Acknowledgements

Many thanks are due to Shelley Payne, for sharing her immeasurable scientific wisdom with me, and allowing me to pursue my studies in her lab. I also thank both past and present members of the Payne lab. Thanks to Elizabeth Wyckoff and Alexandra Mey, for many stimulating scientific discussions.

Carbon Metabolism Influences *Shigella flexneri* Pathogenesis

Publication No._____

Aja Lynne Gore, Ph.D.

The University of Texas at Austin, 2010

Supervisor: Shelley Marshall Payne

The gram negative bacterium *Shigella flexneri* is an etiological agent of bacillary dysentery, and causes destruction of the human intestinal epithelium. *S. flexneri* is primarily transmitted via the fecal-oral route to its primary infective site in the colon. The bacterium invades and replicates within colonic epithelial cells, ultimately ulcerating the mucosal epithelium. To successfully establish infection, *S. flexneri* must quickly adapt to different environments in the host, including adjusting metabolism in response to changes in available carbon sources. In this study, the importance of the glycolytic and gluconeogenic pathways in *S. flexneri* pathogenesis was examined.

The metabolic regulators CsrA and Cra reciprocally regulate the glycolytic and gluconeogenic pathways. The post-transcriptional regulator Cra activates expression of genes involved in gluconeogenesis and represses glycolysis. Conversely, CsrA activates glycolysis and represses gluconeogenesis. The absence of Cra increased *S. flexneri* attachment and

invasion of cultured epithelial cells. In contrast, the *csrA* mutant was significantly impaired in both adherence and invasion. Both the *csrA* and *cra* mutants formed small, turbid plaques, suggesting that both regulators are required for plaque formation. The opposing phenotypes of the *csrA* and *cra* mutants suggested a correlation between invasion and glycolysis.

The role of glycolysis in *S. flexneri* pathogenesis was confirmed by directly examining the first committed step in the pathway. The glycolytic enzyme phosphofructokinase I (PfkI, encoded by *pfkA*) is repressed by Cra and activated by CsrA. Glycolysis was critical for *S. flexneri* pathogenesis, as a mutation in *pfkA* rendered the bacterium noninvasive. The invasion defect of the *csrA* and *pfkA* mutants was due to reduced expression and secretion of the *Shigella* invasion plasmid antigen (Ipa) effectors. Expression of the master virulence regulators *virF* and *virB* was significantly reduced in the *pfkA* mutant, and is the principle reason for decreased invasion. The data presented show that glycolysis is required for invasion, but that plaque formation requires both glycolysis and gluconeogenesis. Because expression of the master virulence regulators is repressed in the *pfkA* mutant, *S. flexneri* may use carbon as an environmental regulator of virulence gene expression.

Table of Contents

List of Tables

List of Figures

I. INTRODUCTION

1. *Shigella flexneri* pathogenesis

The gram negative pathogen *Shigella* causes bacillary dysentery, or shigellosis, in humans and higher order primates. *Shigella* invades and destroys the colonic epithelium leading to desquamation of the epithelial layer and subsequent ulceration of the colon. Destruction of the colonic epithelium and the inflammatory response result in characteristic symptoms of the disease, including profuse, bloody stools, fever and abdominal cramps. The bacterium is primarily transmitted via the fecal-oral route, and *Shigella* infections occur primarily in developing countries where dissemination of the bacterium is augmented by poor sanitation. Over 165 million cases of shigellosis occur annually, resulting in approximately 1.1 million deaths (94).

The genus *Shigella* is divided into four species, *Shigella sonnei, Shigella boydii, Shigella dysenteriae* and *Shigella flexneri*, which are further divided into 13 serotypes based on O-antigen variation (56). *S. flexneri* is endemic in developing countries and causes the most communicable form of bacillary dysentery, but the 2a serotype predominates in industrialized countries (56). *Shigella* is closely related to *Escherichia coli*, and these two bacteria are generally thought to comprise a single species (67). Genetic analysis suggests that *Shigella* arose by convergent evolution from several *E. coli* strains. *E. coli* and *Shigella* share common housekeeping genes, including those for nutrient acquisition and central carbon metabolism (145). Enteroinvasive *E. coli* (EIEC)

and *S. flexneri* are very similar, both in disease pathology and virulence mechanisms. *Shigella* and EIEC have acquired a 220-kb virulence plasmid encoding the *mxi-spa* type III secretion system and associated effectors which allow for invasion, replication and spread within the colonic epithelium.

2. Shigellosis

Shigella is primarily transmitted by the fecal-oral route and enters the host by ingestion of contaminated food or water. The bacterium then travels through the host gastrointestinal tract to its infective site in the large intestine. In the primary stages of infection, *S. flexneri* invades the colonic epithelial cells via the basolateral face (Fig. 1) (85). M cells, which sample lumenal contents, transcytose *Shigella* and deposit the bacterium into an intraepithelial pocket (Fig. 1, steps 1-2) (141). It is here that circulating macrophages may phagocytose *S. flexneri*. *S. flexneri* ensures its survival by rapidly inducing apoptosis of the macrophage (Fig.1, step 3) (149).

After release from the macrophage, *S. flexneri* weakly adheres to the basolateral face of the epithelial cell and induces massive cytoskeletal rearrangements (Fig. 1, step 4). By uncoupling the host membrane from the cytoskeletal architecture, *S. flexneri* is able to promote its uptake in a process similar to macropinocytosis (132). After engulfment by the host cell, *S. flexneri* creates a pore in the resulting vacuole, thereby releasing the bacterium into the host cell cytosol (Fig. 1, step 5). Once the bacterium has escaped the vacuole, *S. flexneri* replicates freely within the host cytosol, and spreads intracellularly (Fig. 1, steps 6-7).

By nucleating actin at one pole, *S. flexneri* creates a propulsive force that pushes the bacterium within the host cell (40). Eventually, this movement results in a protrusion of the bacterium into the neighboring cell that is subsequently engulfed. *S. flexneri* again

disrupts the resulting vacuole, thereby gaining access to the host cytosol. By replicating within and spreading between the epithelial layer, *S. flexneri* is protected against the host immune response.

As the bacterium spreads between the mucosal layer, tight junctions are disrupted, thereby allowing lumenal *Shigella* to access the basolateral face of the colonic epithelia. Persistence of the bacterium within the colon recruits polymorphonucleocytes (PMN), which also infiltrate the tight junctions, and further disrupt the monolayer. This destruction of the monolayer allows further dissemination of the bacterium to the basolateral face of the epithelium.

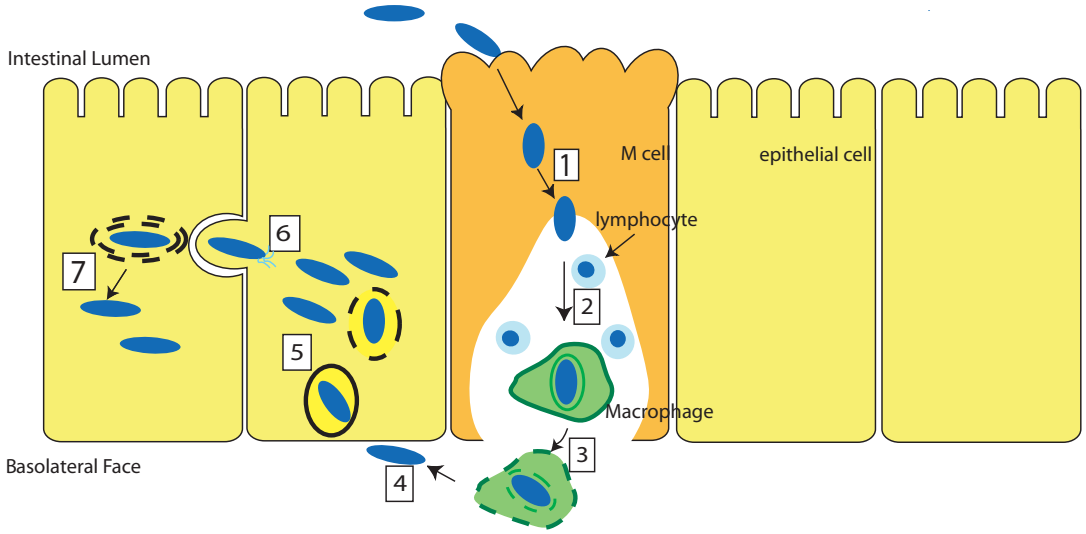

Figure 1. Model of *S. flexneri* pathogenesis.

After traveling to the colon, the bacterium is endocytosed by M cells in the colonic epithelial layer and subsequently deposited in an intraepithelial pocket [1]. Macrophages phagocytose *S. flexneri* [2], and the bacterium ensures its survival by inducing apoptosis of the macrophage [3]. *S. flexneri* attaches to the basolateral face of the colonic epithelial cell [4] and induces its own uptake in via macropinocytosis. The engulfed bacterium is enveloped in a vacuole [5], which *S. flexneri* subsequently lyses. Next, *S. flexneri* replicates within the host cytosol, and spreads to adjacent epithelial cells using an actin-based motility and the bacterial protein IcsA [6]. This movement results in a protrusion, which is engulfed by the neighboring cell [6], and the bacterium lyses the double membrane, thereby allowing the process of intracellular replication and intercellular spread to continue [7]. Figure adapted from Jennison and Verma (56).

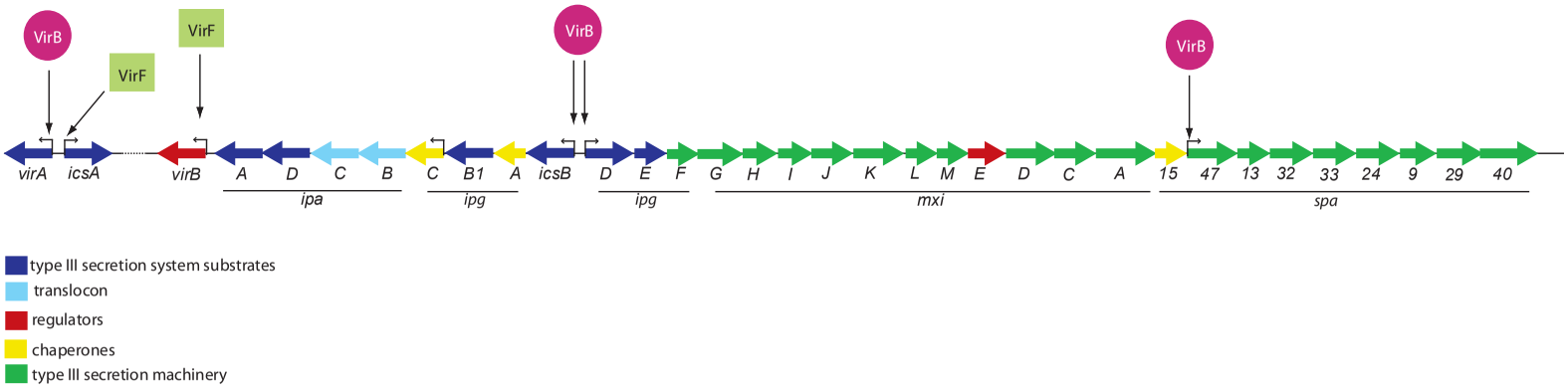
VirB
VirF
VirF
VirB
VirB
virA
icsA
virB
A
D
C
B
C
B1
A
icsB
D
E
F
G
H
I
J
K
L
M
E
D
C
A
15
47
13
32
33
24
9
29
40
ipa
ipg
ipg
mxi
spa
type III secretion system substrates
translocon
regulators
chaperones
type III secretion machinery

Figure 2: Organization of the 31-kb entry region of the *S. flexneri* virulence plasmid.

The genes located in this region are necessary for invasion by *S. flexneri* and are coded according to their function. VirB and VirF activate transcription at the sites indicated. Adapted from Dorman and Porter (29) and Schroeder and Hilbi. (120).

3. Factors involved in *S. flexneri* pathogenesis

3.1 VIRULENCE-PLASMID ENCODED FACTORS

The genes necessary for bacterial entry, survival and spread are encoded on a 31-kb entry region on the virulence plasmid (74, 119). This entry region is comprised of 34 genes which are organized in two clusters (Fig. 2) and includes the necessary genes for the type III secretion apparatus (*mxi-spa*) and its secreted effectors (*ipa, ipg, virA*), chaperones (*ipgA*, *ipgC*, *ipgE* and *spa15)*, and transcriptional activators (120). Additional factors necessary for virulence are encoded elsewhere on the virulence plasmid.

The Ipa (*i*nvasion *p*lasmid *a*ntigen) proteins IpaB, IpaC and IpaD have a central role in *S. flexneri* invasion. Prior to contact with the host cell, IpaB and IpaC are bound to their chaperone protein IpgC within in the bacterial cytosol. The adapter protein IpaD is positioned at the tip of the type III needle, where it acts to regulate secretion of IpaB and IpaC (34). Bile salts induce the presentation of IpaB at the needle tip, and IpaB binds to CD44 receptors present in lipid rafts in the host cell membrane (34, 66, 96). Activation of the needle tip complex by the lipid raft component sphingomyelin results in recruitment of IpaC to the needle tip and subsequently promotes invasion (33). IpaB and IpaC form a translocon pore in the eukaryotic cell, through which additional effector proteins can enter. These effectors, including IpaA, IpgD and VirA, are responsible for the membrane rearrangements necessary to induce engulfment of the bacterium (95). Also included in the entry region is *icsA*. IcsA localizes preferentially to the old pole of the bacterium, where it nucleates actin to propel the bacterium inter- and intracellularly (40).

The transcriptional activators VirB and MxiE are also encoded within this region of the virulence plasmid. The combination of environmental cues present in the mammalian intestine, including pH (103), osmolarity (11), and temperature (129, 131), induce expression of the master virulence regulator VirF. VirF, in turn induces expression of

both *icsA* and *virB* (Figs. 2, 3) (115, 130). The transcriptional regulator VirB is a member of the ParB family of partitioning proteins, and directly activates transcription of genes within the entry region (1).

The third regulator, MxiE, is responsible for activation of the second wave of effectors needed by intracellular bacteria (63). Effector secretion via the type III secretion system regulates the activity of MxiE. After IpaB and IpaC are secreted, their chaperone protein IpgC acts as a co-activator of MxiE (76). Additionally, the effector protein OspD1 and its chaperone Spa15 also regulate MxiE activity. Inside the bacterial cytosol, OspD1-Spa15 binds to MxiE, and prevents MxiE from binding to IpgC. Secretion of OspD1 alleviates MxiE repression, allowing activation of MxiE by IpgC (97). In this fashion, activity of MxiE is then regulated by bacterial location, as OspD1 is secreted by intracellular *Shigella*.

3.2 CHROMOSOMALLY-ENCODED FACTORS

During the course of infection, *Shigella* faces varying environmental conditions. Expression of the plasmid-encoded virulence genes is maximally induced in response to environmental signals in the mammalian intestine (11, 103, 129, 131). Temperature appears to be a principal environmental stimulus, and *S. flexneri* is noninvasive at 30°C (75). Expression of *virF*, *virB* and the *ipa-mxi-spa* type III secretion system is thermally inducible. Growth at 37°C only increases expression of *virF* two-fold relative to its expression level at 30°C. However, expression of the downstream regulator *virB* increases ten-fold under permissive conditions, and expression of the effector gene *icsB* increases 100-fold (103). Although regulation of *virF* expression is lax, tight control of *virB* and *ipa-mxi-spa* expression ensures that the structural components necessary for invasion will only be produced under the appropriate conditions (103).

The nucleoid-associated proteins Fis (*f*actor for *i*nversion *s*timulation), IHF (*i*ntegration *h*ost *f*actor) and H-NS (*h*eat-stable *n*ucleoid *s*tructuring protein) have a central role in thermoregulation of expression from the virulence plasmid. At non-permissive temperatures (<32°C), H-NS binds to both the *virF* and *virB* promoters and significantly inhibits transcription of both (Fig. 3) (10). At 37°C, the topology of the promoters changes such that H-NS repression is overcome. Fis and IHF then bind to the *virF* promoter and activate transcription. The level of VirF is also affected by the levels modified tRNAs. The gene products of *tgt* and *miaA* synthesize nucleosides queosine (Q) and 2-methyltio-N^6-isopentenyladenosine (ms^2i^6A37), respectively. The absence of either *tgt* or *miaA* causes a reduction in the amount of VirF, presumably due to poor translation of the *virF* mRNA (32).

The mechanism of thermal regulation of *virB* expression has been well studied. Although some VirF is present at 30°C, it is unable to activate expression of *virB* at this temperature. The accessibility of the *virB* promoter is greatly influenced by supercoiling around this region. Higher temperatures lead to a reduction in linking number at the *virB* promoter, and it is presumed that this modification in promoter topology allows for VirF-mediated activation of *virB*. The alleviation of H-NS repression at the *virB* promoter allows for binding by VirF and IHF (104), thereby activating the virulence gene expression cascade. VirF binds base-pairs -117 to -17 on the *virB* promoter, but it is unclear if VirF activates transcription by directly contacting RNA polymerase or if VirF is required for recruitment of RNA polymerase to the promoter (131).

Both pH and osmolarity influence virulence gene expression via two-component systems. The *ompB* locus encodes the EnvZ histidine kinase and OmpR response regulator, which modulate porin expression in response to osmolarity fluctuations (122). Growth in low osmolarity medium represses expression of genes in the entry region, but this regulation does not supersede thermoregulation (103). Deletion of the *ompB* locus decreases *S. flexneri* virulence and intracellular multiplication (11). Similarly, deletion of

A)

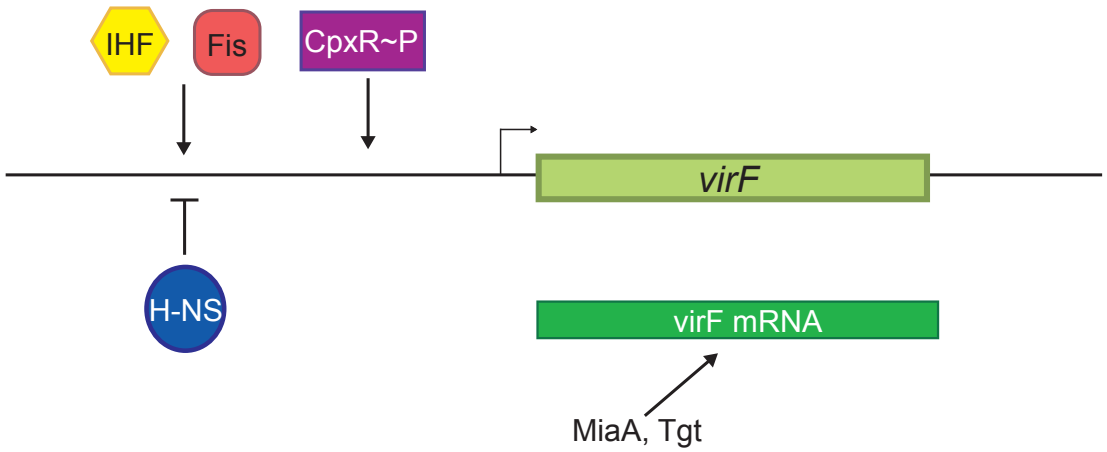
IHF
Fis
CpxR~P
virF
H-NS
virF mRNA
MiaA, Tgt

B)

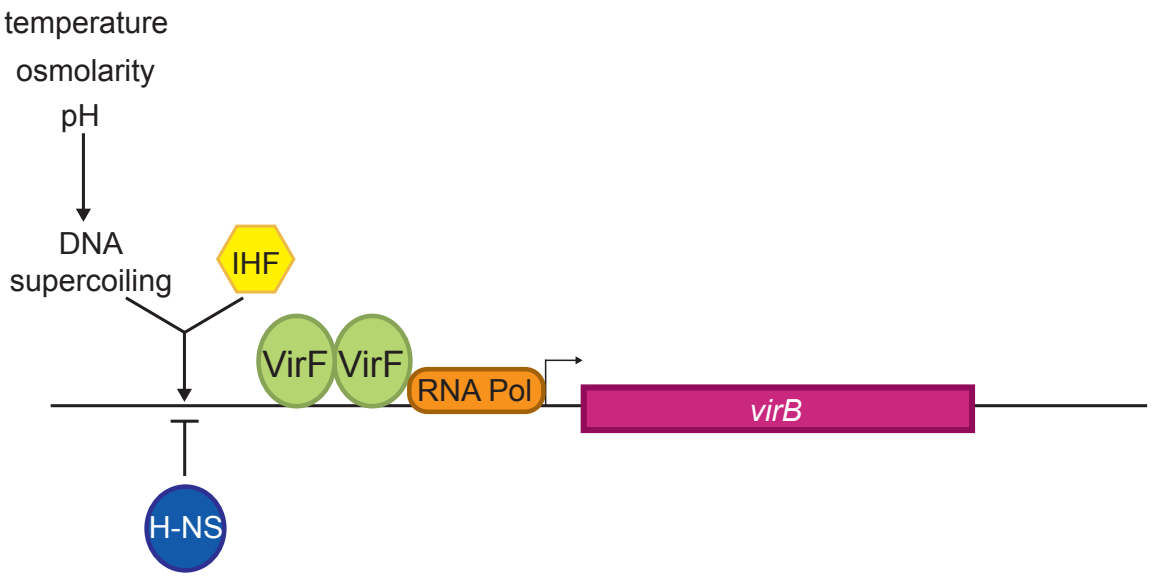
temperature
osmolarity
pH
DNA
supercoiling
IHF
VirF
VirF
RNA Pol
virB
H-NS

Figure 3: Environmental factors regulate expression of *virF* and *virB*.

(A) Expression of *virF* is repressed by H-NS, and activated by Fis, IHF and phosphorylated CpxR (CpxR~P). Translation of the *virF* mRNA is enhanced by the tRNAs made by MiaA and Tgt. (B) Transcription of *virB* is inhibited by H-NS. Temperature, osmolarity and pH increase the supercoiling around the *virB* promoter. This reduction in linking number promotes VirF-mediated activation of the *virB* promoter. VirF binding to the *virB* promoter could recruit or stimulate activity of RNA polymerase (RNA pol). Adapted from Dorman and Porter, 1998 (29).

the OmpR-activated porin OmpC decreases *S. flexneri* virulence in vitro (12). However, no direct role has been identified for OmpR in expression of plasmid-encoded virulence genes.

In *S. sonnei*, the CpxA-CpxR two-component system regulates virulence gene expression in response to changes in pH (89, 90). Expression of *virF* is lower at pH 6.0 versus pH 7.4. Growth at the higher pH induces autophosphorylation of the CpxA histidine kinase. CpxA then donates the phosphate group to its cognate response regulator CpxR. Binding of phospho-CpxR upstream of the *virF* promoter activates *virF* expression (Fig. 3). Although this pH regulation was characterized in *S. sonnei*, the CpxA-CpxR two-component system has been identified in *Shigella spp*., suggesting that this regulation is conserved (89).

4. Role of lipopolysaccharide in *S. flexneri* virulence

The gram negative outer membrane is an effective barrier that protects the bacterium against several harmful agents, including cationic antimicrobial peptides, detergents, bile salts and host defense mechanisms (93). The outer membrane is an asymmetric bilayer, with phospholipid comprising the inner face, and lipopolysaccharide (LPS) as the outer face. LPS is composed of three distinct regions: lipid A, core polysaccharide and O-polysaccharide (Fig. 4).

S. flexneri lipid A is comprised of a glucosamine disaccharide modified with six acyl chains; the primary acyl chains are ligated to the 2, 3, 2' and 3' positions of the sugar molecules, and the secondary acyl chains are conjugated at the 2' and 3' primary chains (41). The addition of the secondary acyl chains requires two acyltransferases, LpxL, which adds laurate to the 2' primary chain, and MsbB, which adds myristate to the 3' primary chain. *S. flexneri* is unique in that it contains two non-redundant *msbB* genes. MsbB1 is present on the chromosome, while MsbB2 is encoded on the virulence plasmid (26). An *S. flexneri msbB1msbB2* double mutant was significantly impaired in destruction of the epithelium in a rabbit model of infection (26). It is thought that both myristoyl transferases may be required for *S. flexneri* survival in vivo, as increased hexa-acylation of lipid A could protect the bacterium from antimicrobial peptides (41).

The LPS core region can be divided into the inner (lipid A-proximal) and outer core regions. *S. flexneri* 2a core belongs to the R3 core type, which is found in several pathogenic *E. coli* species (38). Phosphorylation of the core heptose residues plays an important role in maintaining the barrier function of the outer membrane (93). The core polysaccharide is also required for mediating interactions between LPS and outer

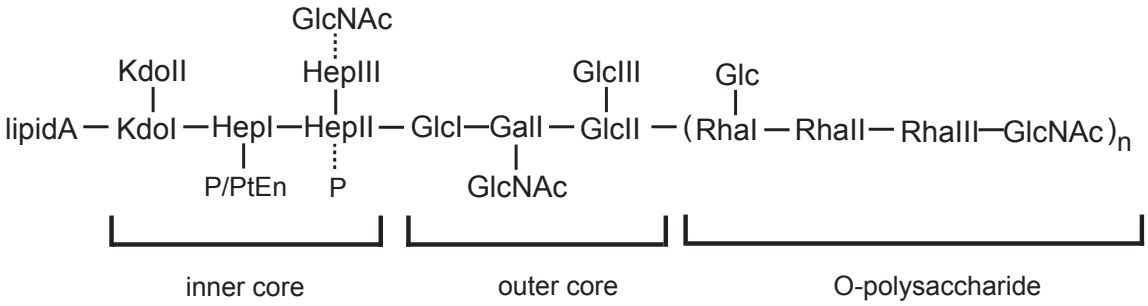

Figure 4: Structure of *S. flexneri* 2a lipopolysaccharide.

Abbreviations: Kdo: 2-deoxy-D-manno-oct-2-ulsosonic acid, Hep: heptose, P: phosphoryl, PtEN: phosphatidylethanolamine, Glc: glucose, Gal: galactose, GlcNAc: N-acetyl-glucosamine, Rha: rhamnose. Dotted lines indicate substoichiometric subsitutions, as HepIII is conjugated to GlcNAc only when HepII is not phosphorylated. GlcII was identified as the O-polysaccharide ligation site by Kaniuk *et al*. (64).

membrane proteins. Most genes required for biosynthesis of the core polysaccharide are encoded on the chromosome. *wabB* (*rfbU*), however, is encoded on the virulence plasmid in both EHEC and *S. flexneri* 2a (64). *wabB* encodes a transferase responsible for the addition of N-acetyl glucosamine (GlcNAc) to heptose III in the inner core. In EHEC, expression of *wabB* is thermoregulated, with maximal expression occurring at 24°C as compared to 37°C (38). The significance of *wabB* on the virulence plasmid has not been experimentally determined, but may indicate coordination of LPS modifications with virulence.

The O-polysaccharide side chain shows wide degrees of heterogeneity, giving rise to different serogroups of *S. flexneri*. In *S. flexneri* 2a strains, the O-antigen repeat unit is composed of a tri-rhamnose-N-acetyl-glucosamine tetrasaccharide, in which the first rhamnose residue is generally glucosylated (Fig. 4).

The presence of O-antigen has a significant effect on *S. flexneri* pathogenesis. A mutation in *rfbD* (blocking dTDP-rhamnose synthesis) is invasive and able to replicate intracellularly in an epithelial cell monolayer, but is impaired in intercellular spread (134). In this mutant, IcsA localizes along the length of the cell body, versus the unipolar localization seen in wild type (134). This heterogeneous pattern of IcsA localization subsequently leads to F-actin polymerization around the perimeter of the cell. A similar pattern of aberrant IcsA localization was seen in the *rfaL* (O antigen ligase) and *rfc* (O-antigen polymerase) mutants (117). Like the *rfbD* mutant, the *rfaL* and *rfc* mutants were impaired in intercellular spread. Sandlin *et al*. (117) postulated that polar localization of IcsA is needed to generate the propulsive force needed for intracellular spread. Thus diffuse IcsA localization in the *rfbD*, *rfaL* and *rfc* mutants fails to generate uniformed, directional F-actin polymerization needed for cell-cell spread. In addition to its role in mediating IcsA localization, the O-antigen is also needed for *S.flexneri* resistance to serum (54).

The above studies were performed using a nonpolar monolayer of epithelial cells. In a polarized epithelial cell model, *rfc* and *rfaL* mutants are severely impaired in invasion (65). This suggests that the entry requirements are different in the two cell types. Kohler *et al*. (65) postulate that at the basolateral membrane, LPS may be the primary adhesin and may also serve to stimulate the proinflammatory events needed for PMN migration.

S. flexneri has two genes that control the length of LPS. wzz_{Sf} is chromosomally encoded and is responsible for the shorter (mode A) distribution of 11-17 O-antigen repeat units. A second gene, wzz_{pHS2} encodes a much longer distribution (>90 repeat units) termed mode B. wzz_{pHS2} is encoded on pHS2, a 3 kb plasmid found in several *S. flexneri* 2a isolates (124). The proportion of the mode A and mode B distributions is regulated in response to growth rate. Although the amount of the shorter, mode A pattern appears to be constant, the amount of mode B increases as the bacteria enter stationary phase (20). Temperature also affects LPS patterns, as growth of *S. flexneri* at 30°C increases the ratio of long chains relative to short chains, as compared to bacteria grown at 37°C (136). Surprisingly, the O-antigen pattern does not appear to change inside the host cell, as compared to bacteria grown in vitro (136).

The O-antigen distribution pattern is also critical for pathogenesis. Mutations in either wzz_{Sf} or wzz_{pHS2} disrupt the modal distribution of O-antigen. A wzz_{Sf} mutant makes shorter O-antigen chains (1-10 repeat units) than wild type along with the longer mode B O-antigen chains. A wzz_{Sf} mutant is less invasive than wild type, and aberrant IcsA localization inhibits intercellular spread in this strain (54, 134). The absence of wzz_{pHS2} prevents the synthesis of the longer mode B O-antigen chain, and thus a wzz_{pHS2} mutant only makes the shorter mode A distribution. The *S. flexneri* wzz_{pHS2} was invasive and able to spread intercellularly. However, this mutant was sensitive to killing by serum. These two O-antigen lengths are therefore needed to balance exposure of the bacterial proteins on the surface while also protecting the bacterium from the host defense mechanism (83).

In addition to regulating the modal distribution of O-antigens, *S. flexneri* also changes the length of the LPS molecule by glucosylation of the O-polysaccharide. This glucosylation is mediated by the phage genes *gtrABX* (3). Glucosylation of the O-polysaccharide is thought to compact the molecule. This transition shortens the overall length of LPS, thereby increasing exposure of the type III needle relative to the outer membrane without affecting the barrier function of the outer membrane (144).

5. Survival in the lumen and intracellular metabolism

During infection, *S. flexneri* encounters several unique microenvironments and thus must adapt to these environments to persist in the host. Most intestinal bacteria require a fermentable carbon source for growth and thus it is assumed that carbohydrate metabolism is required for colonization (99). Regulation of carbon metabolism has been shown to be important for colonization and infection by several enteric bacteria.

Although the mammalian GI tract is rich in carbohydrates, these resources are often consumed by the established intestinal flora. Freter's nutrient-niche hypothesis proposes that nutrient availability defines distinct niches within the intestine (68). Theoretically, each niche is occupied by one species that preferentially consumes a unique metabolite, and the concentration of that metabolite ultimately limits population size. Chang *et al*. expanded on this theory to suggest that differences in metabolite availability and the commensal population may affect the establishment of pathogenic bacteria within the host (21).

Within the gastrointestinal tract, enterohemmoragic *E. coli* (EHEC) lives a scavenging lifestyle, co-metabolizing several carbon sources not consumed by the commensal *E. coli* strains with which it must compete, including hexuronates, galactose, mannose and ribose (35). When the mouse intestine is precolonized with commensal *E. coli*, EHEC strain EDL933 uses glycolytic carbon sources for initial growth, but relies on both glycolytic and gluconeogenic carbon sources for persistence (80). Internal glycogen stores are also a crucial carbon source for *E. coli* colonization (35). The strong genetic similarity between *S. flexneri* and *E. coli* suggests that *S. flexneri* may adopt a similar adaptive strategy to withstand the competitive pressures within the intestine.

S. flexneri is among a small group of pathogens specially adapted for growth in the eukaryotic cytosol. Although prevailing thought suggests the cytosol is a nutrient rich environment, non-cytosolic pathogens were unable to replicate when microinjected into the mammalian cytosol (39). This suggests that *S. flexneri* and other cytosolic pathogens are specially adapted to thrive in this environment. To better understand the metabolic profile of intracellular *S. flexneri*, microarray analysis and GFP-promoter fusions have been employed.

Microarray analysis of intracellular *S. flexneri* revealed differential regulation of over one-quarter of the genome, including several genes involved in carbon uptake and metabolism (73). Notably, *uphT*, encoding a hexose phosphate transporter, was significantly upregulated inside the cytosol (73, 111). Although these data suggest that *S. flexneri* may consume phosphorylated carbon sources intracellularly, microarray analysis also revealed downregulation of several glycolytic and respiratory genes (73). Furthermore, deletion of *uhpT* had no effect on *S. flexneri* virulence in vitro (111). *S. flexneri* may therefore use several carbon sources while inside the host cytosol, or may use hexose phosphates upon entry but switch to alternate carbon sources during the later stages of infection. Data gathered from both lumen and cytosol point to carbon as an important nutrient for *S. flexneri* pathogenesis. Variations in carbon source or its availability may act as an environmental regulator of virulence gene expression.

6. Central Carbon Metabolism

The central metabolic pathways in prokaryotes include the glycolytic (Embden-Meyerhoff-Parnas, EMP), Entner-Doudoroff and Pentose Phosphate pathways (Fig. 5). These metabolic pathways convert carbohydrates, carboxylic acids and acetic acid into energy and precursor molecules for biosynthetic pathways within the cell.

6.1 GLYCOLYSIS AND GLUCONEOGENESIS

Carbohydrate metabolism via glycolysis provides a significant portion of cellular energy. Through a series of ten reactions, the glycolytic pathway degrades glucose into two molecules of pyruvate and simultaneously generates a net of two ATP molecules (Fig. 5). The glycolytic pathway can be divided into two major stages. In the first stage, glucose is phosphorylated twice and converted into fructose 1,6 bisphosphate. This initial stage requires the input of two molecules of ATP to effectively prime the second stage.

In the second half of glycolysis, fructose 1,6 bisphosphate is cleaved by fructose 1,6 bisphosphate aldolase to yield glyceraldehyde 3 phosphate (G3P) and dihydroxyacetone phosphate (DHAP). G3P is then oxidized by NAD^+ and phosphorylated yielding 1, 3 bisphosphoglycerate. High-energy phosphate is donated to ADP to generate ATP via substrate level phoshorylation. 3-phosphoglycerate is converted to 2-phosphoglycerate, and then dehydrated forming phosphoenolpyruvate (PEP). A second substrate phosphorylation event completes glycolysis, generating a second molecule of ATP and pyruvate.

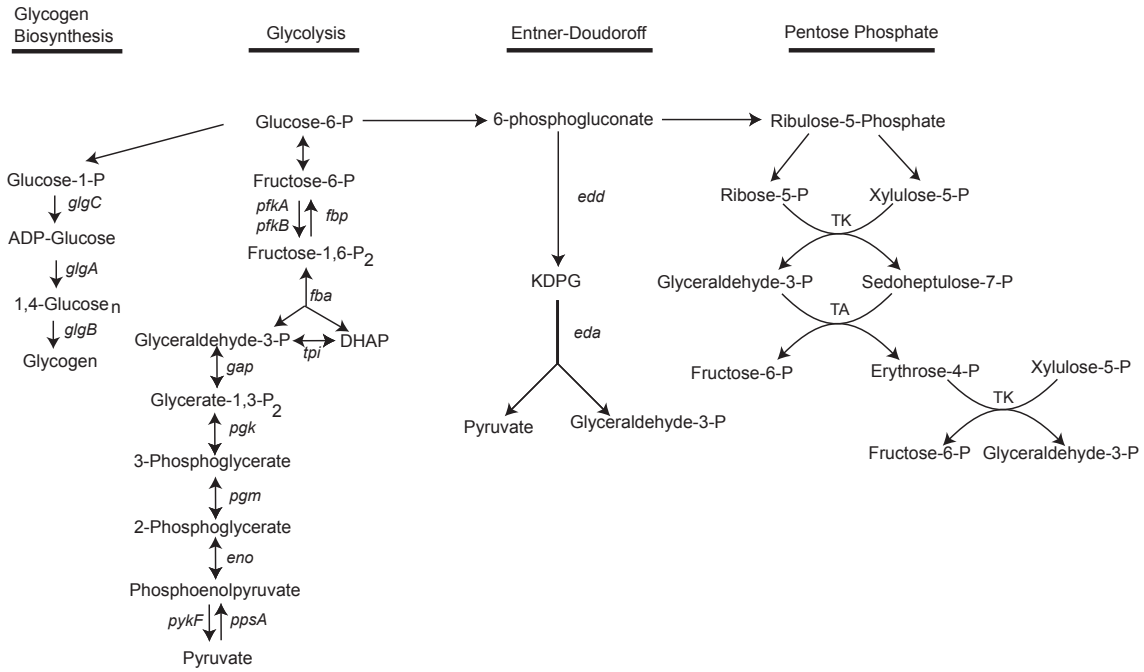

Figure 5. Central metabolic pathways in *Escherichia coli* and *Shigella flexneri*.

The Entner-Doudoroff and Pentose Phosphate pathways diverge from glycolysis via 6-phosphogluconate. Gluconeogenesis is essentially a reversal of the glycolytic pathway, with the exception of the irreversible steps of fructose-6-P phosphorylation and phosphoenolpyruvate dephosphorylation (see text for details). The three pathways shown ultimately generate pyruvate. Enzymes that catalyze the reactions are noted in italics, and are those used in *E. coli*. Abbreviations: DHAP, dihydroxyacetone phosphate; KDPG, 2-keto-3-deoxy-6-phosphogluconate; TK, transketolase; TA, transaldolase.

Several of the glycolytic intermediates serve as biosynthetic precursors for amino acid, lipopolysaccharide, and nucleotide biosynthetic processes. In the absence of carbohydrate carbon sources, these precursors are made from other sources via gluconeogenesis. Gluconeogenesis generally uses glycolytic enzymes, but the reactions that generate fructose 1,6 bisphosphate (phosphofructokinase, *pfkA, pfkB*), and pyruvate (pyruvate kinase, *pykF*) are energetically irreversible. Therefore, these reactions are replaced in gluconeogenesis with energetically favorable reactions, specifically those catalyzed by fructose bisphosphatase (*fbp*), and phosphoenolpyruvate synthase (*ppsA*) (Fig. 5). In this fashion, these irreversible steps also allow for control of carbon flow directionality.

6.2 GLYCOGEN METABOLISM

Glycogen is an important stored nutrient source for bacteria under starvation conditions, and promotes bacterial viability under nutrient-limiting conditions. In *E. coli,* glycogen is composed of glucose linked by 95% α 1,4 linkages and only 5% α 1,6 branched glucosyl linkages (105). Synthesis of glycogen is stimulated under conditions where carbon sources are abundant but other nutrients are limiting. Three enzymes are required for glycogen biosynthesis: ADP-glucose phosphorylase, glycogen synthase and branching enzyme (Fig. 5). The ADP-glucose phosphorylase, encoded by *glgC*, generates ADP-glucose from glucose-1-phosphate and ATP. GlgA, the glycogen synthase, extends the glycogen molecule by transferring glucosyl units from ADP-glucose to the growing polymer. Branching of glycogen is accomplished by the GlgB branching enzyme, which creates the α 1, 6 glycosidic linkages (105). GlgS is also required for glycogen biosynthesis, although it has no defined role in the biosynthetic reactions. Under carbon-limiting conditions, glycogen serves as an important internal

carbon source. Glycogen degradation is mediated by GlgP phosphorylase, which removes glucose from the glycogen molecule, and the GlgX debranching enzyme (105).

The role of glycogen metabolism in virulence is still unclear (14, 77). However, recent studies have shown that this polymer is important for establishment and maintenance of *E. coli* in the host. The absence of the glycogen biosynthetic proteins GlgA or GlgS severely impaired establishment of both commensal and enterohemorragic *E. coli* within the mouse intestine (60). Similarly, deletion of the glycogen degradative enzyme GlgP caused defects in maintainance of commensal and enterohemorragic *E. coli* within the mouse (60). These data suggest that glycogen is an important source of carbon within the lumen, and may provide a nutritional buffer for the bacterium while it scavenges for resources within the host.

6.3 PENTOSE PHOSPHATE PATHWAY

The pentose phosphate pathway can be used alongside the glycolytic or Entner-Doudoroff pathway. In this pathway, glucose-6-phosphate is oxidized to 6-phosphogluconate, and then subsequently oxidized to ribulose-5-phosphate and CO_2 (Fig. 5). Next, ribulose-5-phosphate is converted to a mixture of 3 through 7 carbon sugar-phosphates. A transketolase reaction catalyzes the transfer of two-carbon ketol groups while the transaldolase transfers a three-carbon group from sedoheptulose-7-phosphate to glyceraldehyde-3-phosphate. The pentose phosphate pathway serves both catabolic and anabolic functions within the cell. The NADPH produced during the oxidation steps is an important source of electrons for reduction of molecules during biosynthetic reactions. Additionally, the erythrose and ribose intermediates can be used to make aromatic amino acids and nucleic acids, respectively. The pentose phosphate pathway also allows the cell to use pentoses as either a primary carbon source or for the production of hexose sugars. The pentose phosphate pathway was shown not to be essential for colonization of the

mouse intestine by commensal *E. coli* (21). However, expression of genes in the pentose phosphate pathway were significantly upregulated during intracellular growth of the intracellular pathogen *Listeria monocytogenes*, suggesting that this pathogen primarily uses this pathway for sugar metabolism in the intracellular environment (62)

6.4 ENTNER-DOUDOROFF

The Entner-Doudoroff pathway is exclusive to bacteria and archaea. This pathway is required for oxidation of aldonic acids, which are present in the human intestinal tract (99). As in the glycoytic pathway, the Entner-Doudoroff pathway primes glucose by phosphorylation ultimately generating glucose-6-phosphate. Glucose-6-phosphate dehydrogenase then oxidizes glucose-6-phosphate to 6-phosphogluconate. A subsequent dehydration reaction converts 6-phosphogluconate to 2-keto-3-deoxy-6-phosphogluconate (KDPG). KDPG is then cleaved by KDPG aldolase (encoded by *eda*) yielding pyruvate and glyceraldehyde-3-phosphate (Fig. 5). Disruption of the aldolase encoded by *eda* completely inhibits colonization of the mouse intestine by *E. coli* (127). Additionally, the *eda* mutant is unable to grow in cecal mucus in vitro (127). These data suggest that while in the intestinal lumen, the Entner-Doudoroff pathway is an important metabolic pathway.

7. Metabolic Regulators

7.1 cAMP-CRP

When presented with multiple carbon sources, *E. coli* can either co-metabolize the available carbon sources or preferentially use individual carbon sources in a fashion that allows for usage of the most accessible and most advantageous metabolite. The most classical example of sequential carbon source usage is the glucose-lactose diauxie as described by Jacob and Monod (17). *E. coli* preferentially uses glucose, and the presence of glucose blocks the use of alternative carbon sources in a process known as carbon catabolite repression. In *E. coli*, carbon catabolite repression is mediated primarily by the transcriptional regulator cAMP-CRP (cyclic-AMP bound to *c*AMP-*r*eceptor *p*rotein). In addition to its primary role catabolic regulation, *E. coli* cAMP-CRP acts as a global regulator that activates over 100 promoters, including several catabolic operons, flagellar synthesis and gluconeogenesis (42, 148). The cAMP-CRP complex also plays an indirect role in glycogen metabolism, pH regulation and iron uptake (24).

Carbon catabolite repression is regulated by the phosphorylation state of $EIIA^{Glc}$, a member of the glucose-specific phosphotransferase system (Fig. 6). When glucose is present, phosphoenolpyruvate transiently phosphorylates $EIIA^{Glc}$, which then phosphorylates the $EIIBC^{Glc}$ transporter. Glucose is then phosphorylated as it enters through this transporter. In the absence of active glucose transport, $EIIA^{Glc}$ remains phosphorylated, and is able to activate adenylate cyclase (A.C.), the enzyme responsible

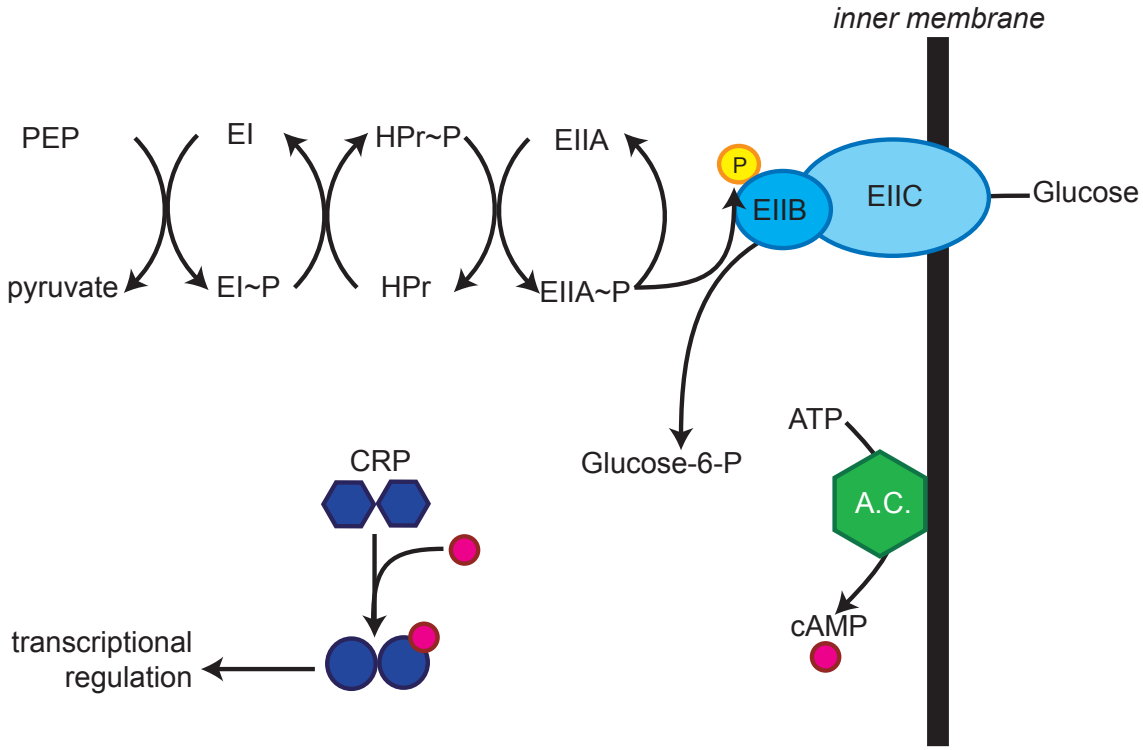

Figure 6: The Phosphotransferase System Regulates the Activity of cAMP-CRP.

Phosphate is transferred from phosphoenolpyruvate (PEP) via a series of phosphotransferase reactions and is ultimately donated to the membrane-bound glucose transporter ($EIIBC^{Glc}$). As glucose is transported into the cell, the phosphate donated by $EIIBC^{Glc}$ to the sugar, thereby coupling glucose uptake with its phosphorylation. In the absence of glucose transport, the level of phosphorylated of $EIIA^{Glc}$ increases and is able to activate the inner membrane-protein adenylate cyclase (A.C.). Adenylate cyclase converts ATP to cyclic AMP (cAMP). This small molecule then binds to a dimer of CRP, thereby forming the active cAMP-CRP complex.

for cAMP production. Concentrations of glycolytic metabolites also affect A.C. activity. Increased proportions of PEP relative to pyruvate leads to increased phosphorylation of $EIIA^{Glc}$, which in turn stimulates A.C. activity. Intracellular concentrations of cAMP are also regulated by synthesis, excretion and degradation of the molecule by cAMP phosphodiesterase (114).

Newly synthesized cAMP binds to its regulatory partner CRP. CRP is a 47-kDa protein that functions as a dimer. cAMP binding induces folding of the CRP protein into two distinct domains. The amino-proximal domain is characteristically comprised of several beta-sheet motifs, which form the cAMP binding pocket. The carboxy-proximal domain is primarily alpha helical, and acts as the DNA binding surface. When not bound to cAMP, CRP is resistant to proteases, and exhibits sequence independent affinity to DNA. Binding of cAMP enhances CRP affinity for DNA, and subsequently makes DNA binding sequence specific. Although each subunit of CRP can bind one molecule of cAMP, stoichiometric and structural studies suggest that the active form of the regulator consists of the CRP dimer complexed with one molecule of cAMP (15).

The cAMP-CRP complex activates expression of several catabolic genes and operons (15, 42, 102, 150). Generally, the genes positively regulated by cAMP-CRP are characterized by weak promoters. cAMP-CRP binds upstream of these promoters and modifies the promoter such that RNA polymerase promoter recognition is enhanced. The cAMP-CRP binding site is a 22-bp palindromic sequence. cAMP-CRP binding induces a structural change near the promoter, and the degree of DNA bending is influenced by distal DNA sequences. DNA bending likely facilitates protein-protein interactions that are important for CRP-dependent promoter activation. CRP binds the RNA polymerase holoenzyme in a cAMP-dependent fashion via the RNA polymerase sigma subunit (15) .

In *E. coli* and *S. flexneri*, adenylate cyclase is encoded by *cyaA*. Expression of *cyaA* is also negatively regulated by cAMP-CRP. The presence of exogenous cAMP represses *cyaA* expression 9-fold (15). Furthermore, the *cyaA* transcript uses a weak UUG initiator codon. However, replacement of the UUG codon with a stronger AUG codon did not increase the translational efficiency of *cyaA*, suggesting that *cyaA* expression is primarily regulated transcriptionally. The *cyaA* upstream region has three promoters, the strongest of which is *cyaA*P2. This promoter contains an operator region containing a CRP binding consensus. The current model proposes that cAMP-CRP binding to *cyaA*P2 blocks DNA binding by RNA polymerase. Expression of *crp* is indirectly inhibited by cAMP-CRP. Binding of cAMP-CRP to the *crp* promoter, *crpP*, activates transcription of an antisense RNA from divergent promoter. This antisense RNA forms a transcription terminating hairpin loop structure that effectively inhibits expression of *crp*.

In addition to its role in carbon metabolism, cAMP-CRP is also important for both cell physiology and virulence. Mutations in either *cyaA* and *crp* lead to abnormalities in cell morphology and significant growth defects (25). Expression of the cAMP-CRP complex is important for virulence of *Yersinia enterocolitica* in the mouse model (102). Both the *crp* and *cyaA* mutants failed to secrete the type III secretion system-dependent virulence proteins necessary for virulence, and were unable to spread to the liver and spleen of infected mice.

7.2 CRA

In *E. coli*, Cra (*c*atabolite *r*epressor *a*ctivator, FruR) is a cAMP-independent regulator of central carbon metabolism (113). Cra was originally identified as a repressor of the

fructose operon. However, further studies showed that this 36-kDa protein has additional roles in controlling carbon flow and also influences utilization of several exogenous carbon sources. Cra is encoded on a monocistronic operon, and the protein has sequence homology to the LacI-GalR family of transcriptional regulators (113). The N-terminal helix-turn-helix domain is required for DNA binding whereas the C-terminal ligand-binding domain is homologous to sugar binding receptors.

In *E. coli* and *Salmonella enterica* serovar Typhimurium (*S.* Typhimurium), Cra regulates central carbon metabolism (23, 107). Cra upregulates expression of genes involved in gluconeogenesis and the Krebs cycle and represses the glycolytic and Entner-Doudoroff pathways. With respect to catabolite regulation, Cra activates transcription of genes subject to catabolite repression while repressing those subject to catabolite activation (Fig. 7). Cra acts as a tetramer (107) and binds to palindromic sequences in the operator of regulated genes. The Cra consensus sequence is characterized by an imperfect palindrome. The protein has stronger interactions at the left half of the palindrome as compared to the right (91), leading to differing binding affinities. This degeneracy may be a result of the multiple roles of Cra and may allow the protein to bind to several different DNA sites (107). Of the known Cra regulated genes, only the *fru* operon contains a perfect palindrome. As expected, Cra binds to this sequence with very high affinity and exhibits its highest fold repression, suggesting that Cra originally evolved as a *fru* operon repressor and later acquired pleiotropic roles (107). The effect of Cra on transcription is determined by the relative position of the Cra binding site to the RNA polymerase binding site (Fig. 7). The glycolytic metabolites fructose-1, 6-bisphosphate and fructose-1-phosphate bind to Cra and block its ability to bind to DNA (107). In this fashion, glycolytic carbon source can derepress expression of glycolytic genes by Cra.

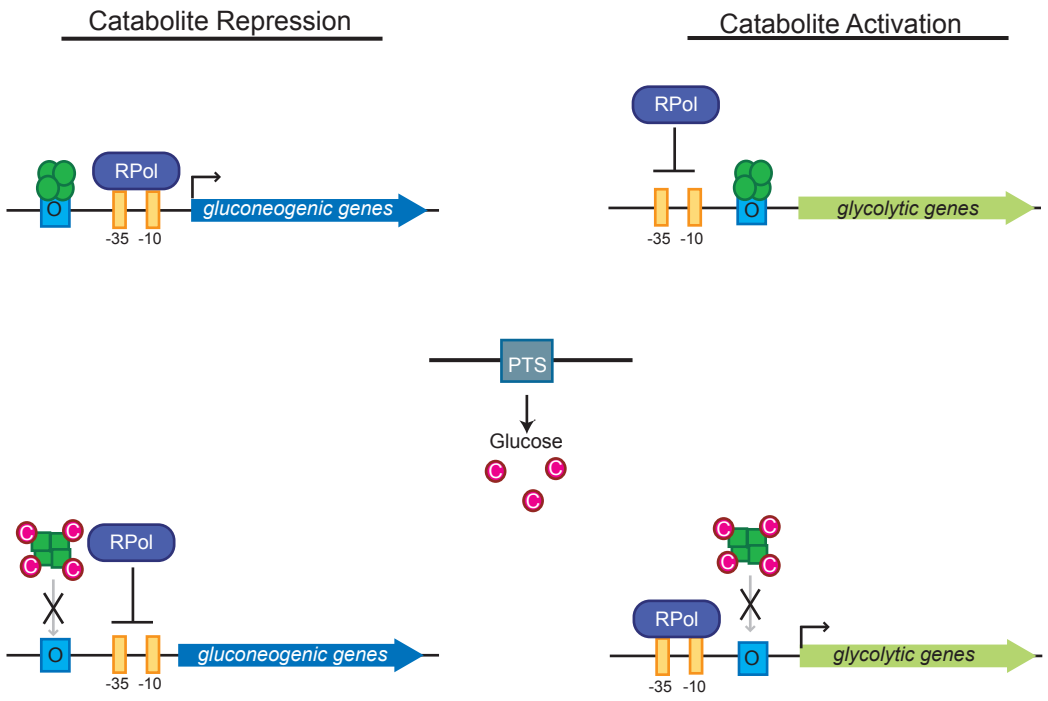

Figure 7. Model of catabolite repression and catabolite activation mediated by the transcriptional regulator Cra.

In the absence of a glycolytic carbon source, Cra binds to operator sequences (O) and either activates (gluconeognic genes) or represses (glycolytic genes) transcription by affecting binding of RNA polymerase (RPol). The presence of a glycolytic carbon source generates fructose 1,6 bisphosphate or fructose-6-phosphate, and these catabolites (C), bind to Cra and change the conformation of this protein thereby preventing Cra from binding to its operator sequences. In those genes repressed by Cra, the presence of a glycolytic carbon source promotes to transcriptional activation (catabolite activation). Conversely, Cra activated genes are repressed by the presence of the glycolytic carbon source (catabolite repression). Abbreviations: PTS, phosphotransferase system; -35, -10, promoter. Figure adapted from (113).

Expression of *cra* is also required for pathogenesis in *S*. Typhimurium (2). When administered to mice perorally, a *cra* mutant of *S*. Typhimurium was avirulent. However, this strain successfully invaded both M-cells and epithelial cells in vitro and grew as well as wild type in mouse mucus in vitro. Although this strain was immunogenic, it failed to persist in the mouse intestine. Similarly, a *cra* mutation in either commensal or pathogenic enterohemorragic *E. coli* (EHEC) led to significant defects in maintenance within the mouse intestine (68). Cra may therefore have an important role in utilization of available carbon sources within the mammalian intestine.

7.3 CARBON STORAGE REGULATOR – CSR

In *E. coli*, CsrA (*c*arbon *s*torage *r*egulator) is a global regulator that post-transcriptionally controls several diverse processes, including carbon metabolism, motility, biofilm formation and cell adherence (6, 72, 109). CsrA is a primary regulator of a larger feedback pathway that includes two non-coding RNAs (ncRNAs), a putative inner membrane protein and a two-component system (Fig. 9). This autoregulatory loop allows the cell to fine tune central carbon metabolism and other physiological responses to external stimuli. Homologs of the Csr system have been identified in several gram negative bacteria where it functions not only in control of cell physiology, but also regulates virulence (Table 1) (72).

Table 1: CsrA homologs in bacteria.

Homologs of *E. coli* CsrA and its RNA antagonists have been identified in several other gram negative bacteria and regulate several distinct steps in pathogenesis. [a] +, activation; -, repression; +/-, mixed response.

Bacteria	CsrA homolog/ RNA antagonist(s)	Role (Response)[a]	Reference(s)
Escherichia coli	CsrA/ CsrB, CsrC	carbon metabolism (+/-) motility (+) biofilm formation (-)	110, 139, 142
Vibrio cholerae	CsrA/ CsrB, CsrC, CsrD	quorum sensing (-)	70
Salmonella enterica Serovar Typhimurium	CsrA/ CsrB, CsrC	pathogenesis (+/-)	4
Pseudomonas aeruginosa	RsmA/ RsmY, RsmZ	pathogenesis (+/-)	18, 86, 101
Legionella pneumophila	CsrA/ CsrB, CsrC	macrophage infection (-) intracellular replication (+)	82
Helicobacter pylori	RsmA/ CsrB1, CsrB2	motility (+) virulence (+)	9
Yersinia pseudotuberculosis	CsrA/ CsrB, CsrC	motility (+) adherence, invasion (+)	49
Campylobacter jejuni	CsrA/ not identified	motility (+) biofilms (+) adherence to epithelial cells (+)	37
Enteroinvasive *E. coli* (EIEC)	CsrA/ CsrB, CsrC	secretion of translocators (+) formation of actin pedestals (+) glycogen metabolism (-)	13

7.3.1 CsrA

Central to the Csr regulon is a 6.8-kDa protein named CsrA. CsrA was originally identified in *E. coli* in a screen for mutants that regulated glycogen metabolism (110). Disruption of this gene led to a twenty-fold increase in internal glycogen stores (110, 112). CsrA was later shown to have pleiotropic effects on central carbon metabolism, specifically activating glycolysis while repressing both gluconeogenesis and glycogen metabolism (112). Like Cra, CsrA regulates metabolism independently of cAMP (110). CsrA is thought to regulate the physiological shifts necessary for transition from exponential to stationary phase, and accordingly expression of *csrA* increases two to four fold upon entry into stationary phase (43).

CsrA functions as a homodimeric protein (31, 44). Each subunit is composed of five beta strands, a small alpha-helix and a flexible C-terminus (Fig. 8) (44). The five beta strands are intertwined with alpha helices forming a wing-like structure near the C-terminus. Although CsrA is not a member of the KH protein family, it contains a conserved GXXG RNA-binding motif. This GXXG motif, located between loops 3 and 4, are likely used to recognize a conserved GGA motif present in target RNAs (44).

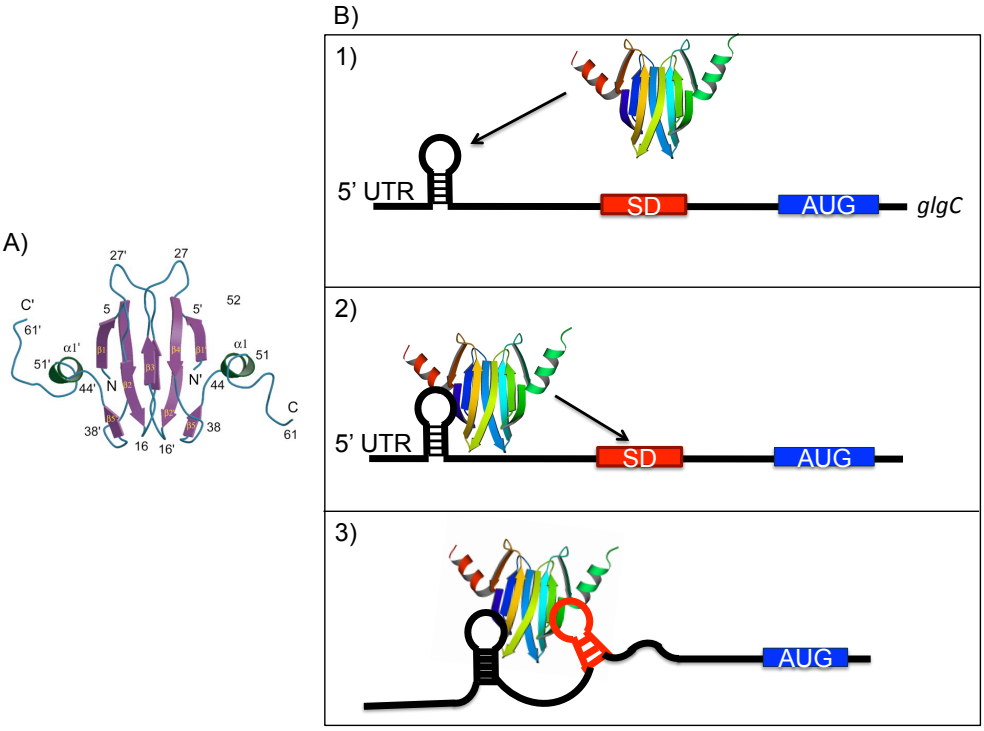

Figure 8: CsrA functions as a post-transcriptional regulator.

(A) The CsrA dimer is composed of two interdigitated monomers linked via five internal β sheets flanked by α helices that form a wing-like structure. The CsrA dimer contains two distinct RNA binding sites, composed of the beta-1 strand of one monomer and beta-5 strand of the second dimer (79). (B) A mechanism of CsrA mediated repression has been described based on the interaction of the protein with the glycogen metabolism message glgC (78). CsrA binds to a high affinity site in the 5' leader sequence of the mRNA, which promotes binding to a second, lower affinity site overlapping the Shine-Dalgarno (SD) sequence. By binding to these sites, CsrA blocks ribosome loading and decreases translation initation. Modified from Mercante *et al*. (78)

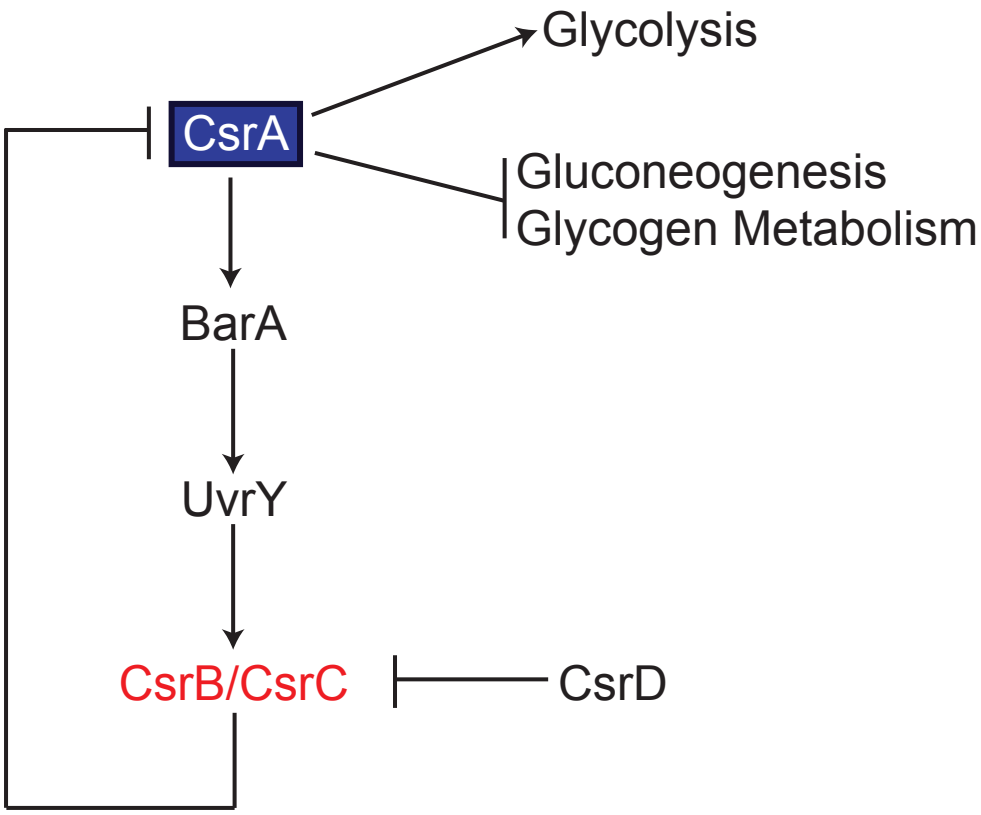

Figure 9. The CsrA regulatory pathway described in *E. coli*.

The post-transcriptional regulator CsrA activates glycolysis while repressing both gluconeogenesis and glycogen metabolism. *E. coli* CsrA modestly stimulates expression of the histidine kinase BarA. Activation of the BarA-UvrY two component system activates expression of the two antagonistic RNAs CsrB and CsrC (highlighted in red). Both CsrB and CsrC bind to CsrA and sequester the protein away from its mRNA targets. The inner membrane protein CsrD promotes RNase-E mediated degradation of CsrB and CsrC. Modified from Babitzke and Romeo, 1997 (6).

With the exception of Hfq mRNA, known CsrA targets contain multiple CsrA binding sites. Despite the variation among these targets, all contain a highly conserved GGA motif within stem-loop structures. To better define the CsrA recognition sequence, SELEX (*s*elective *e*volution of *l*igands by *ex*ponential enrichment) was used to screen a combinatorial library of artificially generated, randomized RNAs for CsrA binding. Using this method, Dubey *et al*. (30) defined the CsrA consensus sequence as RUACARGGAUGU, where the underlined sequences were highly conserved. CsrA affinity for these sequences was confirmed by gel shift mobility assays. These studies also illustrated a role of both primary and secondary structure in CsrA binding. Although CsrA preferentially binds to GGA motifs within hairpin loops, the stem loop alone is neither sufficient nor necessary for binding. Dubey *et al*. (30) showed that CsrA does not bind arbitrarily to stem loop structures, but that the protein will bind to the consensus sequence located in linear RNA. From these data, a model was proposed in which CsrA interacts with the GGA motif within the unpaired loop sequence and partially melts the sequence, allowing for further interaction of the protein with the RNA. This model was expanded upon to suggest that disruption of the stem loop would allow the dimeric protein to bind to bridge two binding sites via the two functional subdomains on opposite sides of the protein (79). CsrA acts as both an activator and repressor of translation. As a repressor, CsrA binds to sequences that overlap the Shine-Dalgarno sequence and competitively inhibits translation initiation by the ribosome (7, 8, 31, 139). However, the mechanism by which CsrA activates translation is not known. It has been postulated that the protein may protect target mRNAs from endonucleolytic degradation (139).

In *E. coli*, CsrA controls expression of several genes in the central metabolic pathways. Specifically, CsrA represses the glycogen metabolic genes *glgCAP* and *glgB*, and the gluconeogenic genes *pckA* and *ppsA* (112). Conversely, CsrA activates the glycolytic genes *pfkA* and *eno* (112). CsrA does not affect the pentose phosphate pathway, and modestly represses the Entner-Doudoroff pathway via an indirect mechanism (88, 112). CsrA has also been shown to regulate metabolism of cyclic di-GMP (c-di-GMP) by modulating expression of GGDEF proteins involved in synthesis and degradation of this second messenger (57). CsrA may also have a more diverse role in cellular processes via its regulation of Hfq. Hfq is a homohexameric protein that pleiotropically regulates cellular function. This protein promotes small RNA-mRNA base pairing necessary for message turnover (81). CsrA binds to a single site in Hfq that overlaps the Shine-Dalgarno sequence, thereby competitively inhibiting ribosome binding (7).

CsrA homologs have been identified in several gram negatives, including enteric pathogens, where this protein affects virulence properties, including production of cytotoxins, adherence, invasion and survival within the host (4, 9, 13, 18, 37, 49, 70, 82, 86, 101, 110, 139, 142) (Table 1). Enteropathogenic *E. coli* (EPEC) is an attaching/effacing pathogen that binds to intestinal epithelial cells and is a major etiological agent of infantile diarrhea (22). Upon infection, the bacterium binds to host cells, inducing massive cytoskeletal rearrangements that result in "pedestal" formation around the adhered bacterium. The proteins necessary for pedestal formation are encoded on the locus of enterocyte effacement (*LEE*). *LEE* consists of several polycistronic operons, including *LEE* 1- 5. In EPEC, CsrA is required for pedestal formation. CsrA binds to the leader segment of the LEE mRNA and increases stability of the message (13). Conversely, overexpression of *csrA* reduces expression of the *LEE* operons. Overexpression of *csrA* inhibits expression of the *LEE* activators GlrA and Ler. In

addition to virulence regulation, EPEC CsrA also regulates central carbon metabolism, as mutation of *csrA* mutant leads to increased glycogen stores (13).

S. Typhimurium causes gastroenteritis in humans (71). This pathogen invades intestinal epithelial cells using the chromosomally encoded SPI-1 type III secretion system, and effector proteins encoded outside this island. Expression of SPI-1 was significantly decreased in the *csrA* mutant, and the mutant was subsequently inhibited in invasion of epithelial cells in vitro. Overexpression of *csrA* also inhibited SPI-1 expression and invasion, suggesting that CsrA may be both an activator and repressor of SPI-1 (4). Unlike in *E. coli*, S. Typhimurium CsrA does not regulate central carbon metabolism. Instead, *S*. Typhimurium CsrA appears to have a pivotal role in metabolism of maltose, maltodextrins, vitamin B12 and ethanolamine. It has been predicted that *S*. Typhimurium CsrA has adapted to govern utilization of carbon sources used by this bacterium the mammalian intestine (69).

7.3.2 CsrB and CsrC

One characteristic feature of the Csr system is two small noncoding RNAs (ncRNAs) that control the intracellular levels of CsrA (Fig. 9). In *E. coli*, the ncRNAs CsrB and CsrC have been identified as antagonists of CsrA. These ncRNAs function as CsrA-sinks, and preferentially sequester the protein away from its mRNA targets. Both CsrB and CsrC contain the GGA motif within several stem-loop structures throughout the RNA (Fig. 10). CsrB is the larger of the two RNAs (366 nt) and can bind up to 10 CsrA dimers, whereas the 245-nt CsrC RNA binds 5 dimers. Expression of the ncRNAs is independent of the other, but both require CsrA for maximal expression (59, 143). Deletion of one of the two ncRNAs leads to a compensatory increase in expression of the second RNA (143). Both CsrB and CsrC have relatively short half-lives ($T_{1/2}$ = 2 min), thereby allowing the cell to respond quickly to stimuli by rapidly modulating the availability of CsrA (43, 143). Like *csrA*, expression of *csrB* and *csrC* increases upon entry into stationary phase. The response regulator UvrY has been identified as a transcriptional regulator of both *csrB* and *csrC* (43, 126, 143). However, in the presence of glucose, expression of *csrC* is only partially dependent on UvrY (59).

The presence of amino acids has also been shown to affect the expression of *csrB* and *csrC* (58). In *E. coli*, growth in minimal media drastically increased the levels of *csrB* and *csrC* as compared to growth in LB. This effect was more pronounced for *csrB* as compared to *csrC*, which the authors suggest is further evidence for differential regulation of the two RNAs. Additionally, the gluconeogenic carbon sources pyruvate, succinate and acetate had a greater effect on RNA expression as compared to glucose. Addition of casamino acids to minimal media drastically reduced the level of *csrB*, arguing that the absence of amino acids in minimal media is responsible for induction of this RNA.

A) CsrB, 366 nt

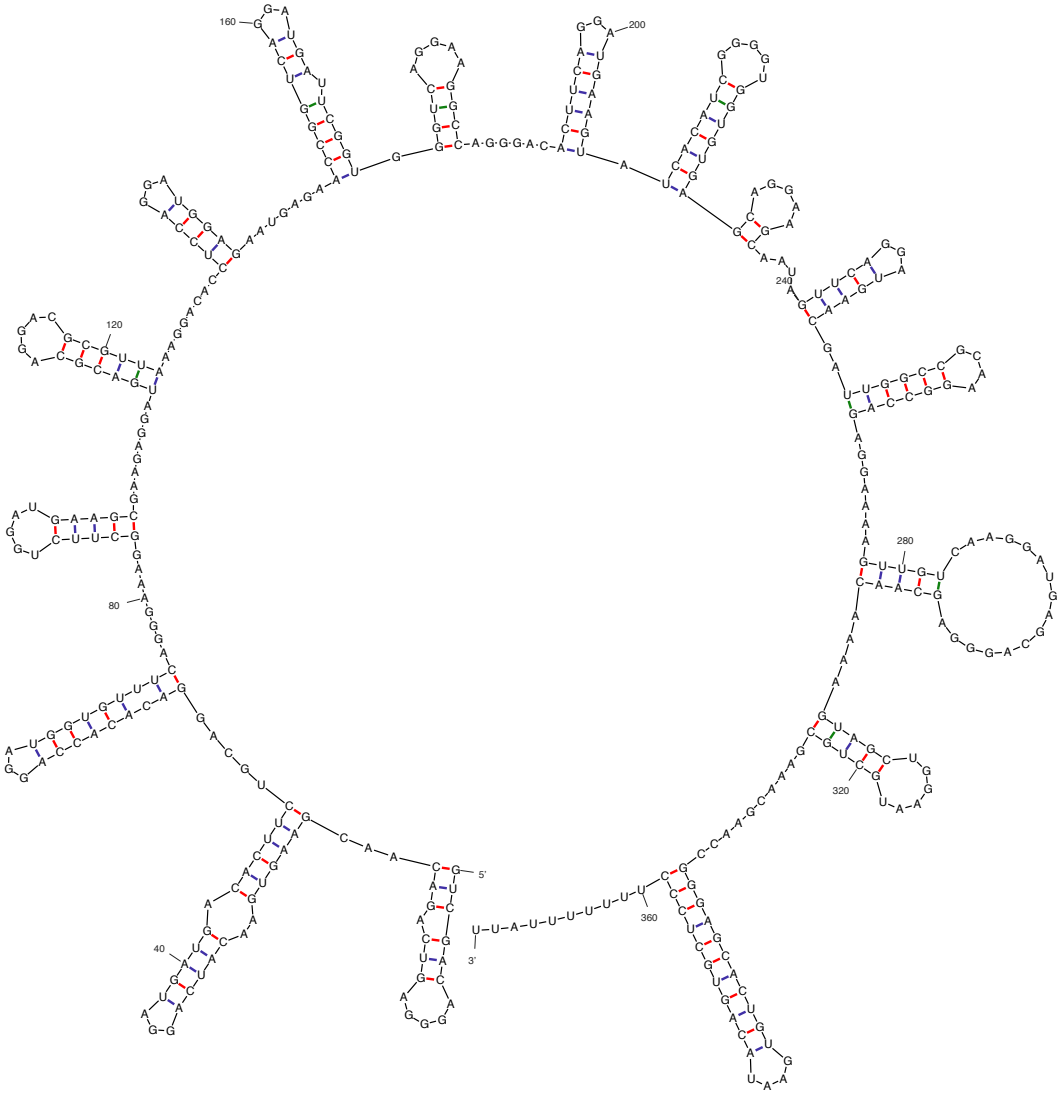

B) CsrC, 245 nt

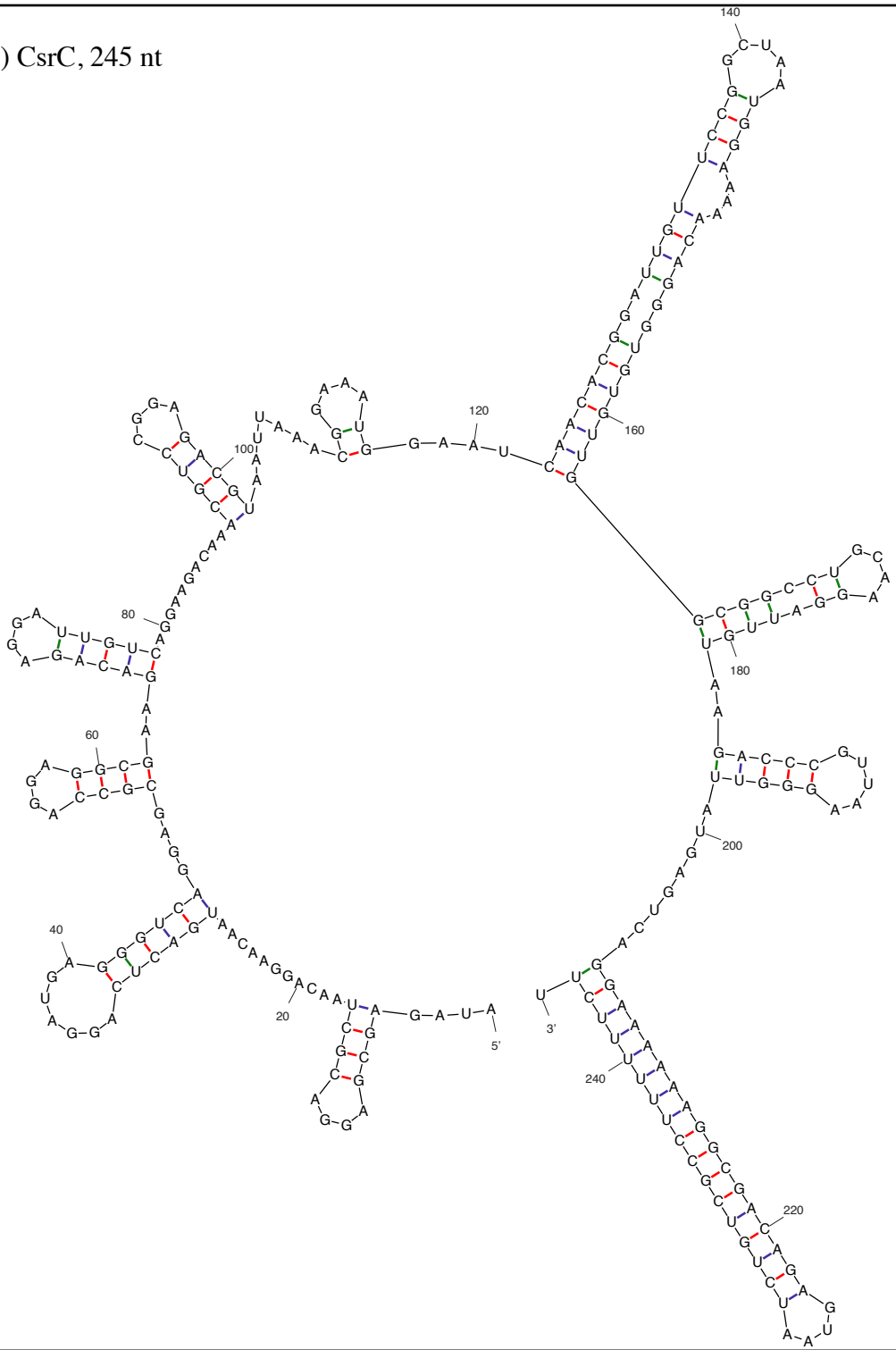

Figure 10: Structure of the antagonistic RNAs CsrB and CsrC from *S. flexneri*.

The small, untranslated RNAs CsrB (A) and CsrC (B) bind CsrA and sequester the protein away from its normal mRNA targets. Both RNAs contain several stem loop structures and multiple copies of the predicted CsrA binding site. The *S. flexneri csrB* and *csrC* sequences are 99% identical to the sequences annotated in *E. coli*. The secondary structure of the RNAs was generated with MFold version 2.3 (http://mfold.bioinfo.rpi.edu), using default parameters for the predictions.

7.3.3 CsrD

Two different groups independently identified CsrD as a regulator of *csrB* and *csrC* expression in *E. coli* (59, 125). CsrD functions as a specificity factor that promotes RNase-E dependent turnover of both ncRNAs, although CsrD is not a general RNA-degradation factor (125). In the absence of *csrD*, the RNA levels and half lives of both ncRNAs is increased (125). This 646 amino acid protein contains a signal sequence, transmembrane and coiled coil domains (59). The inner membrane domain of CsrD is not required for activity, but may act in a sensory capacity or may act to subcellularly localize the protein. In *E. coli*, CsrD was predicted to contain both GGDEF and EAL domains, which are characteristic of proteins required for cyclic-di-GMP metabolism. However, in CsrD these domains do not appear to function in cyclic-di-GMP metabolism (125). Two membrane-spanning regions anchor CsrD in the inner membrane. A HAMP-like domain, implicated in periplasmic sensing, is also required for CsrD function, suggesting that this protein may regulate CsrB and CsrC levels in response to extracellular stimuli (125).

7.3.4 BarA-UvrY Two Component System

In *E. coli*, the BarA-UvrY two-component system also regulates the level of free CsrA. Two-component systems are a mechanism by which a bacterium can sense and relay signals across the inner membrane. These systems allow for adaptive response to environmental shifts through changes in gene expression. Two-component systems are characteristically comprised of two proteins, an inner membrane-bound histidine kinase sensor and a cytoplasmic response regulator. The signal is relayed from the sensor kinase to the response regulator by a series of phosphorylation/dephosphorylation reactions. In

response to stimuli, the sensor kinase autophosphorylates on a conserved histidine residue. The phosphate is then transferred to the response regulator, thereby causing a conformational change in the response regulator that allows it to bind promoters of target genes and regulate gene expression (52).

BarA was originally identified because of its ability to phosphorylate the osmotic response regulator OmpR (55). Because of its ability to rescue osmotic regulation, this protein was named the *b*acterial *a*daptive *r*esponse protein A. The BarA histidine kinase belongs to a unique group of tripartite sensors containing phosphoryl transfer, receiver and histidine phosphotransfer output domains. Tripartite histidine kinases catalyze the phosphorylation of cognate response regulators via an ATP→His→Asp→His→Asp phosphorelay. Likewise, dephosphorylation of the activated response regulator occurs via a reverse Asp→His→Asp→P_i reaction. The periplasmic sensor domain of BarA and its homologs are poorly conserved, implying that these kinases lack a common signal (47).

The response regulator UvrY was so named for its bicistronic linkage to the UV-induced repair gene *uvrC*. Despite this proximity, UvrY has no documented effect on UV-induced DNA repair (100). In laboratory strains of *E. coli*, the BarA-UvrY system regulates the level of free CsrA by activating expression of both CsrB and CsrC (126, 143). Phosphorylation of UvrY by BarA activates the response regulator, which in turn upregulates expression of *csrB* and *csrC*. In *E. coli*, CsrA has also been shown to modestly increase expression of BarA (126), enabling further regulation of the system. The signal to which BarA responds is still unknown, although it has been hypothesized that BarA may respond to an intracellular indicator of carbon availability (126). No other direct targets of BarA-UvrY have been documented.

8. Purpose of this Research

To successfully establish infection, *S. flexneri* must adapt to the unique microenvironments encountered in the host. The bacterium likely encounters different carbon sources throughout infection, as it travels from the external to internal milieu, and as it competes for resources in the host lumen and utilizes available nutrients in the host cytosol. The adaptation to these environments likely relies on one or more the above-mentioned regulators to coordinate metabolic gene expression with the available resources. These regulators may also have a secondary role in coordinating cell physiology and virulence factors with the environment. The purpose of this research is to examine the role of cAMP-CRP, Cra and CsrA in *S. flexneri* pathogenesis, specifically examining how these regulators affect the process of invasion and intercellular survival. By examining the metabolic strategies of *S. flexneri*, these studies provide a better understanding of the mechanisms by which this cytosolic pathogen has adapted to an intracellular lifestyle. Such knowledge may aid in future work to prevent *Shigella* infection, specifically in the development of probiotic therapies that may block initial colonization by the bacterium.

II. MATERIALS AND METHODS

1. Bacterial strains and plasmids

The bacterial strains and plasmids used in this study are listed in Tables 2 and 3, respectively. The *E. coli* strain DH5α was used for cloning of recombinant DNA. The *E. coli* strains TRMG1655 (110), TWMG1655 (143) and RG1-B (43) were kindly donated by Dr. Tony Romeo, University of Florida, Gainesville. Keio mutants were provided by the *E. coli* Genome Analysis Project (5). The *S. flexneri* strain 2457T, a serotype 2a wild type strain, was used to generate all mutants. SA101 is a spontaneous avirulent 2a strain, and was used as a negative control where noted (28).

2. Media, Reagents and Growth conditions

All strain stocks were maintained at -80°C in tryptic soy broth (TSB) supplemented with 20 % v/v glycerol. *E. coli* strains were grown in Luria-Bertani (LB) broth (1% tryptone, 0.5% yeast extract, 1% sodium chloride) or on LB agar plates. *S. flexneri* strains were grown in LB broth or on TSB agar plates containing 0.01% Congo red dye (TSBA-CR). Where noted, the minimal media M63, modified M9 (MM9) or T-medium were used. MM9 contained 30 mg/L monobasic potassium phosphate, 50 mg/L sodium chloride, 100 mg/L ammonium chloride, 6 g/L sodium hydroxide and 30 g/L PIPES. MM9 media was supplemented with 1 mM magnesium sulfate, 100μM calcium chloride, 2 μg/ml nicotinic acid, 20 μg/ml tryptophan and 2 μg/ml thiamine. M63 contained 13.6 g/l monobasic potassium phosphate, 2 g/L ammonium sulfate, 0.5 mg/L ferrous sulfate, and was supplemented with 1 mM magnesium sulfate, 100μM calcium chloride, 2 μg/ml nicotinic acid, 20 μg/ml tryptophan and 2 μg/ml thiamine, 5μg/ml 2-deoxyadenosine and 450 μg/ml methionine.

Table 2: Strains Used in this Study

Strain	Relevant Characteristics	Source or Reference
E. coli		
DH5α	*endAI, hsdR17, supE44, thi-1, recA1, gyrA, relA1, Δ(lacZYA-argF), U169, deoR, [ϕ80*d*lacΔ(lacZ)M15]*	Sambrook and Russell, 2001 (116)
JW1899	BW25113 *uvrY::km*	Keio collection (5)
JW5702-2	BW25113 *crp::km*	Keio collection
JW2757	BW25113 *barA::km*	Keio collection
JW3778	BW25113 *cyaA::km*	Keio collection
JW3221	BW25113 *yhdA::km*	Keio collection
JW0078	BW25113 *cra::km*	Keio collection
JW1692	BW25113 *ppsA::km*	Keio collection
JW3393	BW25113 *glgC::km*	Keio collection
RG1-B	MG1655 *csrB::cm*	T. Romeo
TRMG1655	MG1655 *csrA::km*	T. Romeo
TWMG1655	MG1655 *csrC::km*	T. Romeo
S. flexneri		
2457T	*Shigella flexneri* 2a, wild type	
SA101	*S. flexneri* 2a SA100 spontaneous Crb$^-$	Daskaleros and Payne, 1987 (28)
SA555-148	*S. flexneri* 2a SA100, *rfaX*::Tn*phoA*	Hong and Payne, 1997 (54)
AGS100	2457T *barA::km*	this study
AGS110	2457T *uvrY*::*km*	this study
AGS120	2457T *csrA*::*km*	this study

AGS130	2457T *csrB*::*cm*	this study
AGS140	2457T *csrC*::*tet*	this study
AGS150	2457T csrD::*km*	this study
AGS160	2457T *csrB*::*cm*, *csrC*::*tet*	this study
AGS170	2457T *crp::km*	this study
AGS180	2457T *cyaA::km*	this study
AGS190	2457T *cra*::*km*	this study
AGS200	2457T *ppsA::km*	this study
AGS210	2457T *glgC::km*	this study
AGS220	2457T *pfkA*::km	this study

Table 3: Plasmids Used in this Study

Plasmid	Characteristics	Source or Reference
Cloning Vectors		
pGEM-T Easy	PCR cloning vector	Promega
pQE2	IPTG-inducible gene expression vector	Qiagen
pWSK29	Low-copy number expression vector	Wang and Kushner, 1991 (138)
pWKS30	Low-copy number expression vector	Wang and Kushner, 1991
Gene Expression		
pWCrp	pWKS30 with *crp* promoter and coding region	this study
pWCyaA	pWKS30 with *cyaA* promoter and coding region	this study
pQCsrA	pQE2 with *csrA* under control of IPTG inducible promoter	this study
pQCsrB	pQE2 with *csrB* under control of IPTG inducible promoter	this study
pQCsrC	pQE2 with *csrC* under control of IPTG inducible promoter	this study
pWCsrA	pWSK29 with *csrA* promter and coding region	this study
pWCra	pWKS30 with *cra* promoter and coding region	this study
pWPfkA	pWSK29 with *pfkA* promoter and coding region	this study

T-medium was prepared as described in Simon and Tessman, 1963 (121), and was routinely supplemented with 0.4% carbon source and 2 μg/ml nicotinic acid. EZ rich defined media (EZ-RDM, www.genome.wisc.edu/resources/protocols/ezmedium.html) was also used, and is a modification of the supplemented MOPS minimal media described by Neiderhardt *et al*. (92). Unless otherwise noted, carbon sources were added to EZ-RDM at a final concentration of 0.2% (w/v).

Antibiotics were added at the following concentrations per milliliter: 25μg ampicillin (Amp), 30μg chloramphenicol (Cm), 1.6μg tetracycline (Tet), and 50μg kanamycin (Km). Gene expression was induced by adding isopropyl beta-d-1-thiogalactopyranoside (IPTG) where noted.

3. P1 vir transduction to generate mutants

S. flexneri mutants AGS100 - 220 were generated by bacteriophage P1 *vir* transduction from the *E. coli* strains listed in Table 2, following a modification of the protocol described in Sambrook (116). Bacteriophage stocks were routinely amplified on the *E. coli* strain MG1655 on T-medium agar containing 10 mM calcium chloride and 1 mM dithiothreitol (DTT). Mutant strains were selected by plating recipient cells on TSBA-CR with 2.5 mM sodium citrate with the appropriate antibiotic marker. For those mutants marked with a kanamycin resistance cassette, 200μg/ml kanamycin was added to TSBA-CR selection plates. All mutants were confirmed by polymerase chain reaction (PCR) with primers internal to the antibiotic cassette and flanking the mutated gene.

4. Oligonucleotides and Polymerase Chain Reaction

Oligonucleotides used in this study are listed in Table 4. Primers were designed using Clone Manager software (Sci-Ed Software, Cary, NC), and purchased from Sigma (St. Louis, MO), Invitrogen (Carlsbad, CA) or Integrated DNA Technologies (Coralville,

IA). Lyophilized oligonucleotides were resuspended in sterile Milli-Q (Millipore, Billerica, MA) purified H_2O (H_2O) to a final concentration of 100μM and stored at -20°C.

Table 4: Oligonucleotide primers used in this study

Primer	Sequence (5' – 3')
CRP WKS fwd	GAATCCAAATCGCGCAACGGAAGG
CRP WKS rev	GAGCTCCAGCGTTTGTCGAAGTGCATAG
pWCyaA fwd	GAATTCGTGCTACACTTGTATGTAGCG
pWCyaA rev	GAGCTCGATTGCATGCCCGGATAAGCC
csrA fwd BseRI	ATCTGAGGAGCAGCAAAGTATGCTGATTCTG
csrA rev HindIII	AAGCTTGGGTGCGTCTCACCGATAAAG
pQCsrB fwd	GAATTCATCTTCGTCGACAGG
pQCsrB rev	AAGCTTAAAACTGCCGCGAAGGATAGC
pQCsrC fwd	GAATTCCAAAGGCGTAAAGTAGCACCC
pQCsrC rev	AAGCTTCTTTTGCATGACCTTTGCTGCG
pWCra fwd	GAATTCTGCGAAATCAGTGGGAAC
pWCra rev	GCGGCCGCGTTGGCAGCATTACCTTG
pCC-CsrA fwd	GAATTCACTCGCTTCACGGCATTC
pCC-CsrA rev	AAGCTTAACGGAGGTCTGGCAGATAG
pWPfkA fwd	GTGGACAGGGAGGGTAAACGGTCTATG
pWPfkA rev	GCGGCCGCCTTGCGGGTATATGTTGAGGG
Real Time Primers	
virB2 for	5' TCCAATCGCGTCAGAACTTAACT 3'
virB2 rev	5' CCTTTAATATTGGTAGTGTAGAACTAAGAGATTC 3'
virB2 probe	5' FAM –AGGACTTGAAAAGGC-MGBNFQ 3'
virF for	5' TCGATAGCTTCTTCTCTTAGTTTTTCTG 3'
virF rev	5' GAAAGACGCCATCTCTTCTCGAT 3'
virF probe	5' FAM-TCAGATAAGGAAGATTGTTGAAA-MGBNFQ 3'

PCR for routine screening were performed using Taq polymerase (Qiagen or New England Biolabs) per the manufacturers instructions. Each 100µl PCR reaction contained 100µM each dNTP, template DNA, 10µM each primer in Taq polymerase buffer. For the Taq polymerase PCR reactions, the cycling conditions are as follows: 5 minute denaturation at 94°C, followed by 30 cycles of 30 seconds at 94°C, 50°C annealing for 30 seconds and extension at 72°C for 1 minute per 1000 bp DNA. Taq PCRs were completed by a final extension at 72°C for 15 minutes. Taq plus Pfu (Stratagene, La Jolla, CA) or Platinum Pfx polymerase (Invitrogen) was used for generating DNA fragments for gene expression. Taq plus Pfu PCR reactions were performed as described for Taq reactions. Each Pfx reaction (50µl) contained 300µM of each dNTP, 0.3µM of each primer, and template DNA in Pfx PCR buffer. Three step cycling was used for all Pfx amplifcations as follows: 2 minute denaturation at 94°C, followed by 30 cycles for denaturation at 94°C for 15 seconds, annealing at 55°C for 30 seconds and extension at 68°C for 1 minute per kilobase of DNA. The Pfx PCR reaction was terminated by incubating the product at 4°C.

5. DNA Sequencing

Cloned DNA fragments and PCR products were confirmed by sequencing. Sequencing was performed at the University of Texas at Austin DNA sequencing facility using an ABI 3130 sequencer (Applied Biosystems, Foster City, CA) and automated dye termination procedure. All sequences were analyzed using Clone Manager Professional software.

6. DNA Isolation

Plasmid DNA was isolated from cells using the Sigma (St. Louis, MO) GenElute plasmid prep kit following the manufacturers instructions. DNA fragments were isolated

from agarose gels using the Sigma GenElute gel extraction kit per the manufacturer's instructions. Isolated DNA was eluted with either the provided elution buffer or H_2O and stored at -20°C.

7. Restriction Digests and Ligation

All restriction digests and were performed per the manufacturers directions. Restriction enzymes and DNA size markers were purchased from New England Biolabs. DNA size was estimated using the ϕX DNA-HaeIII and λ DNA-HindIII digests. Ligations were performed by incubating DNA fragments with T4 DNA ligase (Fisher Scientific, Pittsburgh, PA), according to the manufacturer's directions and transformed into the appropriate strain.

8. Transformation of Bacterial Strains

8.1 TRANSFORMATION OF *E. COLI* BY HEAT SHOCK

Ligation products or plasmid DNA was introduced into $CaCl_2$ competent *E. coli* strain DH5α by heat shock transformation. DH5α was made heat-shock competent by subculturing an overnight culture of DH5α 1:100 into LB broth and growing the culture at 37°C until midlog phase. Bacteria were collected by centrifugation at 3000 x g for 10 minutes, and the supernatant was decanted. The bacterial pellet was resuspended in 10 ml ice-cold $CaCl_2$ solution (10 mM PIPES, 60 mM $CaCl_2$, 15% glycerol). The centrifugation and resuspension steps were repeated twice, and after the third centrifugation, the bacteria were resuspended in 2 ml cold $CaCl_2$ solution. Aliquots of 150µl of resuspended bacteria were stored at -80°C. To transform bacteria, plasmid DNA (100 - 200ng) or ligation mixture was added to $CaCl_2$ competent bacteria and incubated on ice for up to two hours. The bacteria were then heat shocked at 42°C for 2 minutes, followed by a 2-minute incubation on ice. The bacteria were inoculated into

850µl LB broth. After a 1-hour incubation at 37°C with aeration, transformed bacteria were isolated by plating the culture on LB agar with the appropriate antibiotics.

8.2 ELECTROPORATION OF *S. FLEXNERI*

To make electrocompetent *S. flexneri*, overnight cultures were subcultured 1:100 into fresh LB broth with appropriate antibiotics, and grown to midlog phase at 37°C with aeration. Bacteria were harvested by centrifugation at 6000 x g in pre-chilled rotor. The bacterial pellet was then resuspended in 20 ml G-buffer (137 mM sucrose, 1 mM HEPES, pH 8.0). The pelleting and resuspension steps were repeated twice, and after the third centrifugation, the bacteria were resuspended in 400µl G-buffer. One hundred microliter aliquots of the cell suspension were stored at -80°C.

To transform *S. flexneri*, 5µl of plasmid DNA and 1.7µl of 20% sucrose were added to 100µl of electrocompetent bacteria. *S. flexneri* was electroporated in a GenePulse electroporator (BioRad, Hercules, CA) using the following settings: 200 Ω, 25 mF, 24V. Bacteria were then inoculated into 800µl of LB broth and incubated at 37°C with aeration for an hour. Transformed bacteria were selected by plating the culture on TSBA-CR with the appropriate antibiotic.

9. Construction of plasmids

9.1 PWCRP

The *crp* mutation in *S. flexneri* strain AGS170 was complemented by expressing the wild type *crp* gene from its native promoter in the low copy vector pWKS30. Wild type *crp* was amplified by PCR from 2457T using primers CRP WKS fwd and CRP WKS rev. The PCR-amplified DNA fragment was digested with EcoRI and NotI, and ligated into similarly digested pWKS30 to create the complementing plasmid pWCrp.

9.2 pWCyaA

The plasmid pWCyaA was used to complement the *cyaA* mutation in *S. flexneri* strain AGS180. To construct this plasmid, wild type *cyaA* was amplified from 2457T by PCR using the primers pWCyaA fwd and pWCyaA rev. The resulting PCR fragment was then ligated into pGEMt-Easy, creating pGWCyaA. The *cyaA* gene was then excised from pGWCyaA by digestion with EcoRI and NotI and ligated into similarly cut pWKS30 (138) to create pWCyaA.

9.3 pQCsrA

Overexpression of *csrA* was achieved by cloning the *csrA* gene under the control of an IPTG inducible promoter in the expression plasmid pQE2 (Qiagen). The *csrA* gene from *S. flexneri* 2457T was amplified by PCR using the forward primer csrA fwd BseRI and reverse primer csrA rev HindIII. The amplified DNA fragment was digested with BseRI and HindIII and cloned under the control of the T5 IPTG-inducible promoter in similarly digested pQE2. The resulting plasmid, pQCsrA, was also confirmed by sequencing.

9.4 pQCsrB and pQCsrC

The *csrB* and *csrC* overexpression vectors, pQCsrB and pQCsrC respectively, were created by amplifying *csrB* and *csrC* from 2457T by PCR. Primers pCsrB fwd and pCsrB rev were used to amplify *csrB*, and *csrC* was amplified using the primers pQCsrC fwd and pQCsrC rev. The resulting DNA fragments were cloned into pGEMt-Easy to create the plasmids pGQCsrB and pGQCsrC. The *csrB* and *csrC* fragments, from pGQCsrB and pQCsrC respectively, were excised using HindIII and EcoRI, and ligated into similarly digested pQE2 to generate pQCsrB and pQCsrC. In these plasmids, both genes are under the T5 IPTG-inducible promoter in pQE2. The resulting plasmids were confirmed by sequencing.

9.5 pWCsrA

To complement the *S. flexneri csrA* mutant AGS120, *csrA* from wild type *S. flexneri* was cloned in the low copy vector pWSK29 under the control of its native promoter. Using genomic DNA from 2457T as template, *csrA* was amplified using the primers pCC-CsrA fwd and pCC-CsrA rev by PCR. The PCR product was ligated into pGEM-T Easy (Promega) thereby generating the plasmid pGWCsrA. The *csrA* fragment was excised from pGWCsrA by digestion with SacII and HincII and ligated into similarly digested pWSK29 (138). The resulting plasmid, pWCsrA was confirmed by sequencing.

9.6 pWCra

For complementation of the *cra* mutant AGS190, *cra* was amplified from 2457T using the primers pWCra fwd and pWCra rev. The resulting PCR product was cloned into the T-overhangs of pGEM-T Easy, yielding the plasmid pGWCra. Both pWKS30 and pGWCra were digested with EcoRI and NotI, and the digested plasmid and *cra* insert were ligated to create pWCra. The cloned *cra* fragment was confirmed by sequencing.

9.7 pWPfkA

The *pfkA* mutant, AGS220, was complemented by PCR amplifying wild type *S. flexneri pfkA* using primers pWPfkA-fwd and pWPfkA-rev. The resulting *pfkA* DNA fragment, which contains *pfkA* under the control of its native promoter, was ligated into pGEM-T Easy, yielding pGWPfkA. The *pfkA* gene in pGWpfkA was excised by digestion with SalI and NotI. The complementing plasmid pWPfkA was generated by ligating the into the low copy vector pWSK29, also digested with SalI and NotI. The cloned *pfkA* gene was confirmed by sequencing.

10. Cell Culture

Henle cells (intestinal 407, American Type Culture Collection) were cultured in minimal essential media (MEM, Gibco) supplemented with 10% bacto-trytone phosphate broth (Difco, Becton-Dickinson Company, Franklin Lakes, NJ), 10% fetal bovine serum (Gibco), 2 mM glutamine and 1X nonessential amino acids (Gibco). Henle cells were routinely incubated at 37°C with 95% air – 5% CO_2.

11. Cell Culture Assays

11.1 Invasion Assays

Invasion assays were performed essentially as described by Hong and Payne (54). Several red colonies from an overnight TSBA-CR plate were used to inoculate LB broth and the cultures were grown at 37°C with aeration to exponential phase. When necessary, the appropriate antibiotic was included in the growth media. Approximately $2x10^8$ cells were added to a subconfluent monolayer of Henle cells in 35 mm 6-well polystyrene plates (Corning) and centrifuged for 10 minutes at 700 x g in a Centra GP8 centrifuge (International Equipment Company, Needham Heights, MA). After centrifugation, the monolayers were incubated for 30 minutes at 37°C with 5% CO_2. To remove extracellular bacteria, the monolayers were washed with phosphate buffered saline (1X PBS-D: 1.98 g/L potassium chloride, 8 g/L sodium chloride, 0.02 g/L monobasic potassium phosphate, 1.4 g/L dibasic potassium phosphate, pH 7.5). Monolayers were then overlaid with two milliliters MEM supplemented with 20μg/ml gentamycin per well. Plates were incubated an additional 40 minutes, washed with 1X PBS-D, then stained with Wright-Giemsa stain (Camco, Ft. Lauderdale, FL), washed with distilled water and air dried. Internalized bacteria were visualized by microscopy at 600X magnification. Henle cells containing 3 or more internal bacteria were scored positive for invasion, and at least 300 Henle cells were examined per well.

In the complement invasion assays involving pQCsrA, cells were grown to mid-logarithmic phase (A_{650} = 0.5), at which point IPTG was added at a final concentration of 150μM. Cultures were then grown to exponential phase, and the invasion assay was performed with an additional 150μM IPTG added to the culture media throughout the duration of the assay. For the pQCsrA overexpression invasion assays, cultures were grown to exponential phase, and 200μM IPTG was added for 30 minutes to induce expression of *csrA*. Cells were similarly grown for the pQCsrB and pQCsrC invasion assays, except that 200μM IPTG was added for 15 minutes to induce expression of the RNAs. 200μM IPTG was added to the culture media where for the duration of the assay.

To test the role of gluconeogenic carbon sources in the invasion of the *pfkA* mutant, several red colonies were used to inoculate an overnight culture in MOPS-minimal media with 0.2% pyruvate as a carbon source. The overnight culture was then subcultured to a starting A_{650} of 0.02 into fresh MOPS medium supplemented with 0.2% carbon source. Cultures were then incubated at 37°C with aeration until exponential phase, and the standard invasion assay protocol was followed.

11.2 ATTACHMENT ASSAYS

To measure adherence of the bacteria to epithelial cells, *S. flexneri* strains were grown to midlog phase in LB broth, and approximately $2x10^8$ bacteria were added to a subconfluent monolayer of epithelial cells in 35 mm 6-well plates. Plates were centrifuged for 5 minutes at 700 x g in a Centra GP8 centrifuge, then incubated for 15 minutes at 37°C in 5% CO_2 prior to staining as described as above. Adherent bacteria were counted by microscopy at 600X magnification. One hundred Henle cells were examined in each experiment, and the total number of bacteria present per cell was recorded for each strain.

11.3 PLAQUE ASSAYS

The plaque assay was performed as previously described (45, 54). Approximately 10^5 exponential phase bacteria grown in LB broth were added to confluent monolayers of Henle cells cultured in 6 well polystyrene plates. Bacteria were centrifuged on to monolayers for 10 minutes at 700 x g in a Centra GP8 centrifuge, and then incubated for 45 minutes in a 5% CO_2 atmosphere at 37°C. Monolayers were then washed with 1X PBS-D, then overlayed with MEM containing 0.3% glucose and 40 μg/ml gentamycin. The gentamycin selectively kills any extracellular bacteria, ensuring that any plaques formed are the result of intracellular spread by *S. flexneri*. After 48 hours incubation, wells were washed with 1X PBS-D and stained with Wright-Giemsa. Plaques are scored for size and clarity, as these features correlate with efficiency of *Shigella* to grow within the eukaryotic cytosol and propagate to adjacent cells.

11.4 RECOVERY OF EXTRACELLULAR AND INTRACELLULAR *S. FLEXNERI*

Bacteria were grown as described in the invasion assay, and $5x10^9$ cells were added to a confluent monolayer of Henle cells grown in a 96 cm^2 Roboflask (Corning). Bacteria were centrifuged onto the monolayer in a Centra GP8 centrifuge for 10 minutes at 700 x g, then incubated for 30 minutes in a 5% CO_2 atmosphere at 37°C. After the initial incubation, the media was removed by pipetting and noninvaded (extracellular) bacteria were collected by centrifugation for 7 minutes at 6000 x g in a Sorvall rotor. The extracellular bacterial pellets were then resupsended in 100μl 1X PBS-D. Monolayers were then washed with PBS-D, overlayed with MEM supplemented with 80μg gentamycin, and incubated an additional 2 hours at 37°C with 5% CO_2. Monolayers were washed again with PBS-D, and intracellular bacteria were released by lysing Henle cells with 2.5% w/v saponin for 8 minutes at 37°C. The cell lysate was recovered by centrifugation at 6000 x g for 7 minutes in a Sorvall SS34 rapid access rotor (Thermo-Fisher Scientific, Rockford, IL). Cell pellets were washed with 1X PBS-D and

centrifuged twice, and after the final spin, the recovered bacteria were resuspended in 200µl 1X PBS-D.

12. Real Time PCR

Colonies grown overnight on TSBA-CR plates were used to inoculate LB broth, and strains were grown to exponential phase at 37°C with aeration. Approximately $8x10^8$ cells were used for isolation. RNA was isolated using the Qiagen RNeasy mini prep kit. After elution, RNA was treated with 10 units of DNase (Invitrogen) and precipitated overnight. Samples were then washed with ethanol, then resuspended in 40µl DEPC-treated H_2O. RNA was quantified using an ND-1000 spectrophotometer (NanoDrop, Wilmington, DE). Approximately 2µg RNA was used to make cDNA using the High Capacity cDNA Reverse Transcription kit (Applied Biosystems) per the manufacturer's directions. cDNA was then diluted 1:10 in DEPC-treated H_2O, and 2.5 µl of this dilution was used as template for real-time PCR. The reaction was performed using minor groove binding (MGB) primers and FAM-labeled probes previously described by Murphy and Payne (87) using Primer Express. The real time reaction was performed using a 7300 real time PCR system (Applied Biosystems) under standard conditions. Samples were normalized to the *dksA* control, and calibrated to the wild type strain 2457T.

13. Protein Analysis

13.1 Isolation and detection of whole cell proteins

Several colonies grown on TSBA-CR plates were used to inoculate LB broth and cultures were grown to exponential phase at 37°C with aeration. Cultures were centrifuged to collect bacteria, and approximately 10^9 cells were resuspended in 100µl 1X PBS-D and 100µl 2X sample buffer (0.001% v/v β-mercaptoethanol, 2% w/v SDS, 10% v/v glycerol, 5% bromophenol blue, 63 mM Tris-Cl). Samples were lysed by boiling for

10 minutes, and 10μl of cell lysate was resolved on a 12% sodium dodecyl sulfate polyacrylamide gel (SDS-PAGE), then visualized by Coomassie staining.

13.2 ISOLATION AND DETECTION OF SECRETED PROTEINS

Secreted proteins were examined using a modification of the protocol described by Murphy and Payne (87). Approximately 10^9 bacteria from cultures grown to exponential phase in LB broth were centrifuged and resuspended in 100μl 1X PBS-D. Congo red was added at a final concentration of 0.005% to cell suspensions, and the suspensions were incubated at 37°C for 20 minutes without aeration. Bacteria were removed by centrifugation for 10 minutes at 16,300 x g. To precipitate the secreted proteins, 10 μl of 100% trichloroacetic acid was added to 100μl of the resulting supernatant. Secreted proteins were precipitated overnight at 4°C, and collected by centrifugation for 15 minutes at 16,300 xg at 4°C. Protein pellets were washed with 100% cold acetone and dried. The precipitated proteins were resuspended in 25μl 1X PBS-D and 25μl 2X sample buffer, and 10μl of sample was electrophoresed on a 12% SDS-PAGE gel, then visualized by silver staining as described by Morrissey, 1981 (84). Protein size was estimated using precision plus dual color protein marker (BioRad) for all SDS-PAGE gels.

13.3 PREPARATION OF PROTEINS FROM INTRACELLULAR BACTERIA

One hundred microliters of 2X SDS-PAGE buffer was added to 100μl of recovered extracellular or intracellular bacteria. Samples were boiled for 10 minutes, and 10 μl of sample was loaded onto a 12% SDS-PAGE gel. Proteins recovered from extracellular bacteria were diluted 1:10 in 1X PBS-D prior to loading. After electrophoresis, proteins were visualized by silver staining, following the protocol of Morissey, 1981 (84).

13.4 IMMUNOBLOTTING OF IPA PROTEIN SAMPLES

After electrophoresis, proteins were transferred to a 0.45μm pore-size nitrocellulose membrane (Hybond-ECL, GE). Blots were probed with monoclonal anti-IpaB or monoclonal anti-IpaC antibodies (E. V. Oaks, WRAIR), followed by goat anti-mouse HRP conjugated secondary antibody (BioRad). Signal was detected by developing the blot with the Pierce ECL-detection kit (Thermo-Fisher Scientific)

14. IcsA localization

Approximately 10^9 bacteria from cultures grown to exponential phase in LB broth were used to examine IcsA localization. Bacteria were fixed in 4% paraformaldehyde for 15 minutes at 25°C, and then washed with 1X PBS-D. Bacteria were incubated for 1 hour at 25°C with 1:100 dilution of rabbit anti-IcsA antibody made in PBS-D. After washing in PBS-D, bacteria were labeled in the dark with 100μl of FITC anti-rabbit antibody for an additional hour at 25°C. Unbound FITC was removed by washing the bacteria with PBS-D, and labeled bacteria were spread on a glass microscope slide. Slow Fade Gold (Invitrogen) was added to prevent photobleaching. IcsA localization was observed under a light microscope using a FITC-filter, and images were captured with SpotAdvance software (Diagnostic Instruments, Sterling Heights, MI).

15. Analysis of Lipopolysaccharide

15.1 PREPARATION OF LIPOPOLYSACCHARIDE SAMPLES

Lipopolysaccharide extraction was performed essentially as described by Hitchcock and Brown (51). Strains were grown to midlog phase in LB broth, and 10^9 bacteria were harvested by centrifugation. Bacterial pellets were resuspended in 50μl LPS lysis buffer (2% w/v SDS, 4% v/v 2-mercaptoethanol, 10% v/v glycerol, 1M Tris-Cl (pH 6.8), 0.05% bromophenol blue), and boiled for 10 minutes and cooled on ice.

Twenty-five micrograms of proteinase K (Sigma-Aldrich) was added to samples, and then samples were incubated for 1 hour at 65°C. LPS samples were then boiled an additional 5 minutes, then 2.5 - 5µl was loaded on a 12% tricine SDS-PAGE gel.

15.2 ISOLATION OF LIPOPOLYSACCHARIDE FROM INTRACELLULAR BACTERIA

Bacteria recovered from the extracellular or intracellular environment were collected by centrifugation and resuspended in 100µl of LPS lysis buffer. Samples were boiled for 10 minutes then cooled on ice. One milligram of proteinase K was added and samples were incubated at 60°C for 1 hour. LPS samples were boiled an additional 5 minutes, and 5µl of sample was loaded onto a 12% tricine SDS-PAGE gel. Extracellular samples were diluted 1:20 in LPS lysis buffer before loading.

15.3 SILVER STAINING OF LIPOPOLYSACCHARIDE SAMPLES

Silver staining of LPS samples was performed as described by Tsai and Frasch (133). After electrophoresis, gels were fixed in isopropanol fixative (40% isopropanol, 5% glacial acetic acid) for 1 hour or up to overnight. After fixation, gels were soaked in 0.7% periodic acid (made in isopropanol fixative), for 15 minutes, then washed three times in Milli-Q purified H_2O. Gels were then soaked for 10 minutes in 20% silver nitrate, and washed three times with Milli-Q purified H_2O. After washing, LPS was visualized by soaking gels in developing solution (0.0185% v/v formaldehyde, 50µg/ml citric acid). Development was stopped by washing gels repeatedly in Milli-Q purified H_2O.

15.4 IMMUNOBLOTTING OF LIPOPOLYSACCHARIDE SAMPLES

After electrophoresis, LPS samples were transferred from the gel to a 0.2μM pore-sized nitrocellulose membrane (GE) at 100 mA for 2 hours. To visualize total LPS, membranes were probed with rabbit group B antisera (Difco) for 2 hours, followed by a one-hour incubation with goat anti rabbit HRP conjugated secondary antibody (BioRad). *S. flexneri* LPS core was detected by probing membranes with the mouse antibody MASF-2a (19) for 18 hours, followed by a 90 minute incubation with goat anti-mouse HRP conjugated secondary antibody (BioRad). Signal was detected using the Pierce ECL detection kit (Thermo-Forma Scientific).

16. Glycogen staining

Glycogen staining was performed as described in Romeo *et al*. (110). Strains were streaked onto Kornberg agar (1.1% dibasic potassium phosphate, 0.85% monobasic potassium phosphate, 0.6% yeast extract) supplemented with 1% glucose, and incubated overnight at 37°C. Plates were then inverted over iodine crystals for 15-30 seconds to stain internal glycogen with iodine vapor.

17. BioLog phenotype microarrays

To examine differences in carbon source utilization, BioLog phenotype microarrays (BioLog, Hayward, CA) were performed. Colonies were harvested from TSB agar plates without Congo red and resuspended in 1 ml saline, then diluted to a final concentration of 10^9 cfu per ml in saline. The cell suspension was next diluted to 10^7 cfu per ml in inoculating fluid (BioLog) supplemented with 2μg/ml nicotinic acid. Each well of the phenotype microarrays was inoculated with 10^6 cfu and incubated at 37°C for 24 hours. The absorbance at wavelength of 595 was recorded every 2 hours using an Opsys MR plate reader (Dynex, Chantilly, VA).

18. Detergent sensitivity

Bacteria were inoculated into LB broth and grown to exponential phase at 37°C with aeration. The equivalent of an absorbance unit at 650 nm of 1 (approximately $8x10^8$ cells) was centrifuged at 16,300 xg for 5 minutes, and resuspended in 1 ml of 25 mM Tris-Cl (pH 7.5) to a final A_{650} of 1.0. After an initial absorbance reading (T_0), sodium dodecyl sulfate (SDS) was added at a final concentration of 0.1% to one set of samples per strain. Samples were incubated at 37°C without aeration. Bacterial lysis was recorded as the ratio of absorbance at each time point (T_n) versus the absorbance at time zero (T_0), and expressed as a percentage (% relative A_{650}).

III. RESULTS

1. Role of metabolic regulators in *S. flexneri* pathogenesis

During the course of infection, *S. flexneri* is faced with several diverse and dynamic environments. To successfully establish infection, the invading bacterium must adapt to these environments to avoid clearance and proliferate within the host. Several global regulators mediate the adaptation to variations in carbon source. To examine the role of carbon metabolism in *S. flexneri* pathogenesis, mutants were constructed in the major carbon flux regulators cAMP-CRP, CsrA and Cra. These regulators were chosen based on their documented role in *E. coli* carbon metabolism, colonization and persistence in the host. The metabolic regulators Cra and CsrA control several processes in central metabolism, but overlap with respect to regulation of glycolysis and gluconeogenesis (Fig. 11). Because of the strong genetic similarity between *S. flexneri* and *E. coli*, it is likely these regulators have similar functions in these two species. The constructed mutants were assayed for defects in *S. flexneri* pathogenesis using cell culture models.

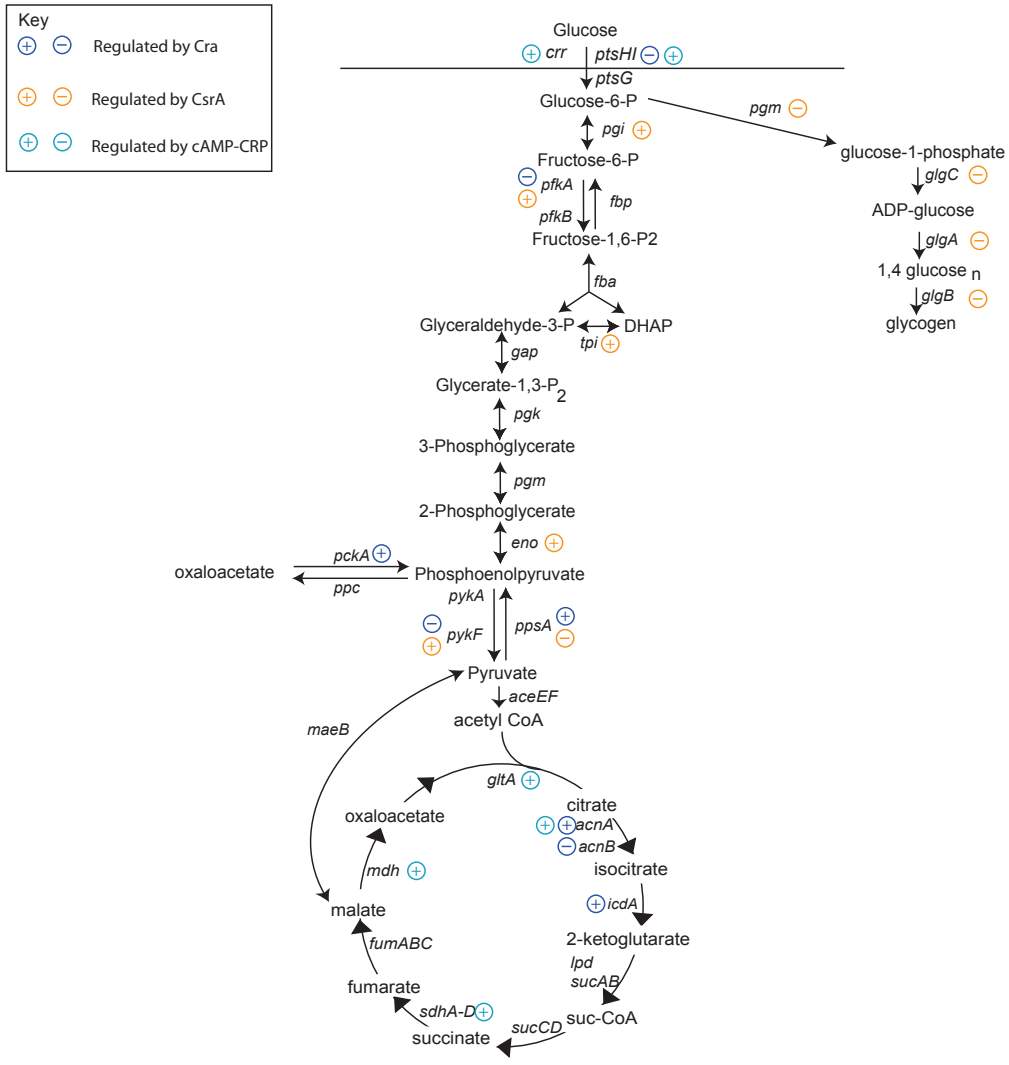

Figure 11: Regulation of central carbon metabolism by CsrA, Cra and cAMP-CRP.

The metabolic regulators CsrA, Cra and cAMP-CRP modulate central carbon metabolism by regulating expression of key genes in the glycolytic and gluconeogenic pathways. Figure modified from Sabnis *et al*. (112).

1.1 GROWTH AND VIRULENCE PROPERTIES OF THE *CRP* AND *CYAA* MUTANTS

Catabolite regulation is mediated in part by the cAMP-CRP transcriptional regulator. To study the role of cAMP-CRP in *S. flexneri* pathogenesis, mutations were constructed in both *crp* and *cyaA* (encoding by adenylate cyclase). The *crp* and *cyaA* mutations were transduced from *E. coli* strains JW5702 and JW3778, respectively, into wild type *S. flexneri* 2457T.

In *E. coli*, the absence of the cAMP-CRP complex results in slower growth rate (25). To test this in *S. flexneri*, the growth characteristics of the *crp* and *cyaA* mutants were examined. Strains were grown in LB broth, and cell growth was monitored by reading the optical density of the cultures at regular intervals. In comparison to wild type, the *crp* mutant demonstrated a modest reduction in growth rate (Fig. 12A). The *cyaA* mutant, however, was significantly impaired in growth (Fig. 12B). Both mutants were able to recover to wild type cell density by 24 hours, but this recovery may be due to suppressors, as cAMP-CRP is a pleiotropic regulator necessary for several cellular functions.

Glucose uptake via the phosphotransferase system inhibits adenylate cyclase activity, thereby preventing formation of a functional cAMP-CRP regulator (Fig. 6). Therefore, exogenous glucose may increase the growth rate of the *crp* and *cyaA* mutants, as production of the cAMP-CRP regulator should be reduced under these conditions. To test this hypothesis, the *crp* and *cyaA* mutants were grown in LB broth supplemented with 0.2% glucose and growth was monitored. The addition of glucose modestly stimulated growth of the *crp* mutant (Fig. 12A), but did not restore growth of the *cyaA* mutant (Fig. 12B). The inability of the *cyaA* mutant to grow in the presence of glucose suggests there is an essential role of cAMP in the cell, and that this role may be independent of the CRP receptor protein.

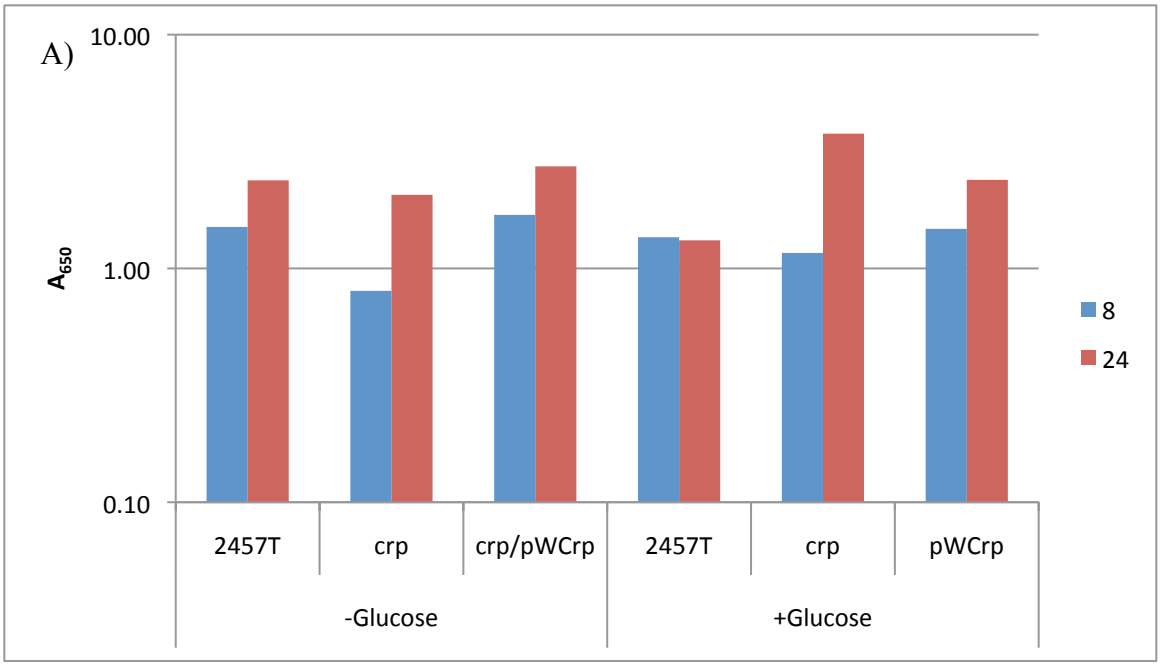
A)
10.00
1.00
0.10
A_{650}
2457T
crp
crp/pWCrp
2457T
crp
pWCrp
-Glucose
+Glucose
8
24

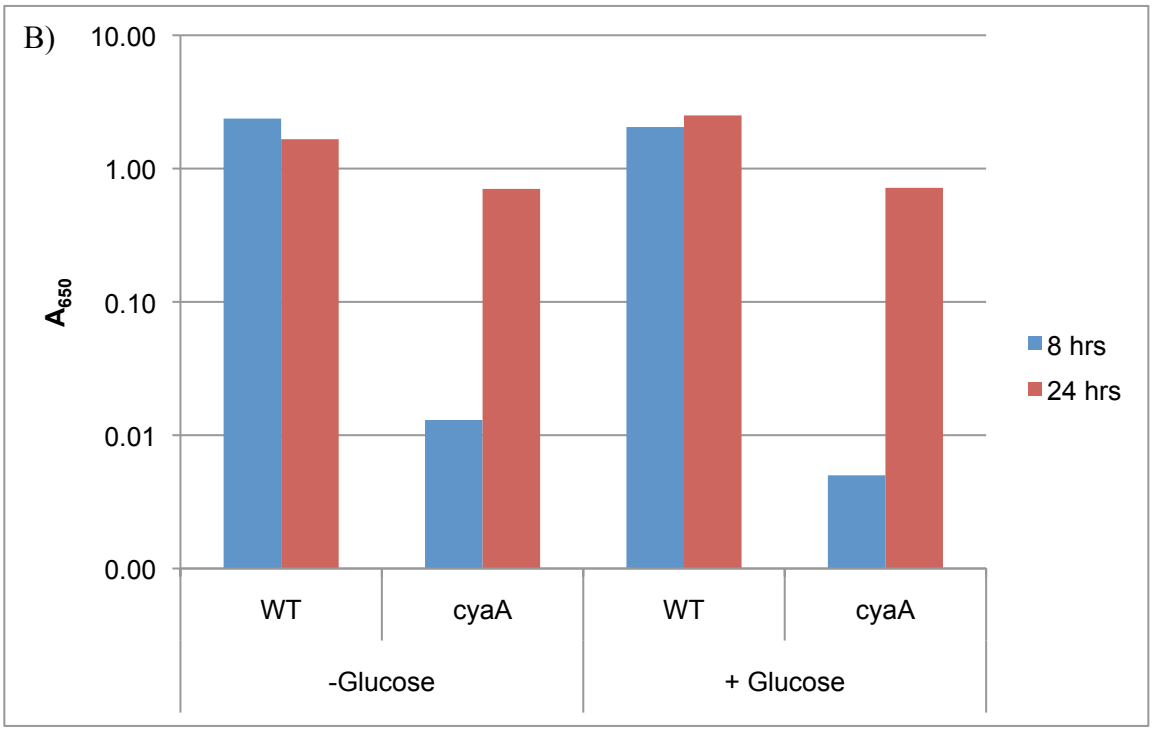
B)
10.00
1.00
0.10
0.01
0.00
A_{650}
WT
cyaA
WT
cyaA
-Glucose
+ Glucose
8 hrs
24 hrs

Figure 12: cAMP-CRP is not essential for growth in rich media.

Several colonies from a TSBA-CR plate were used to inoculate LB broth, and cultures were grown overnight with aeration at 30°C. Overnight cultures were then subcultured to an A_{650} equal to 0.02 into fresh LB-broth with or without 0.2% glucose, and grown at 37°C with aeration. Ampicillin was added to maintain the plasmid pWCrp where indicated. Growth was monitored by reading the optical density of the culture at 650 nm (A_{650}) at 8 and 24 hours after inoculation. (A) End-point growth analysis of wild type (WT, 2457T), *crp* mutant (AGS170) and *crp* mutant carrying the complementing plasmid pWCrp. (B) End-point growth analysis of the *cyaA* mutant (AGS180). Data shown is a representative experiment.

When grown on TSB agar plates supplemented with 0.01% Congo red, wild type *S. flexneri* binds the dye forming characteristic red colonies. The ability to bind Congo red is an indirect indicator of invasive ability, as strains defective in Congo red binding are avirulent (98). The *crp* mutant, however, grew as smaller colonies and bound less dye, resulting in a characteristic pink-white color. Similarly, the *cyaA* mutant, which is defective in cAMP production, also bound less Congo red, forming smaller, pink-white colonies on TSB agar. The small colonies formed by the mutants were consistent with the growth phenotype in LB broth.

To examine the role of cAMP-CRP in *S. flexneri* pathogenesis, a cell culture invasion assay was used. As indicated by their Congo red binding defects, both the *cyaA* and *crp* mutants were less invasive than wild type. The *crp* mutant invaded at 20% of the wild type level, and invasion was restored by expression of *crp* from a plasmid (Fig. 13). In comparison, the *cyaA* mutant was noninvasive. The decreased invasion in both strains suggests that cAMP-CRP is a regulator of *S. flexneri* pathogenesis, though the mechanism by which cAMP-CRP influences pathogenesis is unclear. It is likely that the virulence defects are due to one of the pleiotropic effects of this regulator on cellular metabolism and physiology rather than a direct effect of cAMP-CRP on virulence gene expression.

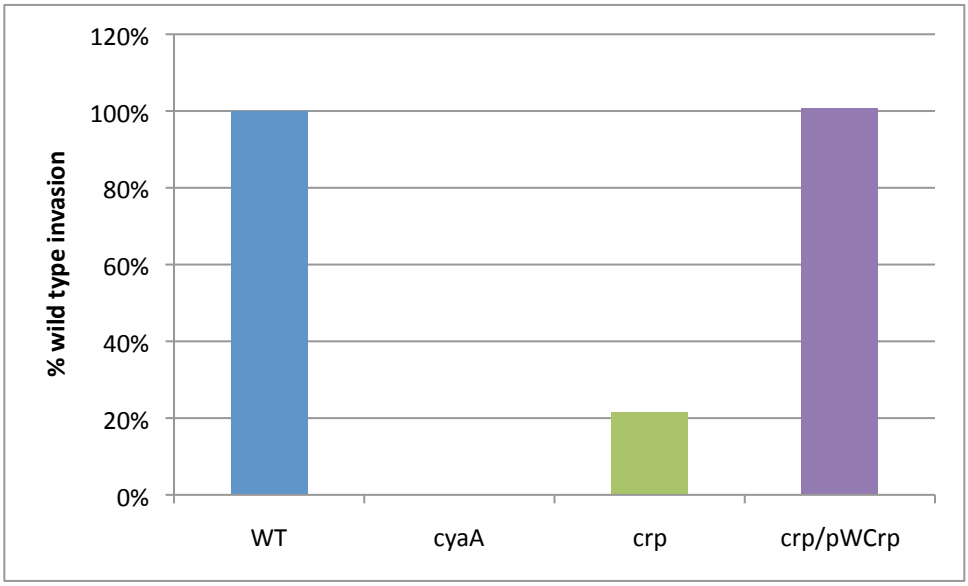

Figure 13: Decreased invasion by the *crp* and *cyaA* mutants.

Wild type (2457T), *cyaA* (AGS180), *crp* (AGS190) and the *crp* complement (crp/pWCrp) were added to a subconfluent monolayer of Henle cells and allowed to invade for 1.25 hours before staining and enumeration. A Henle cell was considered invaded if it contained 3+ intracellular bacteria. At least 300 epithelial cells were counted. The invasion percentage of the *cyaA* mutant, the crp mutant and the *crp* complement (*crp*/pWCrp) were normalized to the invasion efficiency of the wild type (2457T). Data shown is a representative experiment.

1.2 CHARACTERIZATION OF THE *CRA* MUTANT

As the bacterium transits through the host, *S. flexneri* likely relies on metabolic regulators to adapt to changing environmental conditions. In addition to its role in catabolite repression (Fig. 11), the metabolic regulator Cra is required for persistence of EHEC in vivo (68). To examine if Cra is also important for *S. flexneri* pathogenesis, the mutant *cra* allele in JW0078 was transduced into wild type *S. flexneri* 2457T.

1.2.1 Growth and BioLog phenotypic microarray

The in vitro growth properties of the *S. flexneri cra* mutant were examined first, as this protein likely has similar roles in both species. An *E. coli cra* mutant is unable to grow with gluconeogenic substrates as the sole carbon source (113). As predicted, the *S. flexneri cra* mutant did not grow in minimal media when the gluconeogenic carbon source lactate was the sole carbon source (Fig. 14B). Furthermore, this mutant had a slight growth defect versus the wild type strain when grown in LB broth (Fig. 14A).

BioLog phenotype microarrays were performed to assess differences in carbon source utilization of the *cra* mutant versus the wild type strain (Table 5). This assay relies on cellular respiration as an indicator of the bacterium's ability to use a provided substrate, as active respiration leads to reduction of a tetrazolium dye. At 24 hours, the *cra* mutant had reduced absorbance readings on several gluconeogenic carbon sources, indicative of reduced utilization of these substrates (Table 5). In agreement with previously published data in *E. coli*, the *S. flexneri cra* mutant was better able to utilize mannose, glucose-6-phosphate, fructose and glucose (108). Increased consumption of these carbon sources is likely due to derepression of glycolytic gene expression in the absence of Cra. There were some discrepancies between the previously published *E. coli* data and the data gathered from the *S. flexneri cra* mutant. This may be due to differences in data collection methods, as the *E. coli* studies relied on visual scoring

versus absorbance readings (108), or could be due to differences between *E. coli* and *S. flexneri*.

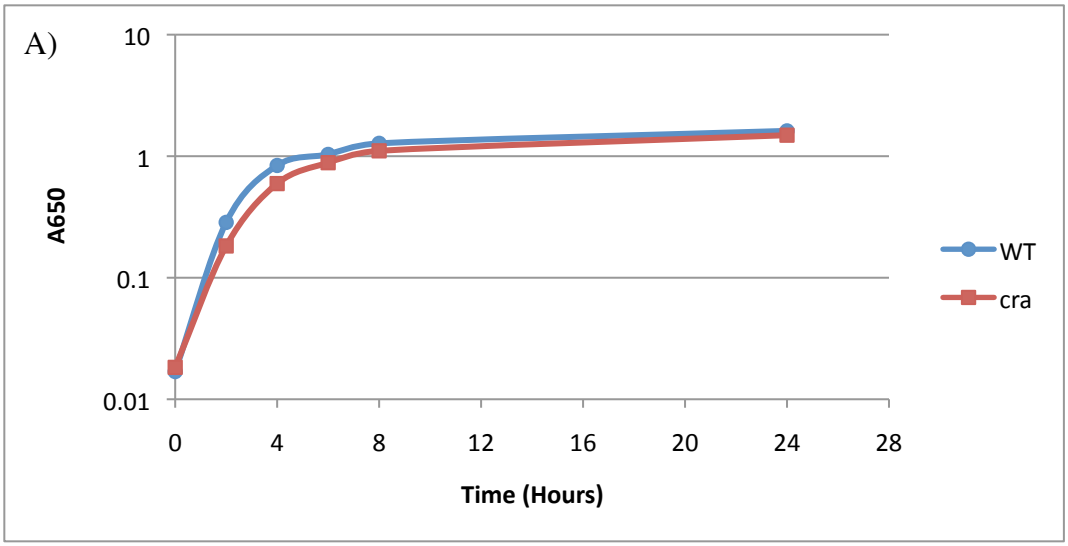

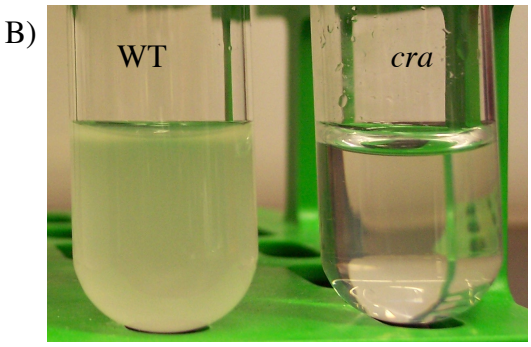

Figure 14: Growth phenotypes of the *cra* mutant

(A) The *cra* mutant has a slight growth defect in rich media. Strains were grown overnight in LB broth at 30°C, and subcultured to an A_{650} equal to 0.02 in 8 ml LB broth. Strains were grown at 37°C with aeration, and growth was monitored by reading the optical density (A_{650}) at 2 hour intervals.

(B) The *cra* mutant is unable to utilize gluconeogenic carbon sources for growth. Cultures were grown overnight at 30°C, and diluted 1:100 into MM9 with 0.2% lactate. Photograph was taken after 16 hours growth at 30°C.

Table 5: BioLog phenotype microarray of 2457T (wild type) versus *cra* (AGS190)

[a]: data from Ramseier *et al*. (108). Legend: -, no color; ±, faint color; + , strong color; ++ very strong color. Differences of at least two-fold are shown in bold.

Carbon Source	Substrate type	*S. flexneri*		*E. coli*[a]	
		wild type	*cra*	wild type	*cra*
Negative Control	negative control	0.08	0.06		
L-Aspartic Acid	amino acid	0.57	0.34		
D-Alanine	**amino acid**	**0.7**	**0.07**	++	-
L-Asparagine	**amino acid**	**0.55**	**0.17**	+	±
L-Serine	amino acid	0.64	0.45		
L-Threonine	**amino acid**	**0.34**	**0.09**		
L-Alanine	**amino acid**	**0.81**	**0.16**		
Ala-Gly	**amino acid**	**0.75**	**0.29**		
Succinic Acid	carboxylic acid	0.52	0.36		
D-Glucuronic Acid	**carboxylic acid**	**1.19**	**0.8**		
D-Gluconic Acid	carboxylic acid	0.21	0.14	++	++
L-Lactic Acid	**carboxylic acid**	**1.42**	**0.49**		
D,L-Malic Acid	carboxylic acid	0.67	0.43		
a-Ketoglutaric Acid	**carboxylic acid**	**0.21**	**0.10**		
Fumaric Acid	carboxylic acid	0.62	0.37	+	-
L-Malic Acid	carboxylic acid	0.68	0.37		
Pyruvic Acid	carboxylic acid	0.6	0.74		

D-Galacturonic Acid	carboxylic acid	1.82	1.4	+	+
Methylpyruvate	ester	0.71	0.49		
L-Arabinose	**carbohydrate**	**0.66**	**0.07**		
N-Acetyl-D-Glucosamine	carbohydrate	0.8	0.91	++	++
D-Galactose	carbohydrate	0.97	0.54	++	++
D-Mannose	carbohydrate	0.8	1.05	±	++
Glycerol	**carbohydrate**	**1.09**	**0.49**		
D,L-a-Glycerol Phosphate	carbohydrate	0.79	0.79	++	±
D-Mannitol	carbohydrate	0.9	1.02	+	++
D-Glucose-6-Phosphate	carbohydrate	1.5	1.47	+	++
D-Ribose	carbohydrate	0.11	0.06		
D-Fructose	carbohydrate	0.84	0.67	+	++
a-D-Glucose	carbohydrate	0.65	0.95	+	++
D-Melibiose	**carbohydrate**	**0.97**	**0.12**		
Thymidine	carbohydrate	1.28	1.12	++	++
a-Methyl-D-Galactoside	**carbohydrate**	**0.54**	**0.09**	**++**	**-**
Uridine	**carbohydrate**	**0.75**	**0.34**	**++**	**++**
D-Glucose-1-Phosphate	carbohydrate	1.33	1.29	++	++
D-Fructose-6-Phosphate	carbohydrate	1.36	1.4	++	++
2'-Deoxyadenosine	carbohydrate	1.03	1.34	++	++
Adenosine	carbohydrate	0.63	1.09	++	++
Inosine	carbohydrate	1.42	1.27	++	++

1.2.2 Virulence properties of the *cra* mutant

The *S. flexneri cra* mutant was assessed for its role in invasion and intracellular spread in a cell culture invasion assay. In this assay, the *cra* mutant was approximately 30% more invasive than wild type and demonstrated an increase in the number of intracellular bacteria 1.5 hours post-invasion (Fig. 15). Based on this phenotype, it was proposed that the absence of *cra* increased *S. flexneri* adherence or increased the rate of intracellular replication. However, both the brevity of the invasion assay and the in vitro growth phenotype of the mutant argued that the increased invasion was more likely due to an increase in attachment to host cells. In agreement with this hypothesis, the *cra* mutant was approximately 7-fold more adherent than wild type (Fig. 16).

The role of *cra* in plaque formation was also examined, as metabolic regulation may be needed for survival in the host cytosol. Although the *cra* formed approximately the same numbers of plaques as the wild type, the plaques formed by the mutant were generally smaller and more turbid (Fig. 17A). The turbidity of the plaques was suggestive of incomplete lysis of the monolayer.

Because plaque formation is a multistep process, both intracellular replication and intercellular spread were assayed. To rule out differences in intercellular spread as a primary cause of defective plaque formation, IcsA localization was examined. Cultures were grown as in the invasion assay, and immunostained with anti-IcsA antibody, and labeled with FITC secondary antibody. IcsA localization was then detected by immunofluorescence microscopy. When grown in vitro, there was no obvious difference in the polar localization of IcsA in the *cra* mutant versus the wild type strain (Fig. 17B), arguing against defects in actin-based motility.

The intracellular replication of the *cra* mutant was also examined, as failure to replicate within the host cell could lead to defects in plaque formation. To determine intracellular replication, the invasion assay was done as described in methods, reducing the number of *cra* mutant bacteria added by a factor of 5 to compensate for the increased

invasion of this strain. The number of intracellular bacteria was determined over time by counting bacteria per Henle cell by microscopy and by plating. Within a subconfluent monolayer of epithelial cells, the *cra* mutant did not demonstrate any discernable difference in replication compared to the wild type (data not shown).

The above data argue against intracellular replication defects as a cause of aberrant plaque formation by the *cra* mutant. However, the morphology of the *cra* mutant within the host cell was examined, as the plaque defect may be caused by failure of the *cra* mutant to escape to the host cytosol, or other abnormalities of the mutant within the intracellular environment. Microscopic analysis of the *cra* mutant within a confluent monolayer of Henle cells revealed the presence of several bacteria within vacuoles in comparison to the wild type (Fig. 17C). These anomalies may be representative of inefficiencies or intracellular defects of the *cra* mutant that could account for the aberrant plaque morphology.

A)

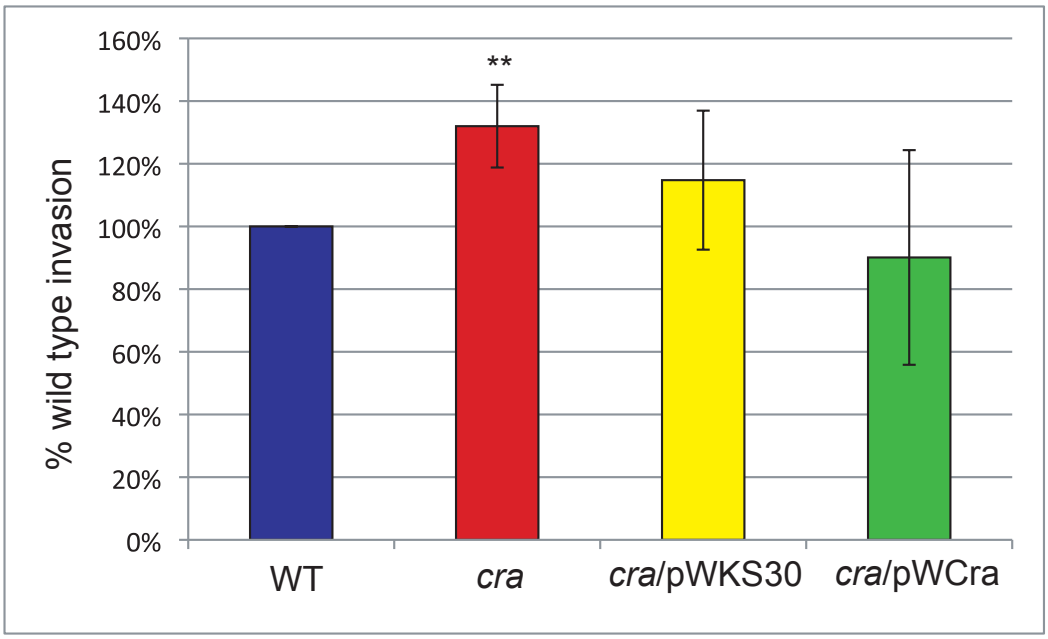
160%
140%
120%
100%
80%
60%
40%
20%
0%
% wild type invasion
**
WT
cra
cra/pWKS30
cra/pWCra

B)

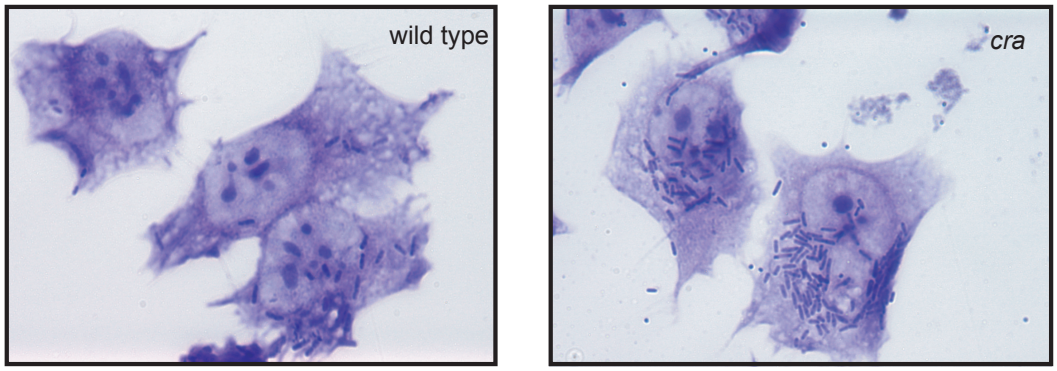
wild type
cra

Figure 15: Cra inhibits *S. flexneri* invasion.

A) *S. flexneri* invasion increases 30% in the absence of *cra*. The invasion percentages of the *cra* mutant and complements were normalized to that of the parental strain 2457T (wild type). The *cra* mutant was complemented by expression of *S. flexneri cra* from the low-copy vector pWKS30. Data shown is the average of three independent experiments, and error bars represent standard deviation. The relative invasion of the mutant and wild type were compared using an unpaired student's T-test. ** represents a P-value < 0.01. B) The increased invasion of the *cra* mutant correlates with an increase in the number of cytosolic bacteria.

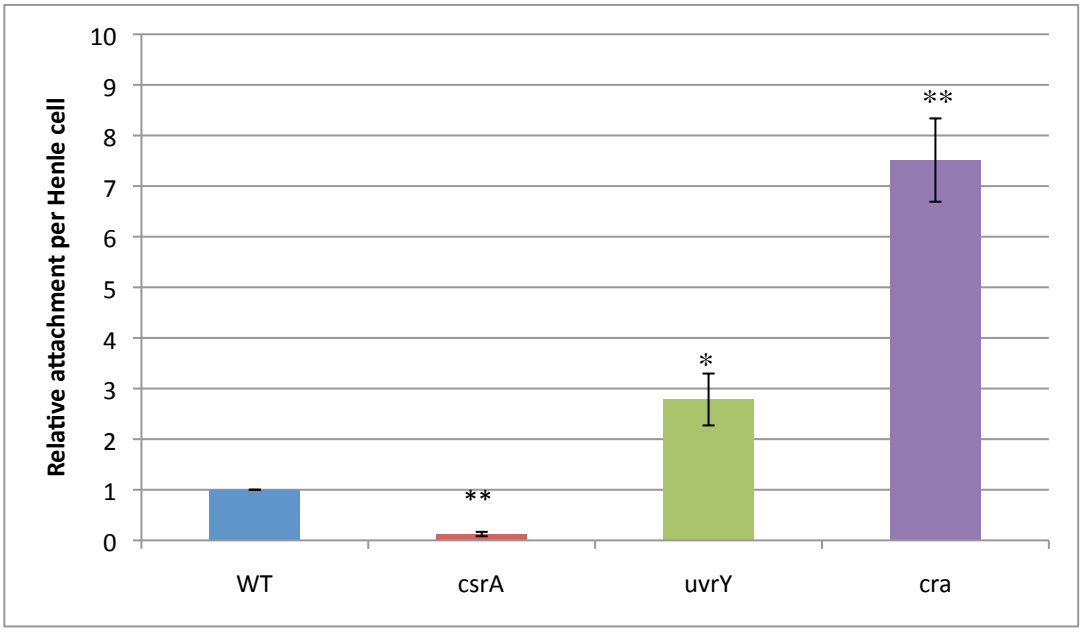

Figure 16: *S. flexneri* attachment to eukaryotic cells is affected by CsrA and Cra

The total number of bacteria attached to 100 Henle cells was counted by microscopy for each strain. Values shown are the average of three independent experiments, and are normalized against the wild type within each experiment. Error bars represent standard deviation. Unpaired student's T-test was used to compare the relative attachment of the mutant strains to the wild type. * denotes a *P*-value <0.05, ** denotes a *P*-value <0.01.

A)

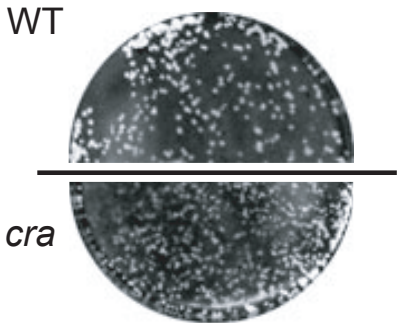

B)

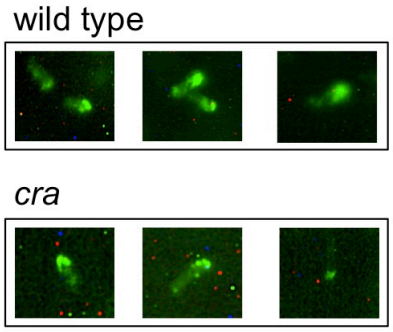

C)

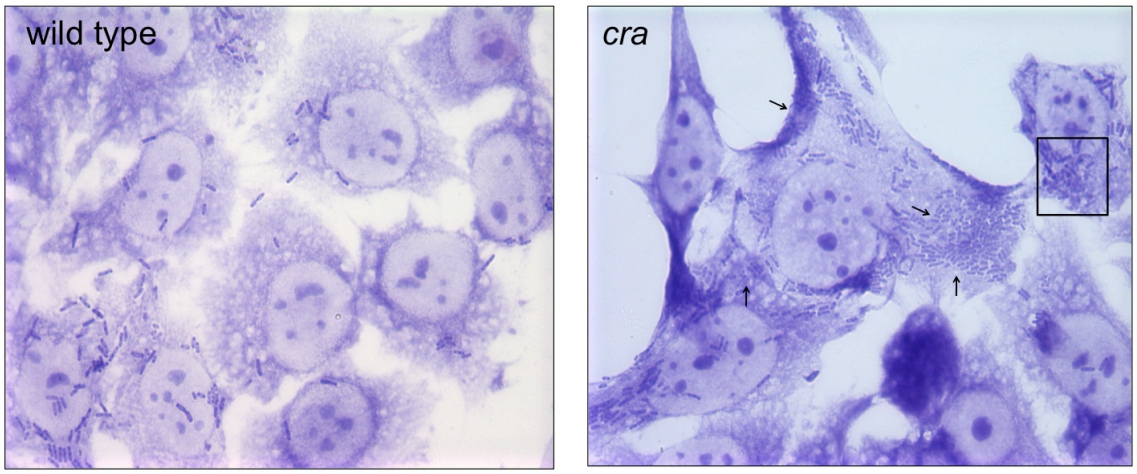

Figure 17: The *cra* mutant has an altered morphology inside the epithelial cell.

(A) The *cra* mutant forms turbid plaques in comparison to wild type (WT). Cultures were inoculated and grown as in the invasion assay. Approximately equal numbers of cells ($2x10^8$ cells) were used to inoculate a confluent monolayer of Henle cells. Bacteria were spun onto the monolayer for 10 minutes, then allowed to invade for 45 minutes. Monolayers were then overlayed with media containing gentamycin, and incubated for an additional 48 hours prior to washing and staining.
(B) IcsA localization in the *cra* mutant. Strains were grown to exponential phase in LB broth, and fixed and immunostained with anti-IcsA (VirG) antibody, followed by labeling with FITC secondary antibody. Signal was detected by fluorescence microscopy. There was no discernable difference in polar localization of this protein in the wild type and mutant strain.
(C) Unique morphology of *cra* mutant within Henle cell. Strains were grown and inoculated in a confluent monolayer of epithelial cells as outlined in (A). After a 90 minute incubation, monolayers were washed and stained. Box: microcolonies; Arrows: vacuolar bacteria.

1.3 CHARACTERIZATION OF THE ROLE OF CSRA IN *S. FLEXNERI*

The phenotype of the *S. flexneri cra* mutant suggests that disruptions in carbon metabolism affect both invasion and plaque formation. Because Cra and CsrA exert opposing effects on carbon metabolism (Fig. 11), it was predicted that disruption of *csrA* in *S. flexneri* would inhibit invasion. To examine if *csrA* is also important for *S. flexneri* pathogenesis, an *S. flexneri csrA* mutant was constructed and tested in the cell culture assays.

1.3.1 Growth and metabolic properties of the *csrA* mutant

The role of CsrA in *S. flexneri* had not been empirically assessed. To determine if CsrA has similar roles in *E. coli* and *S. flexneri*, the in vitro growth properties of the *S. flexneri csrA* mutant were examined. In LB broth there was no obvious growth difference between the *S. flexneri* wild type and *csrA* mutant strains, a phenotype also noted with the *E. coli csrA* mutant (110). A defining characteristic of *E. coli csrA* mutants is an increase in internal glycogen stores (146). The *csrA* mutant has the same effect on glycogen metabolism in *S. flexneri* (Fig. 18), indicating that CsrA represses glycogen metabolism in both *E. coli* and *S. flexneri*.

In the BioLog phenotype microarrays, the *csrA* mutant was better able to utilize adenosine and 2-deoxyadenosine, and also showed increased consumption of the gluconeogenic carbon sources pyruvate, fumarate and bromosuccinate. The *csrA* mutant characteristically was less able to metabolize several glycolytic carbon sources (Table 6), which is consistent with the role of this protein in activation of glycolytic gene expression. However, the reduction in glycolytic carbon source utilization did not apply to all glycolytic carbon sources examined, including mannose, fructose and glucose (Table A1). This inconsistency may be due to residual activity of the *csrA*::Kn allele (128).

Table 6: BioLog phenotype microarray of 2457T versus *csrA* (AGS120).

Differences of at least two-fold are shown in bold.

Carbon Source	Substrate Type	wild type	*csrA*
Negative Control	negative control	0.08	0.09
L-Arabinose	carbohydrate	0.66	0.45
N-Acetyl-D-Glucosamine	carbohydrate	0.8	0.68
Succinic Acid	carboxylic acid	0.52	0.66
D-Galactose	carbohydrate	0.97	0.82
D-Trehalose	carbohydrate	1.12	0.81
D-Sorbitol	carbohydrate	0.09	0.68
D-Glucuronic Acid	carboxylic acid	1.19	0.93
D-Gluconic Acid	**carboxylic acid**	**0.21**	**0.42**
D-Mannitol	carbohydrate	0.87	0.73
D-Glucose-6-Phosphate	carbohydrate	1.52	1.39
D-Ribose	**carbohydrate**	**0.11**	**0.4**
D-Fructose	carbohydrate	0.84	0.98
a-D-Glucose	carbohydrate	0.65	0.7
L-Asparagine	amino acid	0.55	0.78
a-Ketoglutaric Acid	carboxylic acid	0.21	0.41
Uridine	carbohydrate	0.75	0.52
D-Glucose-1-Phosphate	carbohydrate	1.33	1.24
D-Fructose-6-Phosphate	carbohydrate	1.36	1.28

2'-Deoxyadenosine	carbohydrate	1.03	1.5
Adenosine	carbohydrate	0.63	1.23
Gly-Asp	amino acid	0.42	0.53
Fumaric Acid	carboxylic acid	0.62	0.82
Bromosuccinic Acid	carboxylic acid	0.42	0.69
Gly-Glu	amino acid	0.43	0.26
L-Serine	amino acid	0.64	0.74
L-Threonine	amino acid	0.34	0.25
L-Alanine	amino acid	0.81	0.96
Ala-Gly	amino acid	0.75	0.92
Acetoacetic Acid	**carboxylic acid**	**0.09**	**0.21**
Mono-Methylsuccinate	carboxylic acid	0.17	0.3
Methylpyruvate	ester	0.71	0.8
L-Malic Acid	carboxylic acid	0.68	0.72
Pyruvic Acid	carboxylic acid	0.6	0.79

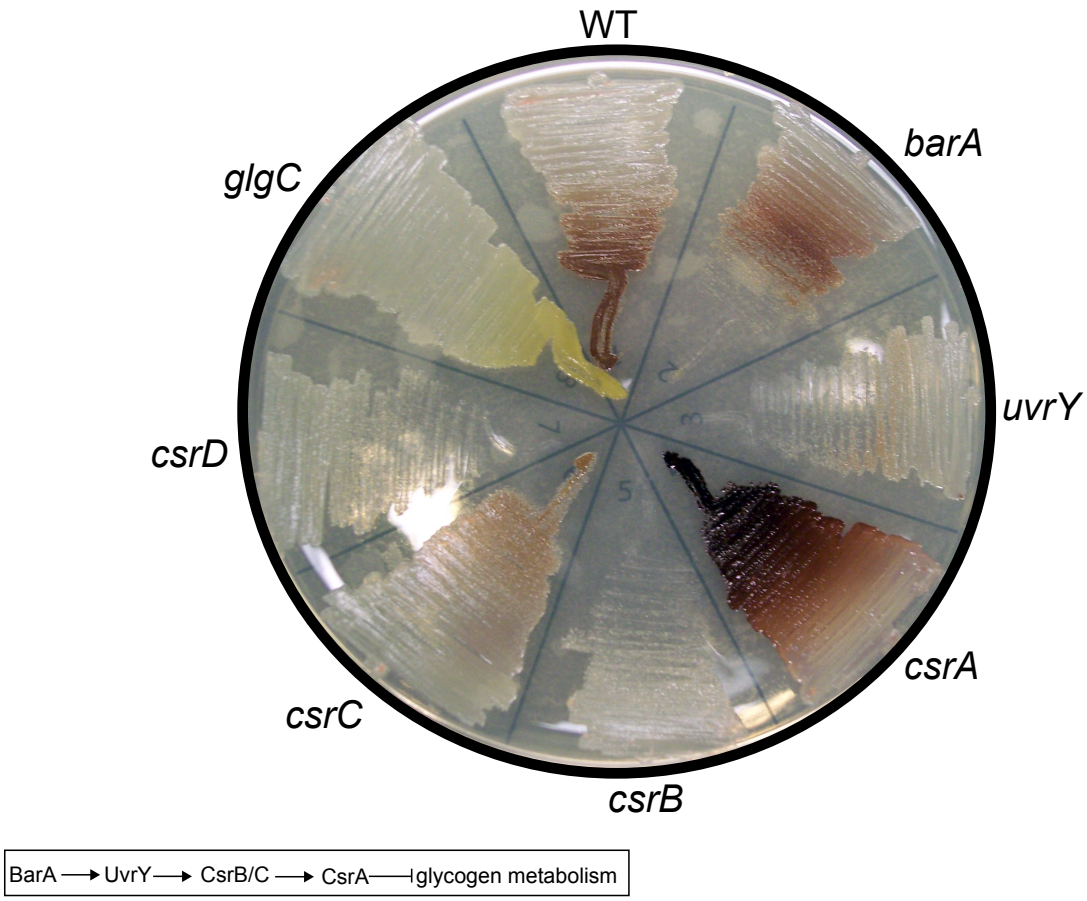

Figure 18: Glycogen accumulation in the Csr mutants.

Strains were streaked onto Kornberg agar containing 2% glucose and incubated overnight at 37°C. Internal glycogen stores were detected by staining with iodine vapor for 15 – 30 seconds. The intensity of staining is proportional to the level of internal glycogen. The *glgC* mutant, defective in glycogen production, was included as a negative control.

1.3.2 Virulence properties of the *csrA* mutant

Homologs of CsrA have multiple roles in pathogenesis (Table 1), and it has been proposed that this protein may coordinate physiological traits with progression through the virulence cycle (72). To determine if CsrA also regulates *S. flexneri* pathogenesis, the *S. flexneri csrA* mutant was tested for both invasion and plaque formation. When grown on TSB agar containing Congo red, the *S. flexneri csrA* mutant produced a mix of strongly and weakly pigmented colonies. Complementation of the *csrA* mutant using either the IPTG-inducible plasmid pQCsrA or the low-copy pWCsrA restored Congo red binding to near-wild type levels. This variation in Congo red binding may be due to variations in the level of CsrA activity in the mutant strain.

In comparison to wild type, the *csrA* mutant demonstrated a significant reduction in both attachment and invasion (Figs. 16, 19). Complementation of the *csrA* mutant with pWCsrA only restored invasion of the mutant to approximately 20% of the wild type level. Induction of *csrA* from the IPTG-inducible promoter in pQCsrA restored invasion to 50% of wild type (Fig. 19).

As expected from the defect in invasion, the *csrA* mutant formed fewer plaques than wild type. The plaques formed by this mutant were also characteristically smaller and more turbid than wild type, indicative of defects in intracellular replication or intercellular spread (Fig. 20). The defect in plaque formation may be due to misregulation of carbon metabolism of bacteria residing within the eukaryotic cytosol. Complementation of the *csrA* mutant in the plaque assay with pQCsrA increased the number plaques formed, but these plaques were still smaller and more turbid in comparison to wild type. This incomplete complementation may be due to inherent difficulties in maininting the plasmid within the host cell, or to more general inhibition of wild type CsrA dimers. Timmermans *et al*. (128) have shown residual activity of the *csrA::kn* allele, which is still able to dimerize and regulate mRNA stability. The difficulties in complemenation of the *S. flexneri csrA* mutant may, therefore, be due to the

formation of less functional complexes that interfere with formation and activity of wild type CsrA homodimers.

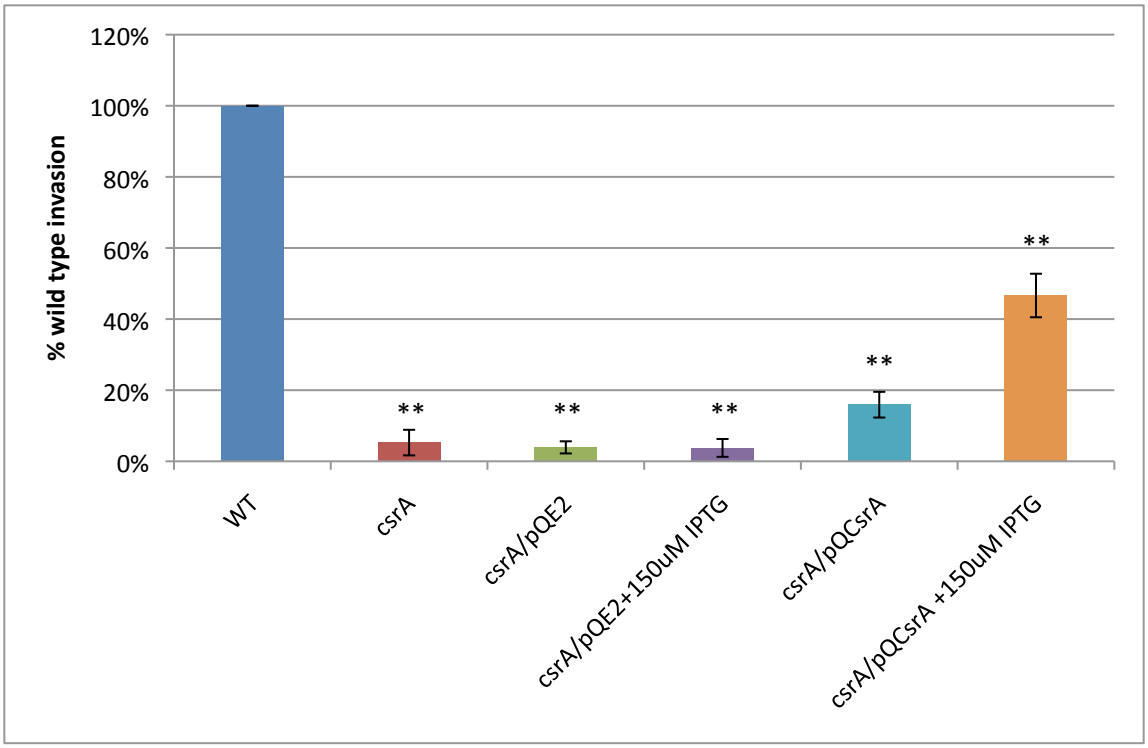

Figure 19: Invasion is significantly impaired in the *csrA* mutant.

The *csrA* mutant invaded at approximately 5% of the wild type level. In the presence of IPTG, expression of *csrA* from the plasmid pQCsrA restored invasion of the *csrA* mutant to approximately 50% of the wild type level. The vector pQE2 was included as a control. Invasion was normalized to the percent invasion of the wild type strain in each experiment. Data shown is the average of three independent experiments performed in triplicate. Error bars represent standard deviation. Samples were compared using an unpaired student's T-test. ** denotes a *P*-value <0.01.

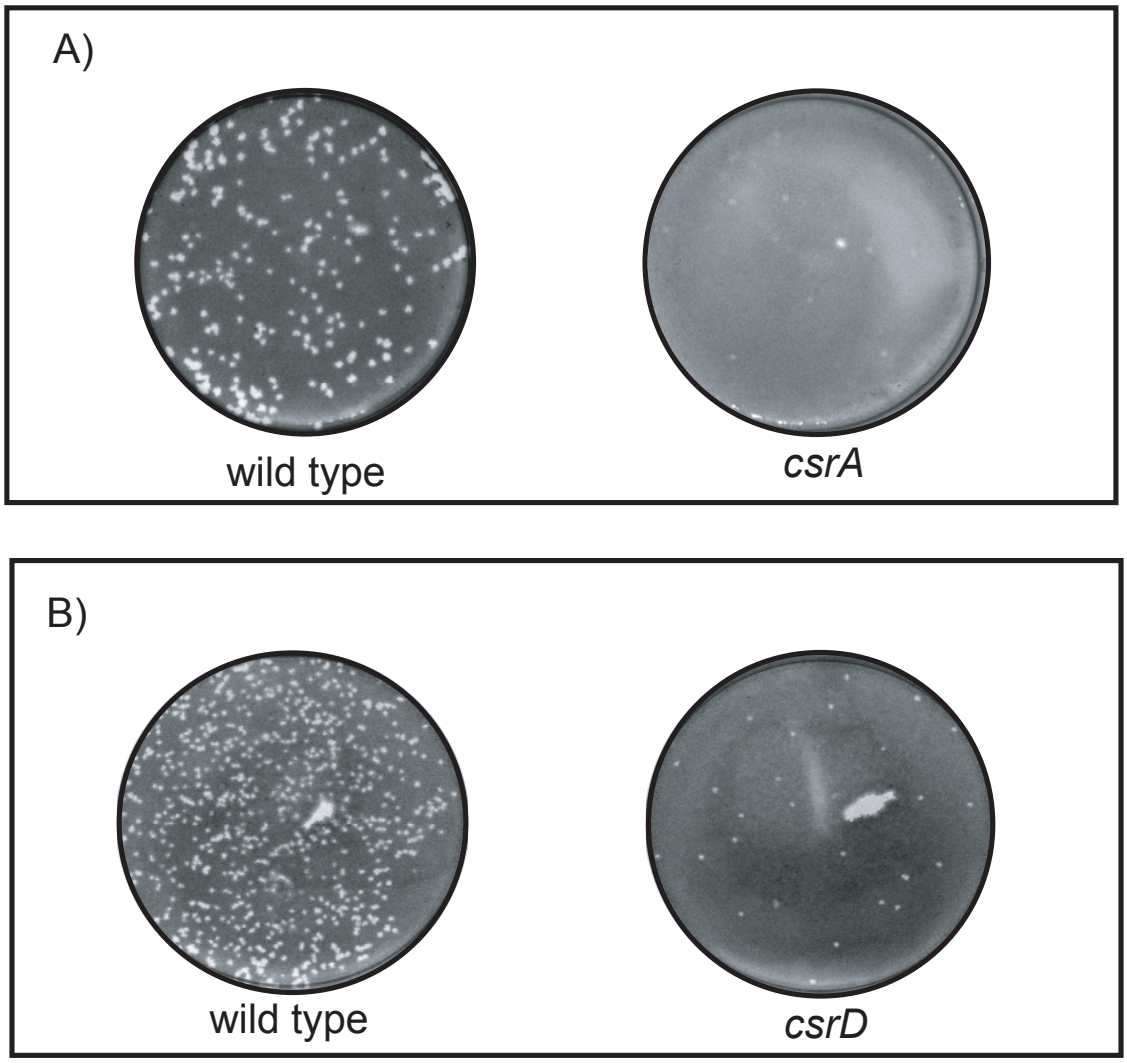

Figure 20: Decreases in free CsrA inhibit plaque formation.

A) Disruption of *csrA* decreases the number of plaques formed and the size and clarity of the plaques. Approximately 10^4 cells were added to a confluent monolayer of Henle cells, and monolayers were stained after 72 hours. B) The *csrD* mutant formed fewer plaques than wild type, but the plaques had wild type morphology. 10^5 cells were added to the confluent monolayer of Henle cells, and visualized after a 48-hour incubation.

1.3.3 Overexpression of *csrA* in *S. flexneri*

In *S.* Typhimurium, it has been shown that the level of CsrA must be carefully regulated, as both deletion and overexpression of *csrA* are inhibitory to invasion in vitro (4). Therefore, the effect of CsrA overexpression on *S. flexneri* invasion was also examined. Overexpression of *csrA* in *S. flexneri* from the IPTG-inducible plasmid pQCsrA significantly inhibited invasion (Fig. 21). This suggests that CsrA may have dual roles in *S. flexneri* pathogenesis, specifically as an inhibitor and activator of virulence properties. The inhibitory effect of CsrA overexpression on *S. flexneri* invasion may be due to disruptions in timing of CsrA expression, as this protein is characteristically expressed upon entry into stationary phase. Overexpression of *csrA* in wild type *S. flexneri* may therefore cause misregulation of genes necessary for efficient invasion.

1.4 CsrA REGULATORS AND *S. FLEXNERI* VIRULENCE

In *E. coli*, the level of free CsrA is governed by an autoregulatory loop that includes two antagonistic RNAs and the BarA-UvrY two component system (Fig. 9). Based on the phenotype of the *S. flexneri csrA* mutant, it was predicted that a reduction in the level of CsrA would inhibit invasion. Conversely, increased amounts of CsrA were predicted to increase invasion, as increased glycolysis correlated with increased invasion in the *cra* mutant (Fig. 15). To better understand the role of CsrA in *S. flexneri* pathogenesis, mutations were constructed in each of the known regulatory elements and tested in the cell culture invasion assay.

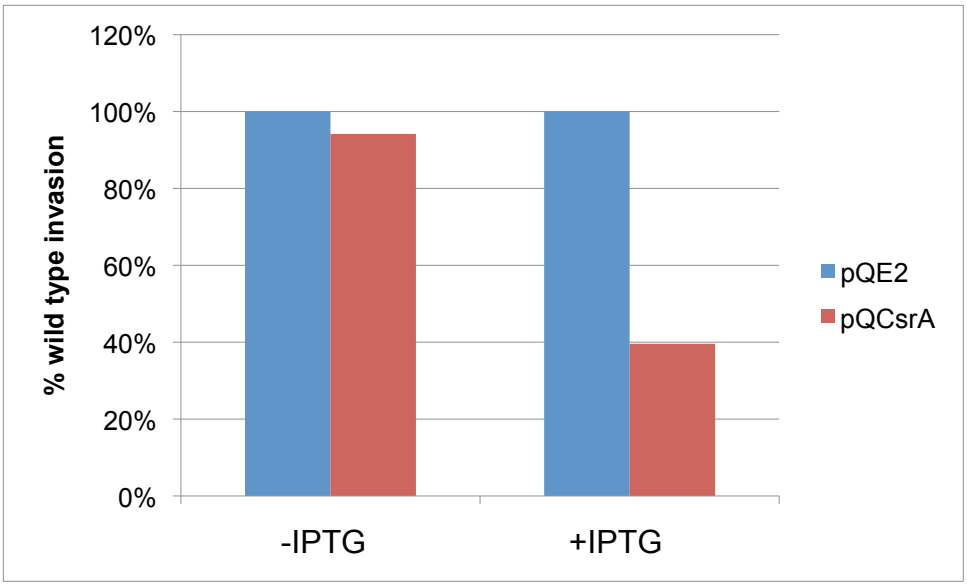

Figure 21: Overexpression of *csrA* in wild type *S. flexneri* inhibits invasion.

Wild type *S. flexneri* carrying the empty vector pQE2 or the IPTG-inducible *csrA* construct pQCsrA were tested in the invasion assay, and values are normalized to the wild type strain carrying the empty vector in the absence of IPTG. The addition of 200μM IPTG decreased invasion *S. flexneri* carrying pQCsrA to approximately 40% of the wild type level. Data shown are one representative experiment.

1.4.1 Overexpression of *csrB* and *csrC*

The ncRNAs CsrB and CsrC inhibit CsrA activity by binding to the protein, effectively sequestering it away from its targets. Because of the antagonistic roles of both ncRNAs, it was postulated that overexpression of either *csrB* or *csrC* would lead to a decrease in the level of CsrA protein, thereby inhibiting *S. flexneri* invasion. In agreement with this hypothesis, overexpression of *csrB* or *csrC* from the IPTG-inducible plasmids pQCsrB and pQCsrC respectively, decreased *S. flexneri* invasion to approximately 50% of *S. flexneri* carrying the empty vector (Fig. 22). This agrees with the model of CsrA regulation as outlined in *E. coli*, and further implicates CsrA as an important regulator of *S. flexneri* virulence.

1.4.2 Deletion of *csrB* and *csrC*

Based on the *E. coli* model of CsrA regulation, deletion of either *csrB* or *csrC* should alleviate CsrA repression (Fig. 9). This was confirmed for the *S. flexneri* mutants, as both the *csrB* and *csrC* mutants showed a decrease in internal glycogen stores when grown in high concentrations of glucose (Fig. 18). Both the *csrB* and *csrC* mutants were more invasive than wild type (Fig. 24). The relatively modest difference in invasion is likely due to compensatory increases in expression of one RNA in the absence of the other (143), but is consistent with the role of these ncRNAs in inhibition of CsrA activity. Despite the increases in invasion, there was no difference in plaque formation by either mutant. This may be due to expression patterns of the ncRNAs when the bacteria are growing within the epithelial cell or a consequence of the modest effects of each mutant on CsrA levels.

In *E. coli*, glucose activates *csrC* expression independently of the response-regulator UvrY, but has no effect on expression of *csrB* (59). To test if this phenomenon also occurs in *S. flexneri*, 0.2% glucose was added to cultures grown in LB broth prior to invasion. If glucose does stimulate *csrC* expression in *S. flexneri*, it should decrease the

level of free CsrA and inhibit invasion in the *csrB* mutant. When grown in the presence of glucose, the *csrB* mutant exhibited wild type levels of invasion (Fig. 23). The relative decrease in invasion efficiency in the presence of glucose agrees with increased expression of *csrC*. As predicted, the addition of glucose to the growth media had no discernable effects on the invasion efficiency of the *csrC* mutant (data not shown).

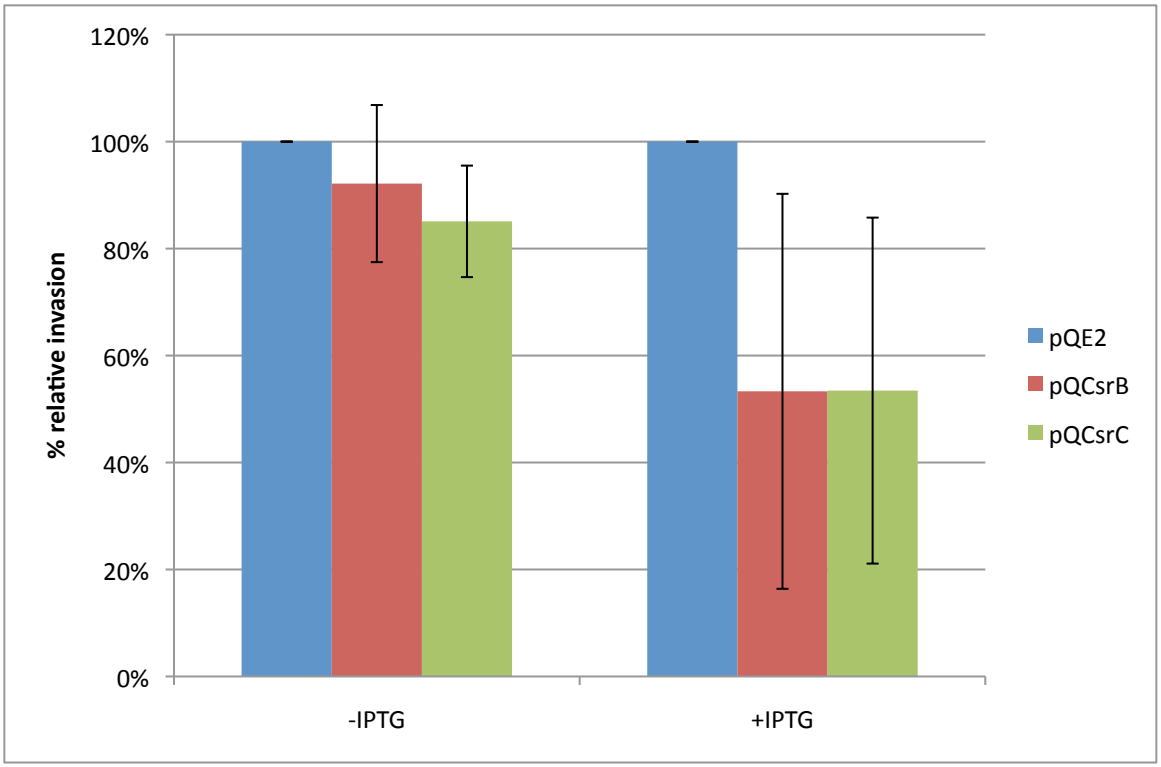

Figure 22: Overexpression of *csrB* or *csrC* inhibits invasion.

In the presence of 200μM IPTG, expression of *csrB* or *csrC* inhibits invasion. The inducer molecule IPTG was added 15 minutes prior to proceeded with the normal invasion assay, and was maintained in the media throughout the assay. Values shown are relative to the wild type invasion value under the same conditions. Data shown are the average of three independent experiments, and error bars represent standard deviation.

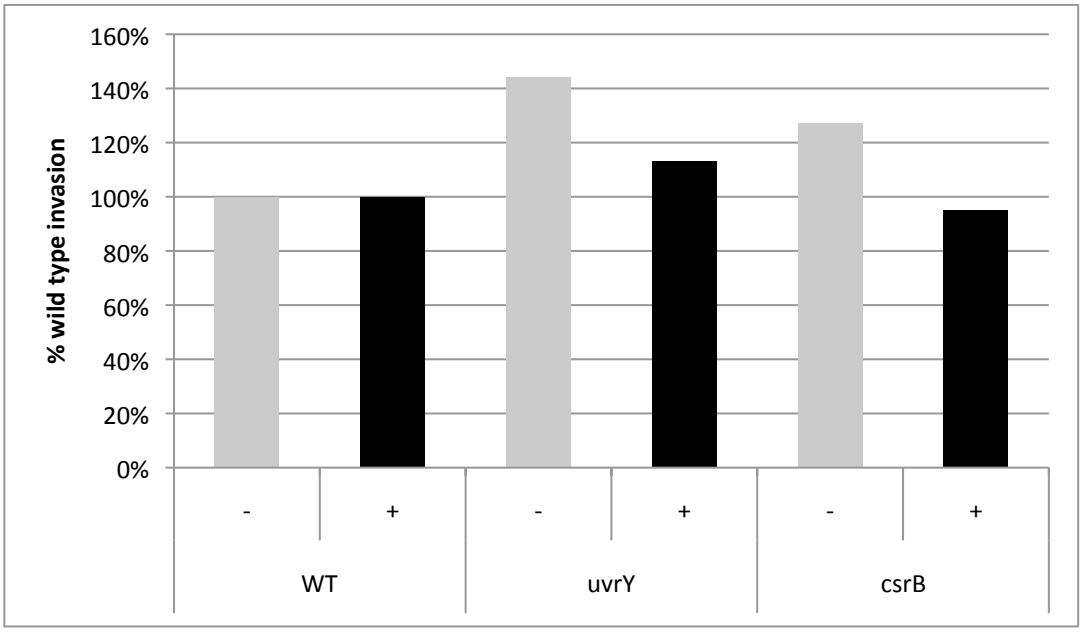

Figure 23: Glucose represses the invasion phenotype of the *csrB* and *uvrY* mutants.

Strains were grown in LB broth with (+) or without (-) 0.2% glucose to exponential phase prior to proceeding with the invasion assay. The invasion percentages shown have been normalized to the wild type invasion under the same conditions. Data shown are a representative experiment.

1.4.3 CsrD

The inner membrane protein CsrD stimulates turnover of both CsrB and CsrC. Thus, in the absence of this protein, both the *csrB* and *csrC* messages are more stable and the level of free CsrA decreases (59, 125). In the glycogen accumulation assay, the *csrD* mutant stained less intensely compared to wild type (Fig. 18). This phenotype is inconsistent with the regulatory model, which suggests that the absence of *csrD* should decrease the level of free CsrA, thereby increasing internal glycogen stores. As CsrD is a predicted inner membrane protein, the absence of this gene could alter membrane properties such that internal glycogen stores may not be detected by iodine staining.

The *csrD* mutant was defective in Congo red binding, a phenotype noted in the *csrA* mutant. As suggested by the defect in Congo red binding, the *csrD* mutant was approximately 60% less invasive than wild type (Fig. 24). The absence of *csrD* led to a 90% reduction in the number of plaques formed, but these plaques appeared normal (Fig. 20). The decrease in invasion and plaque number are consistent with CsrD acting as a regulator of CsrB and CsrC degradation.

1.4.4 UvrY

In response to phosphorylation by BarA, the response regulator UvrY activates expression of both *csrB* and *csrC*, which in turn inhibit CsrA activity (126). Therefore, the absence of *uvrY* should alleviate inhibition of CsrA, subsequently reducing glycogen accumulation and increasing *S. flexneri* invasion. As expected, the *S. flexneri uvrY* mutant had decreased glycogen stores relative to wild type (Fig. 18).

In the invasion assay, the *uvrY* mutant was 40% more invasive than wild type (Fig. 24), and this increase in invasion was coupled with an increase in the number of cytosolic bacteria. The increase in invasion by the *uvrY* mutant is likely due to a three-fold increase in attachment (Fig. 16). As was seen with the *csrB* mutant, the addition of glucose to the growth media blocked the invasion increase, presumably due to increased CsrA inhibition

by CsrC (Fig. 23). There was no phenotype of the *uvrY* mutant with respect to plaque formation. Normal plaque formation in this mutant may be due to the presence of glucose in the tissue culture media, which could induce *csrC* expression, thereby restoring function of the Csr modulon (59).

1.4.5 BarA

In response to an unknown stimuli, BarA autophosphorylates and transfers this phosphate group to its cognate response regulator UvrY. If the overall model of CsrA regulation is correct (Fig. 9), then disruption of *barA* in *S. flexneri* should lead to decreased activation of UvrY, subsequently decreasing expression of *csrB* and *csrC*, and alleviating CsrA repression. There was no discernable difference in iodine staining between the wild type and *barA* mutant when grown on Kornberg agar with glucose (Fig. 18). Deletion of *barA* did not affect *S. flexneri* invasion (Fig. 24) or plaque formation. The absence of a discernable phenotype may be due to promiscuous activation of the response regulator. In the *barA* mutant, the orphaned response regulator may be phosphorylated by another histidine kinase or a small phospho-donor (140), thereby abrogating the effects of a *barA* mutation.

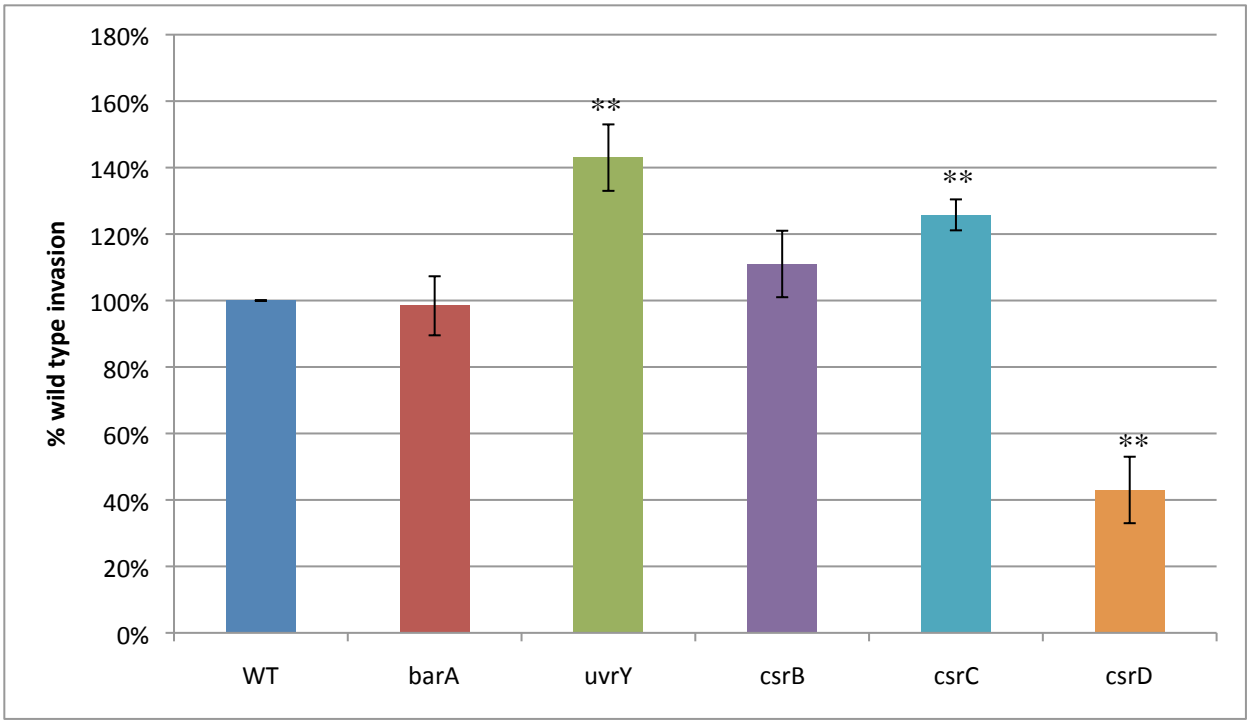

Figure 24: Regulators of CsrA also influence invasion.

Decreases in the level of free CsrA (e.g. *csrD* mutant) decrease *S. flexneri* invasion effiency, whereas mutations that increase the amount of free CsrA (e.g. *uvrY*, *csrB*, *csrC* mutants) increase invasion. Values are normalized to the invasion percentage of the wild type, and data presented are the average of at least three independent experiments. Error bars represent standard deviation. Unpaired student's T-test was used compare the relative invasion of the mutant strains to wild type *S. flexneri*. ** denotes *P* values < 0.01.

2. Central Carbon metabolism and *S. flexneri* pathogenesis

The phenotypes of the CsrA and Cra mutants suggest that regulation of the central carbon metabolic pathways is important invasion and persistence of *S. flexneri* within the host cell. While both pathways appear to be important for plaque formation, increased expression of glycolytic genes, as seen in the *uvrY* and *cra* mutants, correlated with increased attachment and invasion. To directly examine the role of glycolysis and gluconeogenesis in *S. flexneri* pathogenesis, mutants were constructed in a key step of each pathway, and these mutants were examined for invasion and plaque formation.

2.1.1 Gluconeogenesis

The enzyme phosphoenolpyruvate synthase (Pps, encoded by *ppsA*) catalyzes one of the committed steps of gluconeogenesis (Fig. 11). Expression of *ppsA* is activated by Cra, but repressed by CsrA. The phenotypes of the *csrA* and *cra* mutants suggested a correlation between decreased gluconeogenesis and increased invasion. To study the contribution of gluconeogenesis in pathogenesis, a *ppsA* mutant allele in JW1692 was transduced into wild type *S. flexneri*. The absence of *ppsA* had no effect on *S. flexneri* growth in LB broth. In the invasion assay, the *ppsA* mutant was as invasive as the parental strain (Fig. 25). Although these data suggests that Pps and gluconeogenesis are not crucial for invasion, deletion of *ppsA* only inhibits one pathway by which PEP can be generated. Therefore, a double mutant in a redundant pathway may be needed to determine the complete effect of gluconeogenesis on *S. flexneri* pathogenesis.

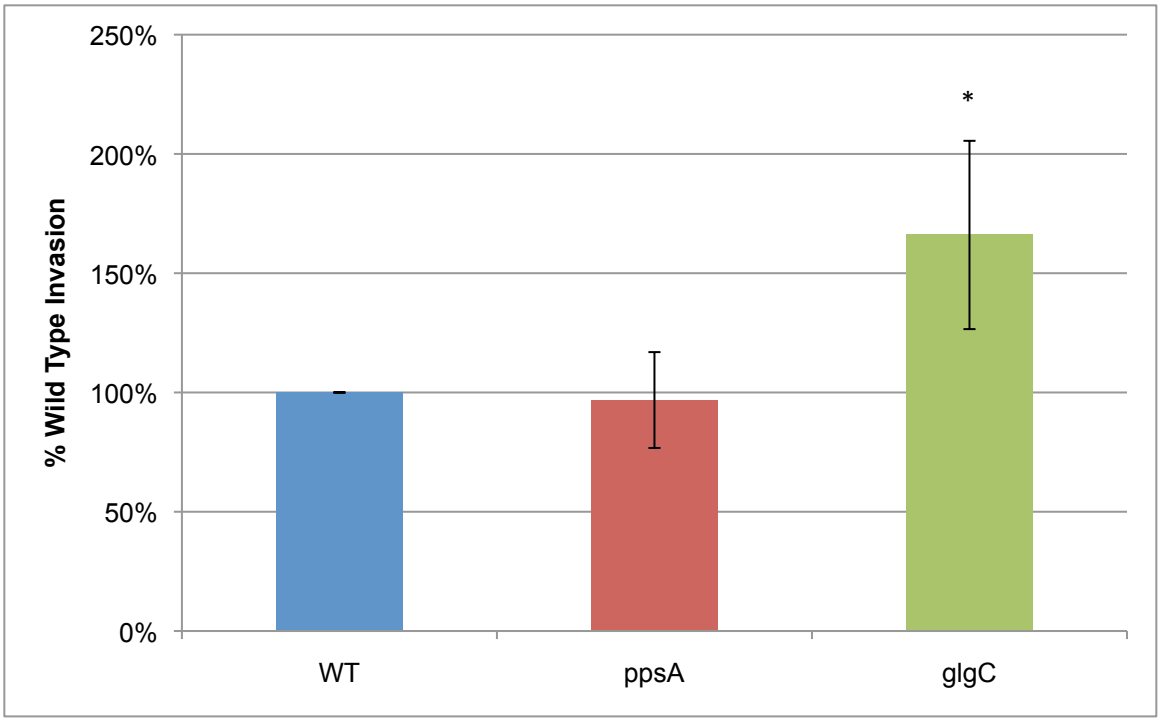

Figure 25: The absence of glycogen biosynthesis increases *S. flexneri* invasion.

The *glgC* mutant, which is defective in the first step in glycogen biosynthesis, was more invasive than wild type. Disruption of the gluconeogenic gene *ppsA* had no significant effect on invasion. The percent invasion shown is relative to wild type, and data given are the average of at least three independent experiments. An unpaired student's T-test was used to compare the percent invasion of the mutant strains relative to wild type. * denotes a *P*-value <0.05.

2.1.2 Glycolysis

The glycolytic enzyme phosphofructokinase (Pfk) catalyzes one of the first committed steps in glycolysis (Fig. 11). Although there are two isozymes, PfkI (encoded by *pfkA*) is the major isozyme, and is responsible for 90% of the Pfk activity in *E. coli* (48). The reciprocal phenotypes of the *csrA* and *cra* mutants suggested a strong correlation between increased glycolysis and increased invasion by *S. flexneri*. To directly examine the effects of glycolysis on *S. flexneri* pathogenesis, the *pfkA* mutant allele in JW3887 was transduced into wild type *S. flexneri*. Consistent with the role of PfkI in glycolysis, the *pfkA* mutant was unable to grow in M63 minimal media when glucose was the sole carbon source (Fig. 26A). The mutant grew as well as wild type on the gluconeogenic carbon source lactate, but exhibited a slight growth defect in LB broth (Fig. 26B).

When grown on Congo red agar, the *S. flexerni pfkA* mutant grew as pink colonies, similar to those formed by the *csrA* mutant. Consistent with the Congo red binding defect, the *pfkA* mutant was completely avirulent in both the invasion (Fig. 27) and plaque assays. Both plaque formation and invasion were complemented by expression of *pfkA* in the vector pWPfkA.

PfkI is required for metabolism of carbon substrates that enter at or above fructose-6-phosphate in the glycolytic pathway (Fig. 11) (137) . If the defect in utilization of glycolytic carbon sources is the cause for the avirulent phenotype of the *pfkA* mutant, then growth in a gluconeogenic carbon source may supersede this defect. Growth of the *pfkA* mutant in minimal medium with either pyruvate or lactate did not restore invasion by this strain (Fig. A1). This result is not completely unexpected, as the *pfkA* mutant likely metabolizes gluconeogenic carbon sources for growth in LB broth and is noninvasive under these conditions (Fig. 27). These data suggests that either a glycolytic byproduct or metabolism via the glycolytic pathway is essential for promoting *S. flexneri* invasion.

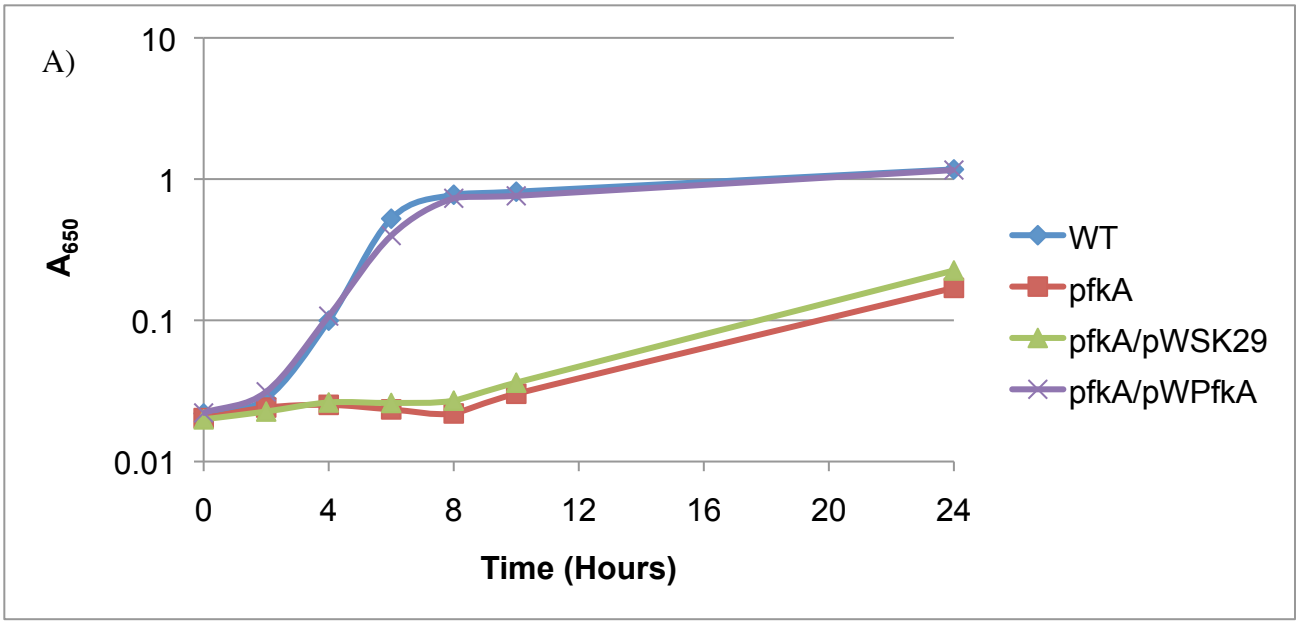
A)
10
1
0.1
0.01
A_{650}
0
4
8
12
16
20
24
Time (Hours)
WT
pfkA
pfkA/pWSK29
pfkA/pWPfkA

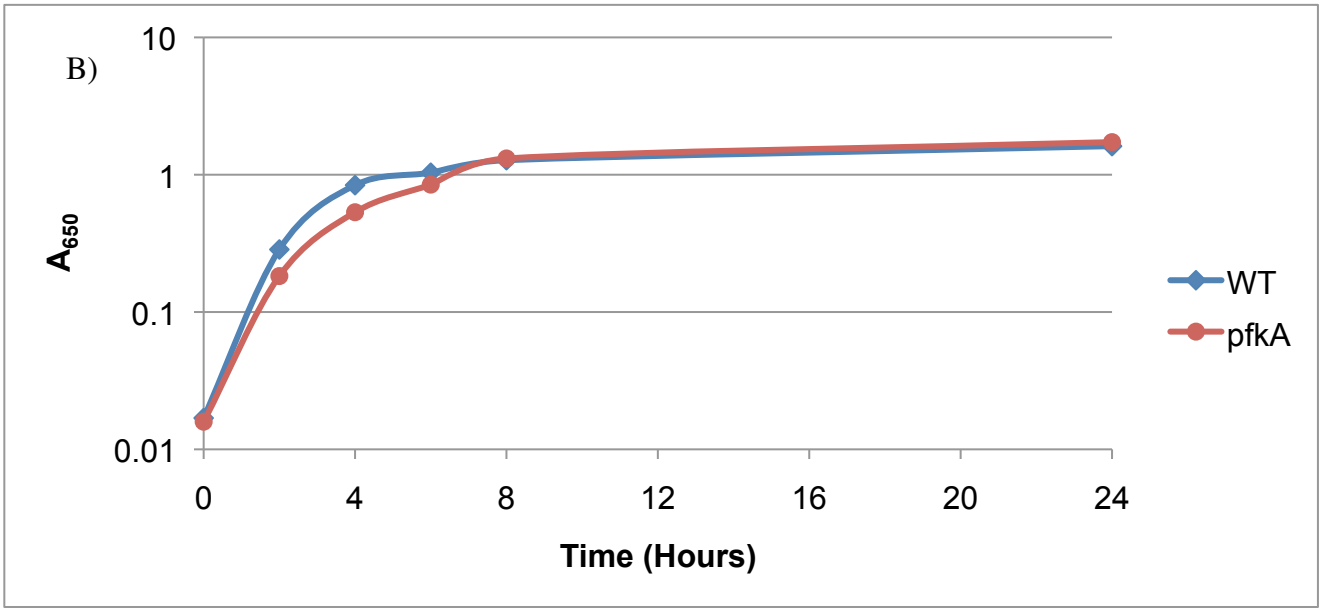
B)
10
1
0.1
0.01
A_{650}
0
4
8
12
16
20
24
Time (Hours)
WT
pfkA

Figure 26: The *pfkA* mutant grows poorly when glucose is the sole carbon source.

Overnights were grown at 30°C in LB broth, then subcultured to a starting absorbance (A_{650}) of 0.02 in M63 with 0.2% glucose (A) or LB broth (B). Cultures were grown at 37°C with aeration, and absorbance readings were taken at two-hour intervals.

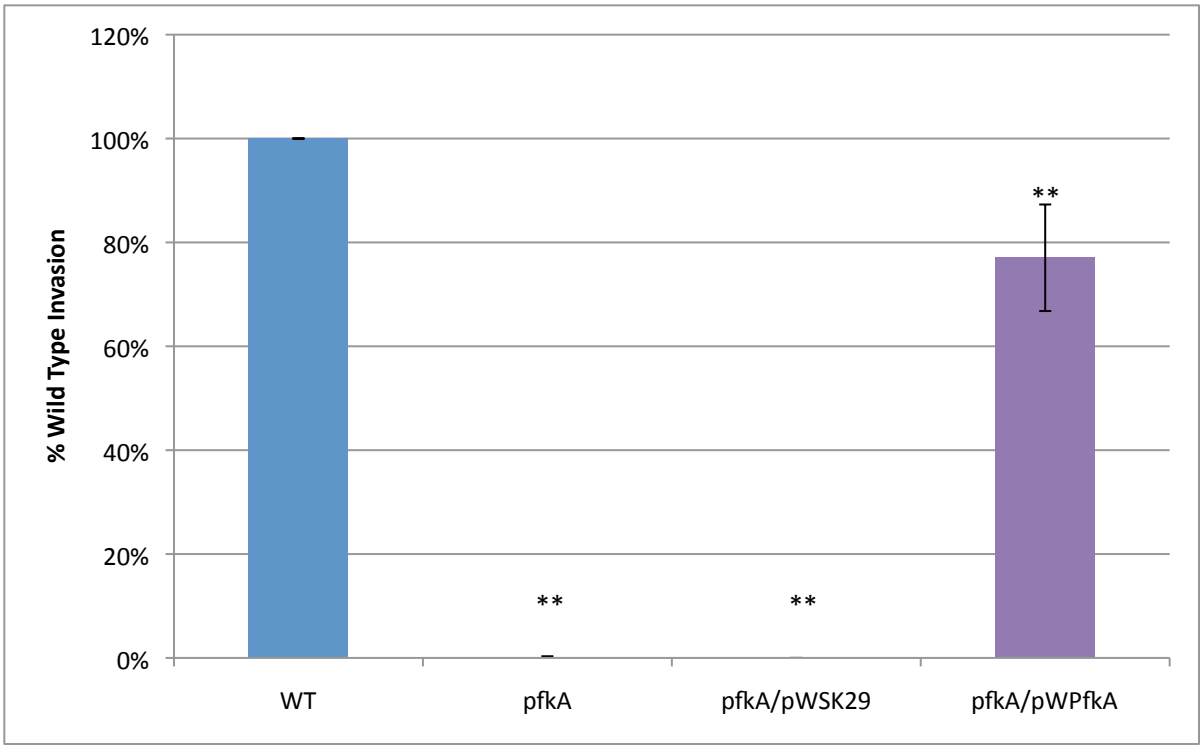

Figure 27: The *pfkA* mutant is noninvasive.

In the invasion assay, the *pfkA* mutant AGS220 was noninvasive, and invasion was restored by expression of wild type *pfkA* from its native promoter on the plasmid pWPfkA. Invasion percentages shown are relative to the wild type, and data given are the average of three independent experiments. Unpaired student's T-test was used to compare the invasion of the mutant strain relative to wild type. ** denotes *P*-value < 0.01. Error bars represent standard deviation.

2.1.3 Glycogen metabolism

Because of the role of CsrA in glycogen metabolism (Fig. 9), it was also possible that the invasion phenotypes seen in the *csrA* mutant were due to disruptions in either synthesis or degradation of this polysaccharide. To directly test the role of glycogen in *S. flexneri* pathogenesis, a mutation was constructed in the first step of the glycogen biosynthetic pathway (glucose-1-phosphate adenylyltransferase, encoded by *glgC*). Deletion of *glgC* had no effect on *S. flexneri* growth in rich media. However, in the invasion assay, the *glgC* mutant was over 60% more invasive than wild type (Fig. 25). This phenotype is opposite that seen in the *csrA* mutant, which suggests that the invasion defect of the *csrA* mutant is not due to blocks in glycogen biosynthesis. The increased invasion of the *glgC* mutant may be due to reallocation of carbon skeletons in the absence of glycogen synthesis. Carbon resources in the *glgC* mutant may be siphoned to other biosynthetic pathways that enhance the overall fitness of the bacterium, thereby increasing invasion. No obvious differences were seen in plaque number or morphology, suggesting that glycogen is not a crucial carbon source for *S. flexneri* in the cell culture assays. This, however, does not rule out a role for glycogen stores in vivo, as the cell culture media used contains an excess of glucose. Glycogen may play an important role in *S. flexneri* survival as it competes with resident microbes in the lumen, or as the bacterium transits the host gastrointestinal tract.

3. Effects of glycolysis on *S. flexneri* physiology and virulence gene expression

3.1 CARBON METABOLISM AND THE *S. FLEXNERI* OUTER MEMBRANE

LPS and O-antigen have an important role in *S. flexneri* pathogenesis. O-antigen polysaccharide length is important for invasion, as longer molecules can mask the type III secretion system (144). LPS is also important for actin-based motility, as mutants lacking the O-antigen exhibit aberrant IcsA localization (117, 118, 134). Because of the role of LPS in *S. flexneri* virulence, it was proposed that changes in carbon metabolism might lead to changes in the LPS, thereby affecting pathogenesis. To better understand the mechanism by which carbon metabolism affects *S. flexneri* pathogenesis, the outer membrane profile of the *csrA*, *cra* and *pfkA* mutants were examined.

3.1.1 Detergent resistance is increased in the *pfkA* and *csrA* mutants

Resistance to the detergent sodium dodecyl sulfate (SDS) assesses differences in the outer membrane composition or permeability, as modifications in the outer membrane make strains more or less resistant to lysis by the detergent. In comparison to wild type *S. flexneri*, both the *pfkA* and *csrA* mutants were more resistant to SDS (Fig. 28). Hong *et al.* (53) have shown a correlation between detergent sensitivity and Congo red binding. The increased detergent resistance noted in the *csrA* and *pfkA* mutants is consistent with this observation, as both mutants were also impaired in Congo red binding. Detergent sensitivity was also tested in the *cra* mutant. However, there was no difference in SDS resistance of the *cra* mutant versus the wild type in this assay.

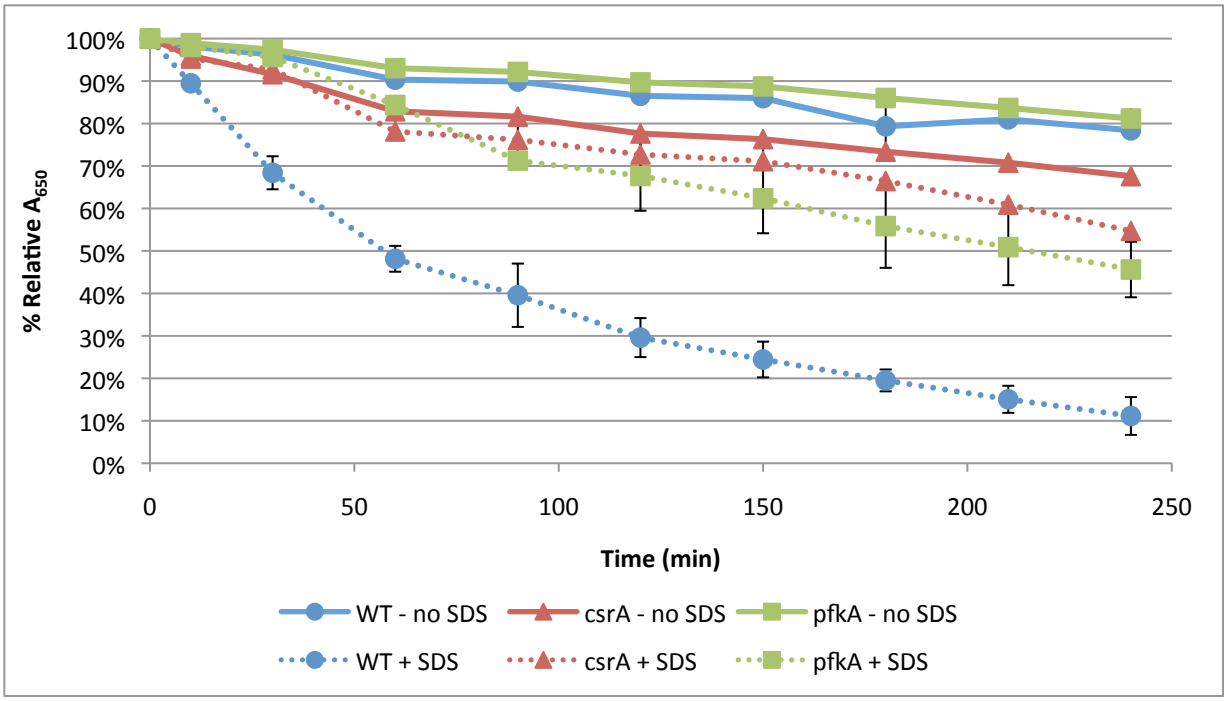

Figure 28: The *csrA* and *pfkA* mutants are more resistant to detergent as compared to wild type.

Bacteria were grown to exponential phase in LB, and equal numbers of bacteria were resuspended in 1 ml of 25 mM Tris-Cl (pH 7.5). After an initial absorbance reading (T_0), sodium dodecyl sulfate (SDS) was added at a final concentration of 0.1% to one set of samples per strain, and samples were incubated at 37°C without aeration. Absorbance was recorded at the time points indicated (T_n) and sensitivity to detergent lysis is expressed as a percentage (A_{650} at T_n/A_{650} at T_n = % relative A_{650}). Data shown is the average of three independent experiments, and error bars are the standard deviation.

3.1.2 Lipopolysaccharide profiles are affected by CsrA and PfkA

To examine specific effects of glycolysis on the outer membrane, LPS was harvested from the *csrA*, *cra* and *pfkA* mutants. Bacteria were grown as in the invasion assay, and LPS was collected from cell extracts treated with proteinase K. Samples prepared from equal numbers of cells were electrophoresed on a tricine SDS-PAGE gel and visualized by silver staining.

The less invasive *csrA* and *pfkA* mutants produced LPS banding patterns in which each repeat unit migrated faster than that of wild type (Fig. 29A). There was no significant difference in LPS migration of the avirulent, Congo red binding negative strain SA101 compared to wild type (Fig. A4), suggesting that the altered LPS was due to differences in metabolism rather than a general effect of decreased virulence gene expression. Because longer O-antigen can mask the type III secretion system, the amount of mode B O-antigen was also examined. Immunoblotting with *Shigella* group B antisera did not reveal differences in the amount of very long LPS produced by either the *csrA* or *pfkA* mutant (Fig. 29B).

The shift in LPS noted in the *csrA* and *pfkA* mutants is indicative of changes in the lipid A or core region of LPS. To examine the core more directly, immunoblotting was also performed using the Shigella group B core specific antibody MASF R3 core-1 (19). This antibody recognizes the R3 core type found in *S. flexneri* 2a strains. Under the conditions used, there was no difference in reactivity of the *pfkA* and *csrA* mutants as compared to wild type (Fig. 29C). Changes in the core polysaccharide were also tested by examining changes in resistance to novobiocin, as modifications in heptose phosphorylation in the core affect sensitivity to this antibiotic (147). Consistent with the immunoblotting data, there was no difference in novobiocin resistance in the *csrA* and *pfkA* mutants versus the wild type. These data suggest that the difference in LPS electrophoretic mobility may be due not to changes in the core polysaccharide, but rather to changes in the lipid A portion of the molecule.

Despite the increase in invasion, there was no discernable difference in the LPS profile of the *cra* mutant versus the wild type. Since LPS is also important for actin-based motility, the LPS was also collected from the *cra* mutant growing within in the host cytosol. Although earlier data argued against IcsA localization defects, it was possible that the defect in intracellular spread occurs within the context of the host cytosol. Strains were allowed to replicate in a confluent monolayer of epithelial cells for 2 hours before collection and sample preparation. Under these conditions, the LPS profiles of the *cra* mutant and wild type were similar (Fig. A2), suggesting that disruption of *cra* affects pathogenesis via other mechanism(s).

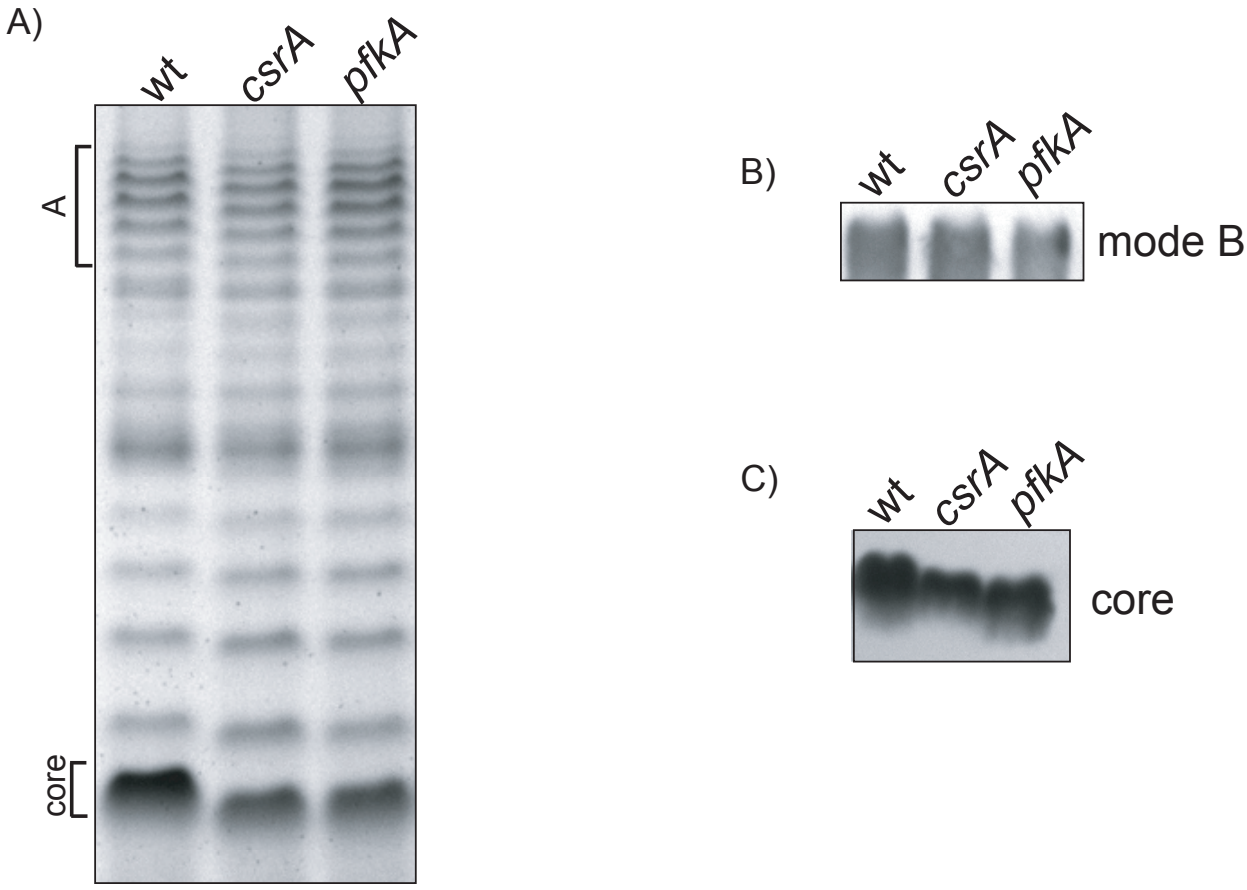

Figure 29: Lipopolysaccharide profiles are altered in the *pfkA* and *csrA* mutants.

LPS was harvested using the protocol of Hitchcock and Brown (51) and visualized by (A) silver staining or immunoblotting using (B) anti-group B *Shigella*, which recognizes the mode B repeats or (C) anti-2a antibodies, which bind the core polysaccharide. Abbreviations: core: lipid A plus the core polysaccharide; A: mode A, core conjugated to 11-17 O-antigen repeat units; B: mode B, core conjugated to 90+ O-antigen repeat units.

3.2 EXPRESSION AND SECRETION OF IPA PROTEINS IS INHIBITED BY DISRUPTIONS IN GLYCOLYSIS

Disruptions in glycolysis, either by mutation of the CsrA or Cra regulators or the glycolytic enzyme PfkI significantly affected *S. flexneri* invasion in the cell culture model. The virulence proteins IpaB and IpaC are central to *S. flexneri* attachment and invasion. Upon contact with the host cell, IpaB and IpaC form a pore in the host cell membrane that promotes phagosome lysis and bacterial uptake. Because of the primary role of these proteins in the preliminary steps of invasion, it was proposed that either expression or secretion of these proteins might be altered in the mutants.

3.2.1 Effector secretion is reduced in the *csrA* and *pfkA* mutants

To examine differences in effector secretion, strains were grown as for the virulence assays. Equal numbers of cells were collected by centrifugation and resuspended in phosphate-buffered saline. Effector secretion was induced by adding Congo red to the cell suspension, as this induces a burst of effector secretion similar to that seen upon host cell contact (106). Secreted proteins were precipitated from the media and electrophoresed on an SDS-PAGE gel. The recovered proteins were visualized by silver staining or immunoblotting with monoclonal anti-IpaB or anti-IpaC antibodies.

There was no significant difference in the amount of Ipa protein secreted by the *cra* mutant (Fig. 30), arguing that gross over-secretion of the Ipa proteins is not responsible for the hyperinvasive phenotype seen in this strain. However, secretion was greatly reduced in the less-invasive *csrA* and *pfkA* mutants (Fig. 30). From these data, it was concluded that decreased secretion of IpaB and IpaC is a contributing factor in the invasion defects of the *csrA* and *pfkA* mutants.

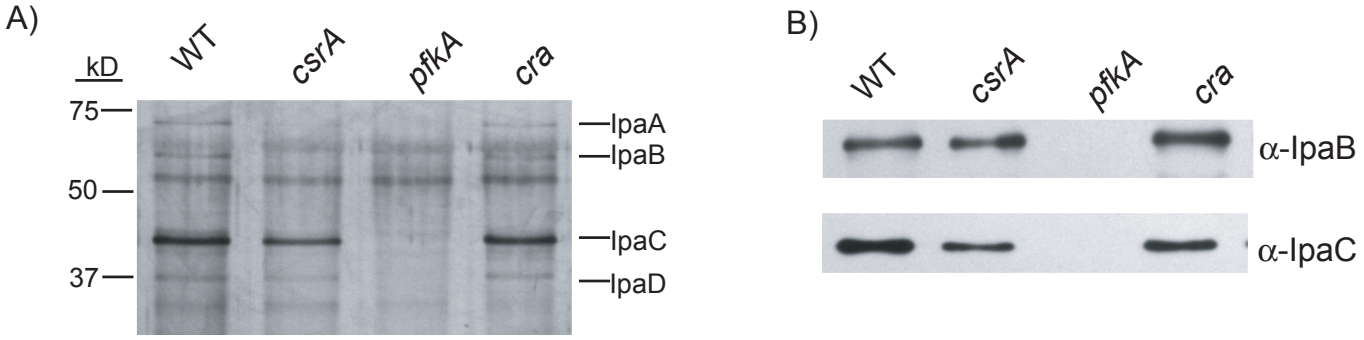

Figure 30: Ipa secretion is reduced in the *pfkA* and *csrA* mutants.

Bacteria were grown to exponential phase in LB broth, and secretion was induced by adding 0.005% (w/v) Congo red to equal numbers of bacteria. Secreted proteins were visualized by silver staining (A) or transferred to a nitrocellulose membrane and hybridized with anti-IpaB or anti-IpaC monoclonal antibodies (B).

3.2.2 Effector production is also reduced in the *csrA* and *pfkA* mutants

To test if the defect in Ipa secretion seen in the *pfkA* and *csrA* mutants was due to a defect in Ipa synthesis, whole cell lysates were resolved on an SDS-PAGE gel and visualized by Coomassie staining or immunoblotting with monoclonal anti-IpaB or anti-IpaC antibodies.

Deletion of *cra* had no effect on the level of IpaB or IpaC produced (Fig. 31). Because of the plaque phenotype, Ipa production of the *cra* mutant within the host cytosol was also examined. After 2 hours growth in a confluent monolayer, bacteria were collected from the host cell, and cell lysates were prepared from the recovered bacteria. The *cra* mutant made similar levels of IpaB and IpaC as the wild type (Fig. A3). Because the absence of *cra* does not affect Ipa production or secretion, is likely that this protein regulates invasion in an Ipa-independent fashion.

There was a significant reduction in IpaB and IpaC levels in the *csrA* and *pfkA* mutants, which accounts for the decreased secretion noted in these strains (Fig. 31). In both strains, Ipa production was restored by expression of the wild type gene from a plasmid. The reduction in Ipa production seen in the *csrA* and *pfkA* mutants suggests a correlation between active glycolysis and expression of the *ipaBCDA* operon.

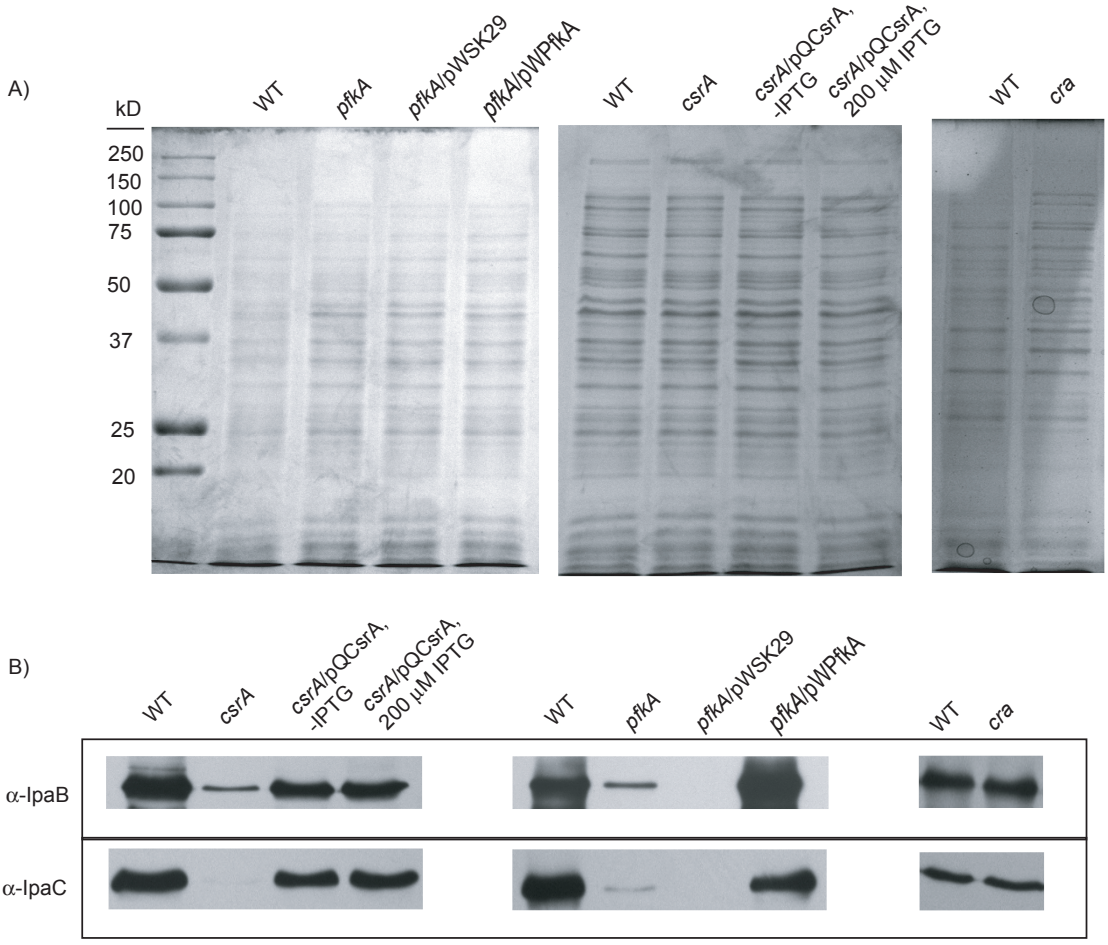

Figure 31: Decreased glycolytic gene expression results in decreased Ipa production.

(A) Proteins were harvested from whole cell lysates and separated by SDS-PAGE electrophoresis and visualized by coomassie staining. (B). Collected proteins were transferred to a nitrocellulose membrane and probed with anti-IpaB or anti-IpaC antibodies.

3.3 DISRUPTIONS IN GLYCOLYSIS INFLUENCE *VIRB* AND *VIRF* EXPRESSION

3.3.1 *virB* expression is reduced in the *pfkA* mutant

The virulence regulator VirB directly activates expression from the 31-kb entry locus, including the *ipaBCDA* operon (1). Thus, the reduced Ipa production in the *csrA* and *pfkA* mutants (Fig. 31) is likely due to decreased transcription of *virB*. To examine if *virB* expression is reduced in the *pfkA* mutant, bacteria were grown under the same conditions as the cell culture assays. RNA was collected, and the relative expression level of *virB* was determined by real-time PCR. The *pfkA* mutant was chosen for study, as this mutation more directly examines the effects of glycolysis on expression from the virulence plasmid. In comparison to the wild type, expression of *virB* was significantly reduced in the *pfkA* mutant (Fig. 32A), suggesting that glycolysis is required for expression of this virulence regulator.

3.3.2 Expression of the virulence regulator *virF* is also reduced in the *pfkA* mutant

In response to environmental stimuli (11, 103, 130, 131), the primary virulence regulator VirF activates expression of *virB*, thereby activating expression from the entry locus (Figs. 2, 3). Therefore, reduced *virF* expression in the *pfkA* mutant may account for reduced expression of *virB*. Consistent with the model, the relative expression of *virF* was significantly reduced in the *pfkA* mutant (Fig. 32B). Thus, the invasion deficiencies of this strain are due principally to reduced expression of the master virulence regulators. Insufficient activation of *virF* and *virB* prevents expression of the *ipa-mxi-spa* type III secretion system, rendering the *pfkA* mutant noninvasive. These data suggest a correlation between glycolytic metabolism and activation of the virulence gene cascade.

Carbon metabolism or carbon source availability may therefore be an additional factor by which *S. flexneri* coordinates virulence gene expression with conditions in the host.

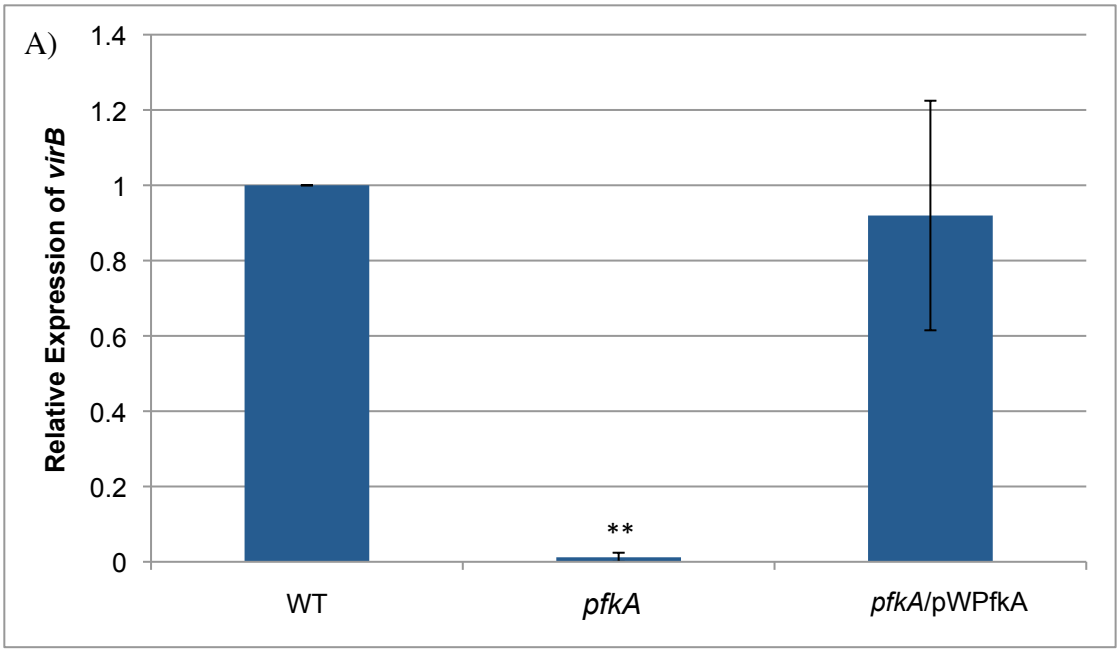
A)
Relative Expression of virB
1.4
1.2
1
0.8
0.6
0.4
0.2
0
**
WT
pfkA
pfkA/pWPfkA

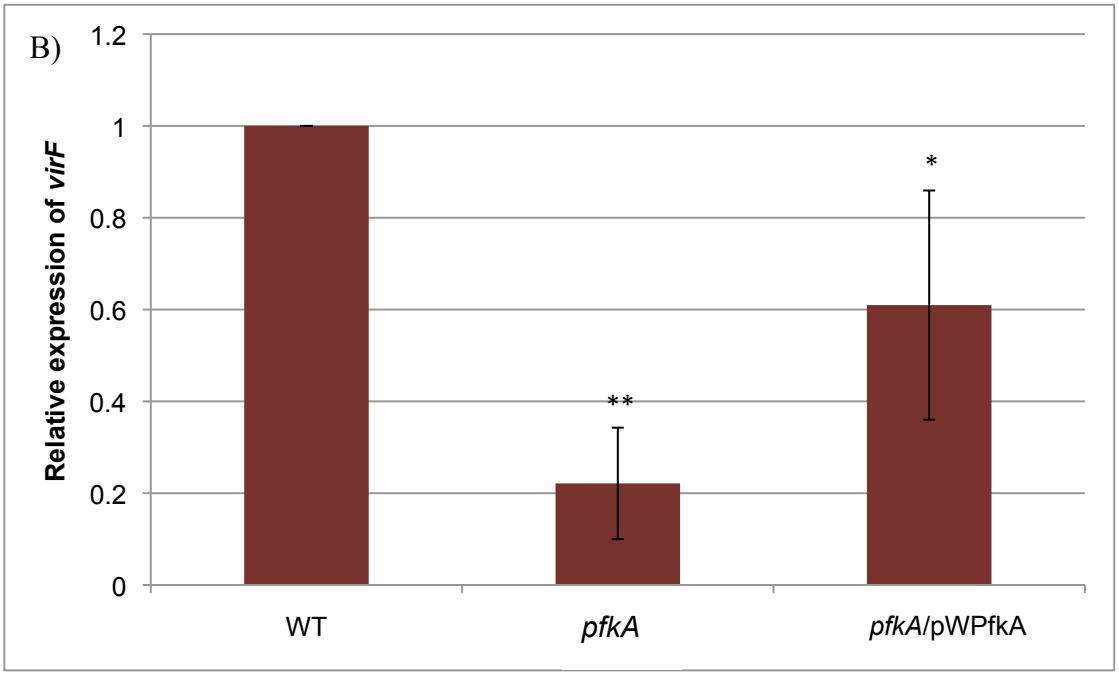
B)
Relative expression of virF
1.2
1
0.8
0.6
0.4
0.2
0
**
*
WT
pfkA
pfkA/pWPfkA

Figure 32: Expression of *virF* and *virB* is reduced in the *pfkA* mutant.

Real-time PCR was used to examine relative expression of *virB* (A) and *virF* (B). Values are normalized to the internal control *dksA* in each sample, and values are normalized to the expression value in wild type. Data are the average of three independent experiments, and error bars represent standard deviation. An unpaired student's T-test was used to compare relative expression of *virB* and *virF*. ** indicates *P*-values < 0.01, * represents *P* -values < 0.05.

IV. DISCUSSION

In order to establish infection, an invading pathogen must (1) colonize and penetrate the host mucosal surfaces (2) subvert the immune response and (3) grow within the host (123). Growth is the keystone of all successful infections, as virulence progression is predicated on replication and proliferation of the pathogen. Growth of the invading pathogen is significantly influenced by the surrounding milieu. The environmental conditions within the host are dynamic and shaped by the metabolic demands of both resident microbes and the invading bacterium. Therefore, to successfully establish infection, a pathogen must respond and adapt to these unique environments.

Within the mammalian colon, *S. flexneri* transitions from the intestinal lumen, to the subepithelial spaces and ultimately replicates within colonocytes. The bacterium must therefore adapt to these distinct environments. In vitro, the shift from growth in media to the eukaryotic cytosol results in significant changes in *S. flexneri* gene expression (73). In addition to regulation of dedicated virulence factors, transition into the host cytosol results in differential regulation of several classes of metabolic genes. This shift in expression is indicative of a coordinated response to the new environment. In the intracellular environment, *S. flexneri* downregulated expression of several glycolytic genes while upregulating expression of key genes in the gluconeogenic pathway (73). These data indicated that coordination of central carbon metabolism is required for successful adaptation to the host cytosol, and may be essential for pathogenesis. As such, this study focused on the known regulators of the glycolytic and gluconeogenic pathway, and the effects of metabolic disruptions on *S. flexneri* pathogenesis in vitro.

1. Decreased glycolysis inhibits initial stages of pathogenesis

Glycolysis is important for the preliminary steps of *S. flexneri* pathogenesis, as the *csrA* and *pfkA* mutants are severely impaired in attachment and invasion (Figs. 16, 19,

27). Additionally, growth of the *pfkA* mutant on gluconeogenic carbon sources did not restore invasion of this strain. This phenotype suggests that the glycolytic pathway, or PfkI itself, is required for virulence.

The defects in invasion are due principally to reduced production and secretion of the effector proteins IpaB and IpaC (Figs. 30, 31). In the *pfkA* mutant, expression of *virF* and *virB* is significantly reduced relative to wild type (Fig. 32). Expression of *virB* was also reduced in the *csrA* mutant (data not shown), further supporting the hypothesis that carbon metabolism and its regulation is essential for *S. flexneri* pathogenesis. Thus, in the absence of glycolytic gene expression, *S. flexneri* does not activate the virulence gene cascade necessary for invasion (Fig. 33).

Binding of the amphipathic dye Congo red is indicative of *S. flexneri* virulence. Consistent with the invasion defect, both the *csrA* and *pfkA* mutants bound less dye relative to wild type (data not shown). Previous data from our lab has shown that glycolysis is essential for Congo red binding, as *S. flexneri* grown on media lacking glycolytic carbon sources does not bind the dye (27).

Reduced glycolytic gene expression also increased detergent resistance (Fig. 28). Reduced effector secretion correlates with increased detergent resistance, as a strain defective in Congo red binding was more resistant to SDS versus its Congo red binding positive counterpart (53). Collectively, these data point to a role of glycolysis in initiation of *S. flexneri* pathogenesis, specifically in the synthesis of effector molecules and secretion via the type III secreton (Fig. 33).

Increased glycolytic gene expression in the *cra* and *uvrY* mutants correlated with increased adherence and invasion (Figs. 15, 16, 24). The mechanism by which glycolysis enhances invasion is unclear. Both the *cra* and *uvrY* mutants synthesized and secreted wild type levels of effectors (Fig. 31, data not shown). As the outer membrane affects invasion (144), the LPS profile of the *cra* mutant was also examined. However, there was no discernable difference in the outer membrane morphology of the *cra* mutant as

compared to wild type (Fig. A4). The increased invasion noted in the *cra* and *uvrY* mutants is likely a result of increased adherence. The factor(s) responsible for *S. flexneri* attachment are unknown, but the process may involve IpaB binding to lipid rafts on the host cell membrane (66). However, the absence of Cra had no effect on Ipa production or secretion (Figs. 30, 31). Additional factor(s) are also involved in *S. flexneri* adherence, as *ipaB* null strains are hyperadherent in vitro (50). Thus, the adhesion phenotypes caused by increased glycolysis is not necessarily due to altered Ipa production or secretion.

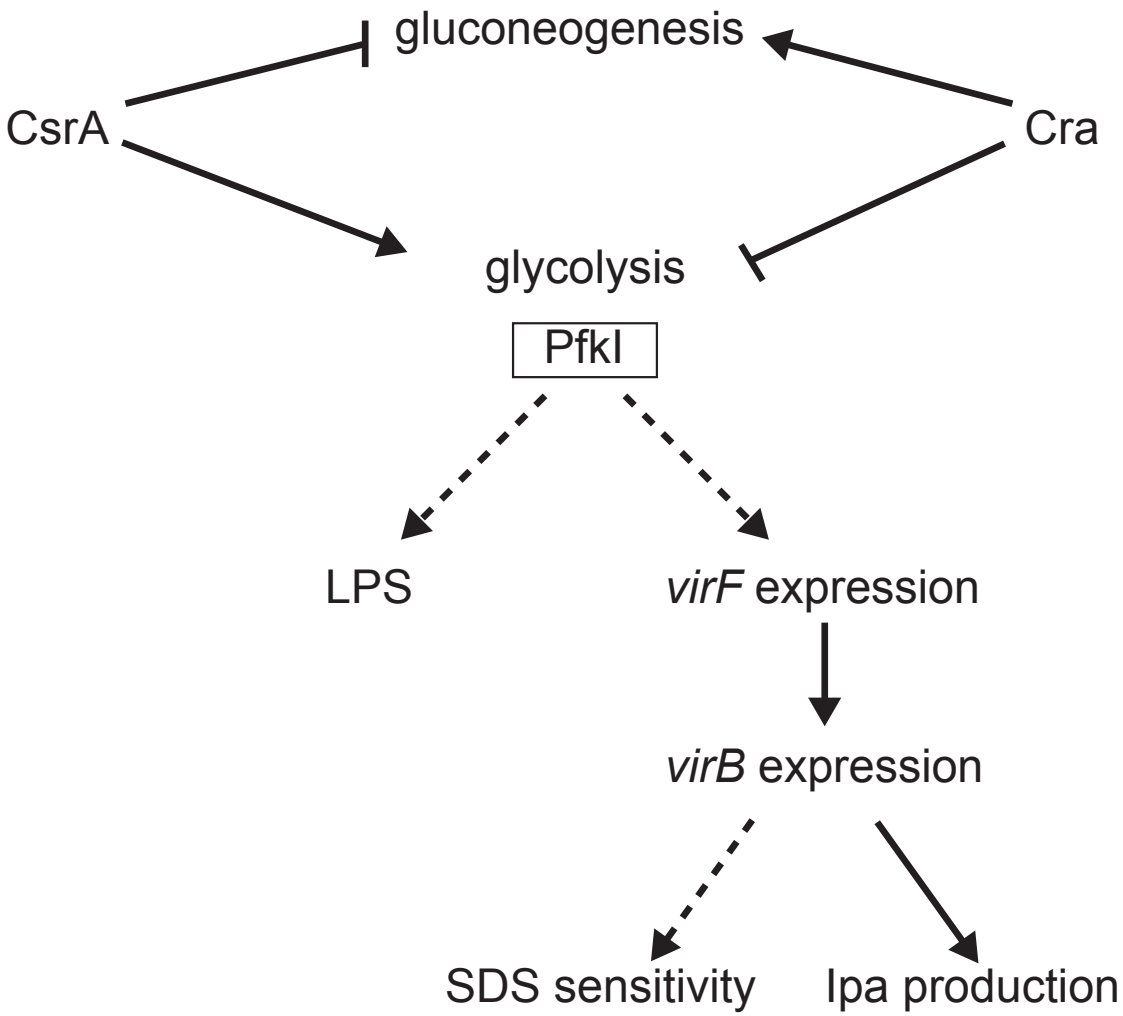
gluconeogenesis
CsrA
Cra
glycolysis
PfkI
LPS
virF expression
virB expression
SDS sensitivity
Ipa production

Figure 33: Glycolytic gene expression affects *S. flexneri* physiology and pathogenesis.

The proposed model suggests a mechanism by which disruptions in glycolytic gene expression could regulate *S. flexneri* pathogenesis. Decreased expression of the glycolytic enzyme PfkI alters the lipid A – core region of LPS. However, the specific effects of this altered LPS on pathogenesis have not been determined. PfkI is also required for expression of the virulence regulator VirF. Decreased expression of *virF* results in decreased expression of *virB* and thus decreased production and secretion of IpaB and IpaC. The decreased effector secretion likely influences *S. flexneri* resistance to the detergent SDS. The mechanism by which increased glycolytic gene expression enhances virulence is unclear, but could be due to subtle changes in effector secretion or production.

2. Persistence in the eukaryotic cytosol requires balanced carbon metabolism

The eukaryotic cytosol is presumably rich in carbon sources, including glycerophospholipids, glycoproteins, phosphorylated carbohydrates and glycerol. However, microinjection studies suggest that pathogens that occupy this niche have specifically adapted to do so (39). Like *S. flexneri*, *Listeria monocytogenes* exploits the eukaryotic cytosol as a replicative niche. Within this environment, *L. monocytogenes* reduces expression of glycolytic genes, while increasing the pentose phosphate pathway (62). It has been proposed that *L. monocytogenes* utilizes alternate carbon sources (e.g. glycerol and phospholipids) via the pentose phosphate and gluconeogenic pathways. In this fashion, the pathogen avoids siphoning valuable resources from the host cell, thereby prolonging the integrity of its replicative niche (61). As *Listeria* and *Shigella* both occupy the eukaryotic cytosol, it is likely *S. flexneri* also relies on multiple carbon sources to persist within the colonocyte.

Similar to *L. monocytogenes*, *S. flexneri* downregulates expression of key glycolytic genes upon entry into the host cytosol, while increasing expression several genes involved in glycogen uptake and gluconeogenesis (73). Prolonged occupation of the host cytosol may also influence S. *flexneri* carbon metabolism. As the number of intracellular bacteria increases, it is likely that competition for resources intensifies, mandating that the bacteria use a variety of carbon sources to persist. The ability to use a wide array of carbon sources likely relies on catabolite-responsive regulators. Consistent with this prediction, both CsrA and Cra were required for plaque formation by *S. flexneri*.

The specific reason for atypical plaque formation by the *cra* mutant still remains unclear, but could stem from several interacting factors. Microscopic examination of the *cra* mutant bacteria within the monolayer showed an increase in the number of bacteria in vacuoles and increased formation of microcolonies. Although these morphological

differences may be an artifact of the increased invasion of this strain, they could also indicate abnormalities that lead to defects in plaque formation. The presence of vacuolar bacteria may be the result of misregulated effector secretion, as IpaB is required for escape from the phagocytic vacuole (50). A mutation in *icsA* results in the formation of microcolonies, as this mutant is unable to move through the host cytosol. Despite the polar localization of IcsA in the *cra* mutant (Fig. 17B), the functionality of this protein within the host cytosol has not been thoroughly examined.

Based on the metabolic phenotypes of the *cra* mutant, misregulation of carbon metabolism is likely a significant contributor to aberrant plaque formation by this strain. Over a 90-minute period, the strain replicates normally within the eukaryotic cell (data not shown). However, the metabolic burden placed on the host cell over a longer period of time may lead to defects responsible for the inability of this strain to replicate within the monolayer. Data presented in this study show that the *cra* mutant has increased consumption of glycolytic carbon sources, but is defective in utilization of gluconeogenic metabolites (Table 5). The increased number of intracellular bacteria may place a large metabolic burden on the host cell. Strict utilization of glycolytic carbon sources could result in competition between the *cra* mutant and its eukaryotic host, increasing metabolic stress on the host cell, and may lead to premature death of the host cell. Increased glycolysis could also lead to excess acetate production, which is likely toxic to the already-stressed host cell.

Like the *cra* mutant, the *csrA* mutant formed smaller, more turbid plaques than wild type. However, the abnormal plaque morphology of the *csrA* mutant is primarily due to reduced effector production (Fig. 31). In addition to a role in invasion, the genes encoded in the entry locus are necessary for intercellular spread.

Reduced effector secretion likely impairs the ability of the *csrA* to invade, and could result in delayed activation of the late-stage virulence regulator MxiE. Activity of MxiE is also dependent on effector secretion. IpgC acts as both an intra-bacterial chaperone of

IpaB and IpaC and as an activator of MxiE (76). Thus, reduced effector secretion could lead to delays in activation of MxiE, and such delays could decrease the overall rate of bacterial spread through the monolayer, resulting in smaller plaques.

Reduced glycolysis also altered the *S. flexneri* LPS profile, resulting in a faster migrating core (Fig. 29A, C), indicative of changes in the lipid A or core portion of the molecule. There was no detectable difference in the core polysaccharide as determined by immunoblotting (Fig. 29C) or novobiocin sensitivity (data not shown). Thus, it is likely that the alteration occurs in the lipid A region. The LPS profile is similar between wild type *S. flexneri* and the avirulent strain SA101 (Fig. 37). Thus, the LPS profile of the *csrA* and *pfkA* mutants is due to disruptions in carbon metabolism and not a result of reduced virulence. The effect of the modified LPS structure on pathogenesis of the mutant strains is unknown. Though lipid A acylation is important for *S. flexneri* pathogenesis in vitro, there are no documented roles of the lipid A region in *S. flexneri* pathogenesis in vitro (26).

It is also possible that misregulated carbon metabolism could contribute to plaque defects by the *csrA* mutant. In the phenotypic microarray the *csrA* mutant preferentially utilizes gluconeogenic carbon sources (Table 6), although the shift in metabolism was relatively modest. However, these defects in carbon utilization may result in increased competition for resources, as the mutant would be unable to fully utilize the array of available carbon sources. The *pfkA* mutant was completely noninvasive (Fig. 27), and thus unable to form plaques. More studies are needed to better examine the role of glycolysis in intracellular survival. Bowden *et al.* (16) speculate that increased glycolysis is inhibitory to intracellular replication, as expression of *pfkA* from a plasmid modestly inhibited *S.* Typhimurium replication within the macrophage vacuole.

3. Carbon metabolism is an environmental regulator of virulence gene expression

Environmental conditions in the host induce maximal expression of the plasmid-encoded virulence genes (Fig. 3). Temperature (37°C), osmolarity and pH activate expression of the transcriptional regulator VirF. VirF activates the second transcriptional regulator VirB, which in turn directly activates the *ipa-mxi-spa* type III secretion system. Carbon metabolism may also be an environmental regulator of virulence gene expression, as *virF* and *virB* expression was significantly reduced in the *pfkA* mutant (Fig. 32).

The mechanism by which carbon metabolism affects virulence gene expression is unclear. There were no canonical CsrA, cAMP-CRP or Cra binding sites identified in *virF* or *virB* (data not shown). Carbon may therefore affect virulence gene expression in a more indirect manner. Changes in DNA supercoiling play an important role in activation of *virF* and *virB* expression. An increase in temperature from 30°C to 37°C results in increased supercoiling around the *virF* (36) and *virB* (130) promoters. This shift in DNA topology alleviates H-NS-mediated repression, and increases RNA polymerase binding at the promoters. Similar to increased temperature, an increase in the [ATP]/[ADP] ratio also increases DNA supercoiling (135). Disruptions in carbon metabolism may affect energy production, in turn affecting DNA topology and accessibility of the *virF* and *virB* promoters.

The Ipa effectors are required for both invasion and intercellular spread. Prior to invasion, *S. flexneri* upregulates expression of the *ipa-mxi-spa* type III secretion system. However, expression from this entry locus gradually decreases during replication within the epithelial cell (46, 73). Concomitantly, expression of *virF* and *virB* also decreases (73). Lucchini *et al*. (73) propose two scenarios to explain the apparent discrepancy. First, the level of effectors needed for intercellular spread may be lower than that needed

for invasion, thus accounting for decreased expression of the *ipa* locus. Alternatively, intracellular *Shigella* could split into smaller subpopulations. In this model, one population maintains the "invasive" status, and spreads intercellularly. The other subpopulation becomes "dormant", down-regulating expression of virulence factors (73).

Carbon metabolism may be the dividing factor between the two populations. Temperature and osmolarity likely remain relatively constant in the intracellular milieu, and carbon metabolism may therefore become a primary regulator of virulence gene expression. As *Shigella* replicates in the host cytosol, competition for available resources increases. In response, the bacteria likely utilize alternative carbon sources such as glycerol, amino acids and nucleotides. Metabolism of these alternative carbon sources would decrease glycolytic metabolism, and in turn decrease expression of *virF* and *virB*. A small subpopulation, however, may still utilize remaining glycolytic carbon sources, thereby retaining the invasive status. Although this model is consistent with the data presented, it remains to be experimentally confirmed.

Disruptions in glycolytic-gluconeogenic carbon flux likely have downstream effects on the Entner-Doudoroff and Pentose Phosphate pathways. Thus, it is possible that the phenotypes noted in this study are not due directly to changes in glycolysis *per se*, but rather a consequence of altered metabolism via the citric acid cycle, the pentose phosphate pathway or the Entner-Doudoroff pathway.

As *S. flexneri* travels the host gastrointestinal tract, the bacterium adapts to several distinct environments. Conditions in the colon, including temperature, pH and osmolarity work in concert to maximize expression of the invasion genes. In this fashion, *S. flexneri* coordinates proper location in the host with production of virulence factors. The data presented suggest that carbon source is an additional environmental regulator of the invasion genes. Central carbon metabolism involves several connecting pathways, and impinges upon a wide array of other cellular processes. In addition to the glycolytic and gluconeogenic pathways, Entner-Doudoroff and Pentose Phosphate pathways may also

affect *S. flexneri* invasion and intracellular survival. Host-cell metabolism also likely affects *S. flexneri* pathogenesis. In this study, immortalized Henle cells were used for cell culture assays. Inherent differences in the culture cell line compared to cells in the mammalian intestine likely influence the metabolism of invading *S. flexneri,* as differences in host cell physiology could affect the nutrient pool available to *S. flexneri*. The data presented in this study show a strong correlation between central carbon metabolism and *S. flexneri* pathogenesis. However, future studies are needed to further elucidate the mechanism by which these pathways influence *S. flexneri* pathogenesis.

Appendices

Table A1: BioLog phenotype microarray - Plate 1, 24-hour comparison

Carbon Source	Substrate Type	Wild type (2457T)	*csrA* (AGS120)	*cra* (AGS190)
Negative Control	negative control	0.075	0.092	0.062
L-Arabinose	carbohydrate	0.659	0.448	0.07
N-Acetyl-D-Glucosamine	carbohydrate	0.798	0.679	0.916
D-Saccharic Acid	carboxylic acid	0.073	0.084	0.062
Succinic Acid	carboxylic acid	0.515	0.663	0.358
D-Galactose	carbohydrate	0.965	0.823	0.537
L-Aspartic Acid	amino acid	0.57	0.582	0.335
L-Proline	amino acid	0.064	0.086	0.062
D-Alanine	amino acid	0.68	0.808	0.067
D-Trehalose	carbohydrate	1.115	0.808	1.33
D-Mannose	carbohydrate	0.79	0.817	1.046
Dulcitol	carbohydrate	0.084	0.101	0.077
D-Serine	amino acid	0.095	0.094	0.07
D-Sorbitol	carbohydrate	0.089	0.682	0.076
Glycerol	carbohydrate	1.085	1.086	0.488
L-Fucose	carbohydrate	0.075	0.083	0.064
D-Glucuronic Acid	carboxylic acid	1.188	0.926	0.8

D-Gluconic Acid	carboxylic acid	0.209	0.421	0.135
D,L-a-Glycerol Phosphate	carbohydrate	0.788	0.933	0.794
D-Xylose	carbohydrate	0.065	0.093	0.073
L-Lactic Acid	carboxylic acid	1.422	1.521	0.486
Formic Acid	carboxylic acid	0.079	0.095	0.062
D-Mannitol	carbohydrate	0.87	0.733	1.024
L-Glutamic Acid	amino acid	0.103	0.115	0.083
D-Glucose-6-Phosphate	carbohydrate	1.52	1.388	1.472
D-Galactonic Acid-g-Lactone	carboxylic acid	0.077	0.082	0.063
D,L-Malic Acid	carboxylic acid	0.673	0.711	0.428
D-Ribose	carbohydrate	0.112	0.396	0.064
Tween 20	fatty acid	0.088	0.103	0.075
L-Rhamnose	carbohydrate	0.068	0.081	0.068
D-Fructose	carbohydrate	0.837	0.976	0.674
Acetic Acid	carboxylic acid	0.066	0.11	0.074
a-D-Glucose	carbohydrate	0.651	0.698	0.946
Maltose	carbohydrate	0.087	0.116	0.071
D-Melibiose	carbohydrate	0.969	1.124	0.121
Thymidine	carbohydrate	1.278	1.359	1.122
L-Asparagine	amino acid	0.545	0.783	0.168
D-Aspartic Acid	amino acid	0.08	0.08	0.064
D-Glucosaminic Acid	carboxylic acid	0.076	0.088	0.072

1,2-Propanediol	alcohol	0.084	0.101	0.071
Tween 40	fatty acid	0.09	0.095	0.077
a-Ketoglutaric Acid	carboxylic acid	0.206	0.411	0.103
a-Ketobutyric Acid	carboxylic acid	0.076	0.11	0.076
a-Methyl-D-Galactoside	carbohydrate	0.536	0.624	0.085
a-D-Lactose	carbohydrate	0.085	0.102	0.078
Lactulose	carbohydrate	0.094	0.114	0.082
Sucrose	carbohydrate	0.091	0.11	0.075
Uridine	carbohydrate	0.75	0.523	0.338
L-Glutamine	amino acid	0.08	0.096	0.067
m-Tartaric Acid	carboxylic acid	0.055	0.07	0.054
D-Glucose-1-Phosphate	carbohydrate	1.328	1.243	1.286
D-Fructose-6-Phosphate	carbohydrate	1.36	1.275	1.414
Tween 80	fatty acid	0.088	0.107	0.076
a-Hydroxyglutaric Acid-g-Lactone	carboxylic acid	0.09	0.106	0.08
a-Hydroxybutyric Acid	carboxylic acid	0.071	0.05	0.065
b-Methyl-D-Glucoside	carbohydrate	0.078	0.096	0.068
Adonitol	carbohydrate	0.084	0.093	0.066
Maltotriose	carbohydrate	0.088	0.11	0.072
2'-Deoxyadenosine	carbohydrate	1.03	1.499	1.335
Adenosine	carbohydrate	0.63	1.232	1.091
Gly-Asp	amino acid	0.416	0.525	0.333

Citric Acid	carboxylic acid	0.075	0.086	0.062
m-Inositol	carbohydrate	0.075	0.084	0.069
D-Threonine	amino acid	0.078	0.123	0.063
Fumaric Acid	carboxylic acid	0.624	0.822	0.374
Bromosuccinic Acid	carboxylic acid	0.42	0.685	0.215
Propionic Acid	carboxylic acid	0.054	0.058	0.056
Mucic Acid	carboxylic acid	0.069	0.093	0.07
Glycolic Acid	carboxylic acid	0.069	0.081	0.066
Glyoxylic Acid	carboxylic acid	0.063	0.051	0.048
D-Cellobiose	carbohydrate	0.093	0.111	0.077
Inosine	carbohydrate	1.417	1.309	1.266
Gly-Glu	amino acid	0.43	0.262	0.356
Tricarballylic Acid	carboxylic acid	0.082	0.091	0.072
L-Serine	amino acid	0.644	0.737	0.449
L-Threonine	amino acid	0.339	0.246	0.089
L-Alanine	amino acid	0.814	0.96	0.155
Ala-Gly	amino acid	0.745	0.918	0.293
Acetoacetic Acid	carboxylic acid	0.088	0.208	0.068
N-Acetyl-D-Mannosamine	carbohydrate	0.122	0.196	0.133
Mono-Methylsuccinate	carboxylic acid	0.165	0.298	0.207
Methylpyruvate	ester	0.711	0.797	0.493
D-Malic Acid	carboxylic acid	0.08	0.097	0.063

L-Malic Acid	carboxylic acid	0.681	0.717	0.374
Gly-Pro	amino acid	0.104	0.112	0.077
p-Hydroxyphenyl Acetic Acid	carboxylic acid	0.078	0.091	0.063
m-Hydroxyphenyl Acetic Acid	carboxylic acid	0.074	0.087	0.061
Tyramine	amine	0.073	0.108	0.064
D-Psicose	carbohydrate	0.077	0.091	0.065
L-Lyxose	carbohydrate	0.061	0.07	0.056
Glucuronamide	amide	0.094	0.12	0.169
Pyruvic Acid	carboxylic acid	0.6	0.789	0.742
L-Galactonic Acid-g-Lactone	carboxylic acid	0.08	0.089	0.067
D-Galacturonic Acid	carboxylic acid	1.821	1.904	1.4
Phenylethylamine	amine	0.078	0.101	0.06
2-Aminoethanol	alcohol	0.079	0.091	0.067

Table A2: BioLog phenotype microarray, Plate 2, 24-hour comparison

Carbon Source	Substrate Type	wild type (2457T)	*csrA* (AGS120)	*cra* (AGS190)
Negative Control	negative control	0.074	0.087	0.065
Chondroitin Sulfate C	polymer	0.064	0.069	0.056
a-Cyclodextrin	polymer	0.107	0.097	0.066
b-Cyclodextrin	polymer	0.095	0.088	0.069
g-Cyclodextrin	polymer	0.077	0.084	0.064
Dextrin	polymer	0.113	0.149	0.068
Gelatin	polymer	0.082	0.09	0.067
Glycogen	polymer	0.085	0.086	0.073
Inulin	polymer	0.081	0.085	0.066
Laminarin	polymer	0.090	0.097	0.07
Mannan	polymer	0.085	0.097	0.075
Pectin	polymer	0.143	0.143	0.11
N-Acetyl-D-Galactosamine	carbohydrate	0.085	0.099	0.066
N-Acetyl-Neuraminic Acid	carboxylic acid	1.115	1.044	1.046
b-D-Allose	carbohydrate	0.070	0.071	0.058
Amygdalin	carbohydrate	0.080	0.093	0.062
D-Arabinose	carbohydrate	0.076	0.084	0.062
D-Arabitol	carbohydrate	0.084	0.087	0.067

L-Arabitol	carbohydrate	0.076	0.093	0.065
Arbutin	carbohydrate	0.081	0.085	0.061
2-Deoxy-D-Ribose	carbohydrate	0.058	0.063	0.056
i-Erythritol	carbohydrate	0.086	0.083	0.069
D-Fucose	carbohydrate	0.085	0.09	0.073
3-0-b-D-Galactopyranosyl-D-Arabinose	carbohydrate	0.054	0.06	0.054
Gentiobiose	carbohydrate	0.086	0.09	0.069
L-Glucose	carbohydrate	0.084	0.078	0.068
D-Lactitol	carbohydrate	0.082	0.101	0.072
D-Melezitose	carbohydrate	0.088	0.08	0.068
Maltitol	carbohydrate	0.088	0.096	0.071
a-Methyl-D-Glucoside	carbohydrate	0.093	0.089	0.066
b-Methyl-D-Galactoside	carbohydrate	0.096	0.097	0.084
3-Methylglucose	carbohydrate	0.098	0.129	0.091
b-Methyl-D-Glucuronic Acid	carboxylic acid	0.092	0.101	0.072
a-Methyl-D-Mannoside	carbohydrate	0.095	0.103	0.077
b-Methyl-D-Xyloside	carbohydrate	0.086	0.103	0.078
Palatinose	carbohydrate	0.104	0.128	0.088
D-Raffinose	carbohydrate	0.804	0.759	0.07
Salicin	carbohydrate	0.072	0.086	0.079
Sedoheptulosan	carbohydrate	0.079	0.088	0.067
L-Sorbose	carbohydrate	0.081	0.082	0.063

Stachyose	carbohydrate	0.086	0.096	0.071
D-Tagatose	carbohydrate	0.090	0.093	0.079
Turanose	carbohydrate	0.100	0.14	0.094
Xylitol	carbohydrate	0.088	0.094	0.075
N-Acetyl-D-glucosaminitol	carbohydrate	0.104	0.121	0.077
g-Amino-N-Butyric Acid	carboxylic acid	0.093	0.106	0.077
d-Amino Valeric Acid	carboxylic acid	0.103	0.123	0.087
Butyric Acid	carboxylic acid	0.097	0.097	0.09
Capric Acid	carboxylic acid	0.082	0.067	0.054
Caproic Acid	carboxylic acid	0.073	0.099	0.066
Citraconic Acid	carboxylic acid	0.067	0.097	0.058
D,L-Citramalic Acid	carboxylic acid	0.085	0.089	0.074
D-Glucosamine	carbohydrate	1.294	1.048	1.003
2-Hydroxybenzoic Acid	carboxylic acid	0.055	0.061	0.047
4-Hydroxybenzoic Acid	carboxylic acid	0.071	0.089	0.057
b-Hydroxybutyric Acid	carboxylic acid	0.084	0.106	0.078
g-Hydroxybutyric Acid	carboxylic acid	0.095	0.081	0.087
a-keto-valeric acid	carboxylic acid	0.085	0.09	0.076
Itaconic Acid	carboxylic acid	0.069	0.071	0.065
5-Keto-D-Gluconic Acid	carboxylic acid	0.086	0.094	0.07
D-Lactic Acid Methyl Ester	ester	0.133	0.114	0.088
Malonic Acid	carboxylic acid	0.089	0.093	0.068

Melibionic Acid	carbohydrate	0.771	0.899	0.1
Oxalic Acid	carboxylic acid	0.090	0.096	0.067
Oxalomalic Acid	carboxylic acid	0.093	0.106	0.074
Quinic Acid	carboxylic acid	0.077	0.082	0.065
D-Ribono-1,4-Lactone	carboxylic acid	0.095	0.096	0.072
Sebacic Acid	carboxylic acid	0.067	0.069	0.06
Sorbic Acid	carboxylic acid	0.047	0.052	0.048
Succinamic Acid	carboxylic acid	0.270	0.228	0.22
D-Tartaric Acid	carboxylic acid	0.068	0.075	0.072
L-Tartaric Acid	carboxylic acid	0.072	0.079	0.065
Acetamide	amide	0.081	0.092	0.068
L-Alaninamide	amide	0.095	0.107	0.078
N-Acetyl-L-Glutamic Acid	amino acid	0.093	0.102	0.072
L-Arginine	amino acid	0.081	0.087	0.063
Glycine	amino acid	0.091	0.105	0.067
L-Histidine	amino acid	0.080	0.098	0.065
L-Homoserine	amino acid	0.084	0.087	0.071
Hydroxy-L-Proline	amino acid	0.078	0.098	0.065
L-Isoleucine	amino acid	0.082	0.092	0.068
L-Leucine	amino acid	0.085	0.096	0.068
L-Lysine	amino acid	0.083	0.089	0.065
L-Methionine	amino acid	0.085	0.083	0.067

L-Ornithine	amino acid	0.075	0.083	0.059
L-Phenylalanine	amino acid	0.085	0.089	0.064
L-Pyroglutamic Acid	amino acid	0.087	0.091	0.065
L-Valine	amino acid	0.084	0.09	0.069
D,L-Carnitine	carboxylic acid	0.084	0.089	0.066
Sec-Butylamine	amine	0.082	0.083	0.066
D,L-Octopamine	amine	0.079	0.081	0.066
Putrescine	amine	0.075	0.087	0.061
Dihydroxyacetone	alcohol	0.067	0.069	0.065
2,3-Butanediol	alcohol	0.094	0.097	0.077
2,3-Butanone	alcohol	0.080	0.096	0.069
3-Hydroxy 2-Butanone	alcohol	0.089	0.105	0.08

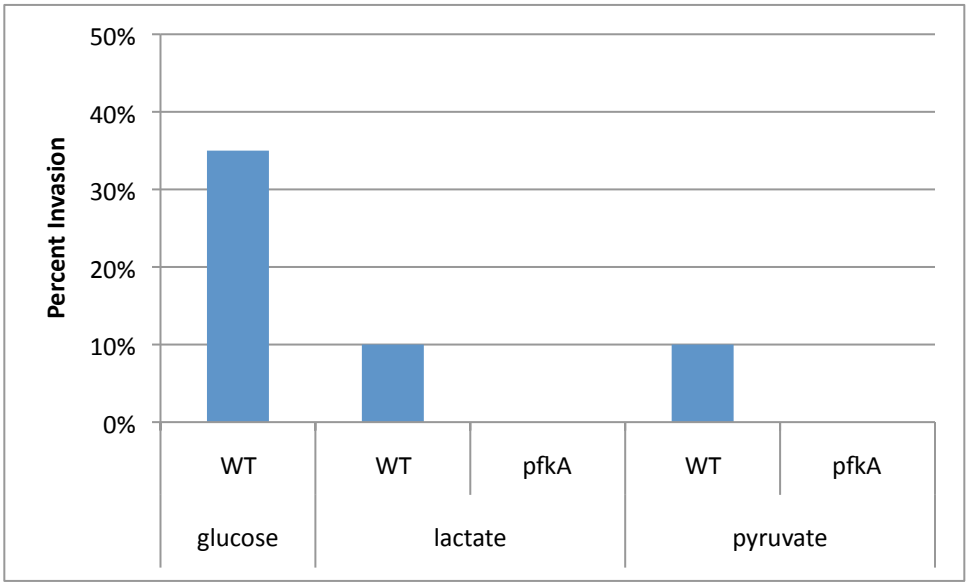

Figure A1: Invasion of *pfkA* grown on gluconeogenic carbon sources.

Strains were grown overnight in minimal media supplemented with 0.2% pyruvate. Overnight cultures were diluted to an optical density (A_{650}) of 0.03 in MOPS media supplemented with 0.2% carbon source and grown to exponential phase at 37°C with aeration. Equal numbers of cells ($2x10^8$) were used in the invasion assay. Data are from one experiment performed in triplicate.

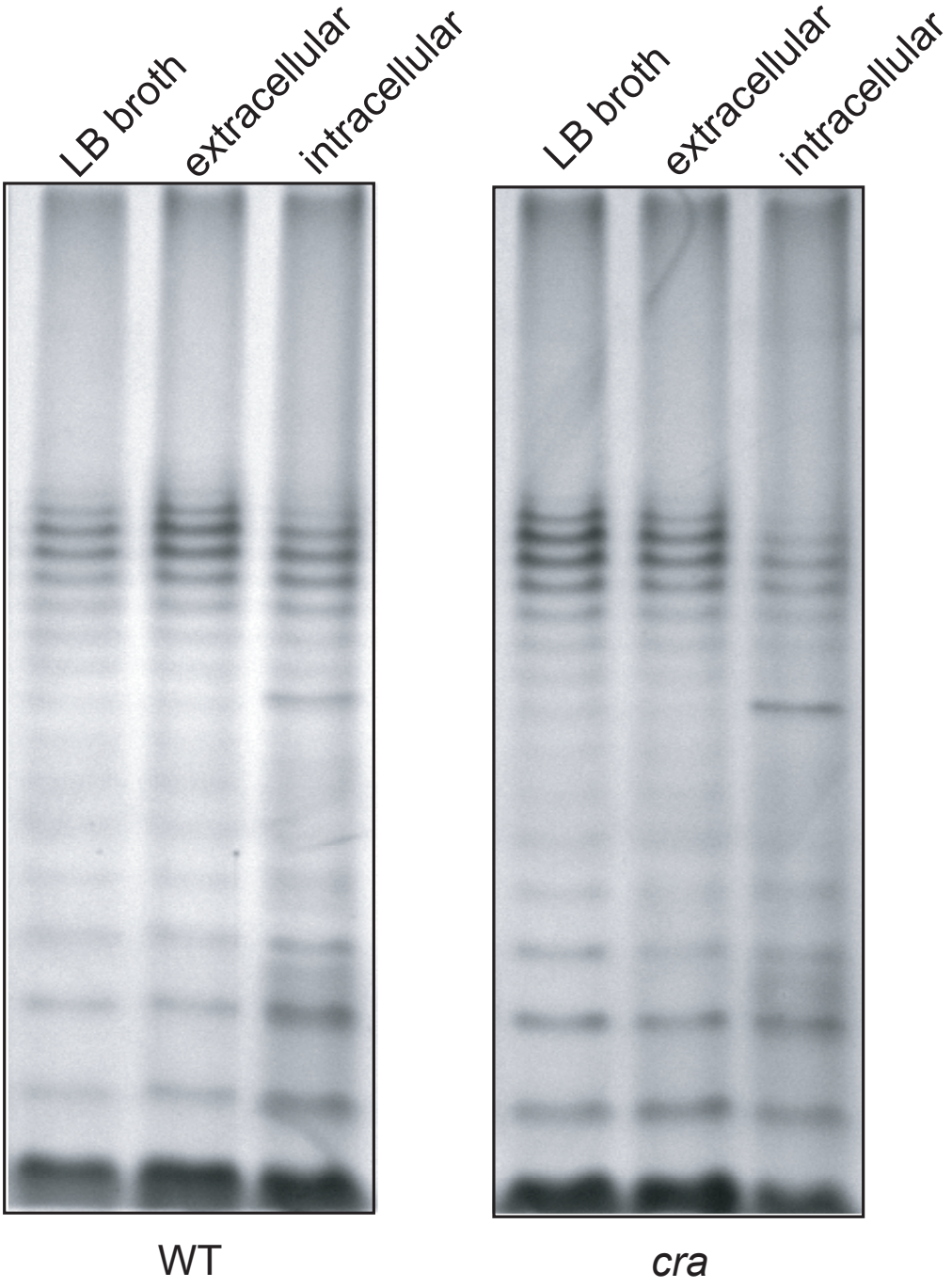
LB broth
extracellular
intracellular
LB broth
extracellular
intracellular
WT
cra

Figure A2: LPS profiles of intracellular bacteria.

Strains were grown to exponential phase in LB broth at 37°C, and $1x10^9$ cells from the culture were used to prepare the pre-invasion (LB broth) LPS. Approximately $5x10^9$ cells from the culture were spun onto confluent monolayer of confluent Henle cells. After a 30 minute incubation, uninvaded bacteria were collected from the media and used to prepare the "extracellular" LPS sample. Monolayers were overlayed with media containing gentamycin, and incubated an additional two hours. Intracellular bacteria were then collected and used to prepare the "intracellular" LPS samples.

A)

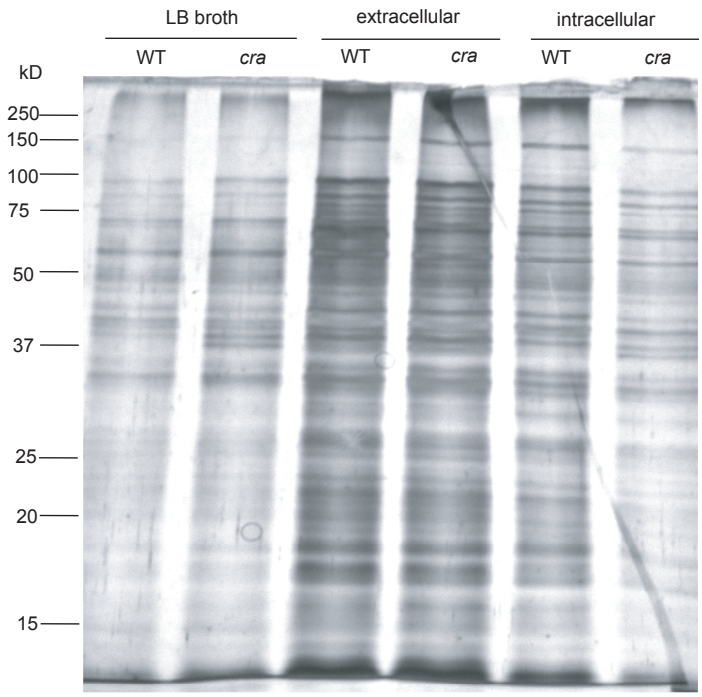
LB broth
extracellular
intracellular
WT
cra
WT
cra
WT
cra
kD
250
150
100
75
50
37
25
20
15

B)

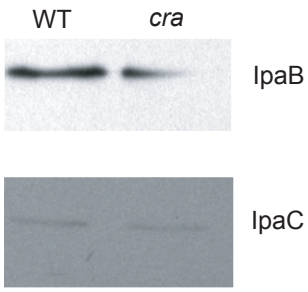
WT
cra
IpaB
IpaC

Figure A3: Protein profile of *S. flexneri* growing inside the host cytosol.

Whole cell lysates from bacteria grown in LB broth, or extracellular and intracellular bacteria were electrophoresed on an SDS-PAGE gel and silver stained (A). The intracellular proteins were then transferred to a nitrocellulose membrane and probed with anti-IpaB or anti-IpaC antibodies (B).

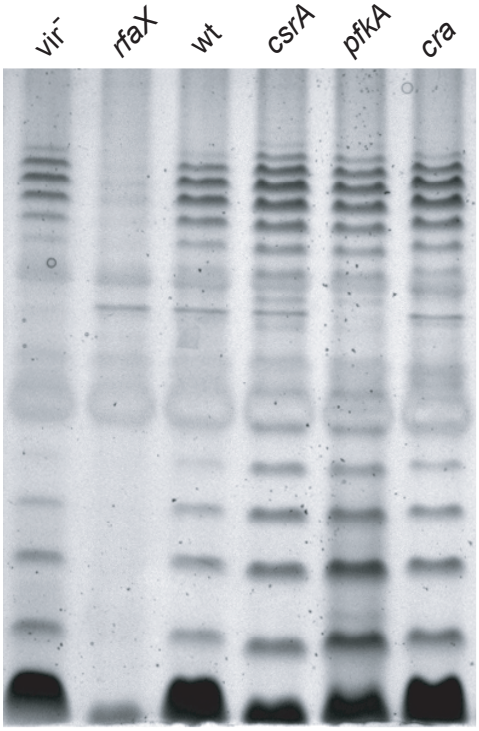

Figure A4: LPS profile of SA101 (vir$^-$).

Strains were grown to exponential phase in LB broth, and approximately 10^9 cells were collected by centrifugation. Cells were lysed by boiling, and the cell lysate was treated with proteinase K. LPS was separated on a tricine SDS-PAGE gel, and visualized by silver staining. SA101 (vir-) is an avirulent *S. flexneri* 2a strain. *rfaX* (SA555-148, renamed *waaJ*) is defective the addition of two glycose residues to the outer core of LPS, and is unable to ligate O-polysaccharide to the lipid A – core molecule (54, 64).

References

1. **Adler, B., C. Sasakawa, T. Tobe, S. Makino, K. Komatsu, and M. Yoshikawa.** 1989. A dual transcriptional activation system for the 230 kb plasmid genes coding for virulence-associated antigens of Shigella flexneri. Mol Microbiol **3:**627-35.
2. **Allen, J. H., M. Utley, H. van Den Bosch, P. Nuijten, M. Witvliet, B. A. McCormick, K. A. Krogfelt, T. R. Licht, D. Brown, M. Mauel, M. P. Leatham, D. C. Laux, and P. S. Cohen.** 2000. A functional cra gene is required for *Salmonella enterica* serovar typhimurium virulence in BALB/c mice. Infect Immun **68:**3772-5.
3. **Allison, G. E., and N. K. Verma.** 2000. Serotype-converting bacteriophages and O-antigen modification in *Shigella flexneri*. Trends in Microbiology **8:**17-23.
4. **Altier, C., M. Suyemoto, and S. D. Lawhon.** 2000. Regulation of *Salmonella enterica* serovar typhimurium invasion genes by *csrA*. Infect Immun **68:**6790-7.
5. **Baba, T., T. Ara, M. Hasegawa, Y. Takai, Y. Okumura, M. Baba, K. A. Datsenko, M. Tomita, B. L. Wanner, and H. Mori.** 2006. Construction of *Escherichia coli* K-12 in-frame, single-gene knockout mutants: the Keio collection. Mol Syst Biol **2:**2006 0008.
6. **Babitzke, P., and T. Romeo.** 2007. CsrB sRNA family: sequestration of RNA-binding regulatory proteins. Curr Opin Microbiol **10:**156-63.
7. **Baker, C. S., L. A. Eory, H. Yakhnin, J. Mercante, T. Romeo, and P. Babitzke.** 2007. CsrA inhibits translation initiation of *Escherichia coli* hfq by binding to a single site overlapping the Shine-Dalgarno sequence. J Bacteriol **189:**5472-81.
8. **Baker, C. S., I. Morozov, K. Suzuki, T. Romeo, and P. Babitzke.** 2002. CsrA regulates glycogen biosynthesis by preventing translation of glgC in *Escherichia coli*. Mol Microbiol **44:**1599-610.
9. **Barnard, F. M., M. F. Loughlin, H. P. Fainberg, M. P. Messenger, D. W. Ussery, P. Williams, and P. J. Jenks.** 2004. Global regulation of virulence and the stress response by CsrA in the highly adapted human gastric pathogen Helicobacter pylori. Mol Microbiol **51:**15-32.
10. **Beloin, C., and C. J. Dorman.** 2003. An extended role for the nucleoid structuring protein H-NS in the virulence gene regulatory cascade of Shigella flexneri. Mol Microbiol **47:**825-38.
11. **Bernardini, M. L., A. Fontaine, and P. J. Sansonetti.** 1990. The two-component regulatory system ompR-envZ controls the virulence of Shigella flexneri. J Bacteriol **172:**6274-81.

12. **Bernardini, M. L., M. G. Sanna, A. Fontaine, and P. J. Sansonetti.** 1993. OmpC is Involved in Invasion of Epithelial Cells by *Shigella flexneri*. Infection and Immunity **61:**3625-3635.
13. **Bhatt, S., A. N. Edwards, H. T. Nguyen, D. Merlin, T. Romeo, and D. Kalman.** 2009. The RNA binding protein CsrA is a pleiotropic regulator of the locus of enterocyte effacement pathogenicity island of enteropathogenic Escherichia coli. Infect Immun **77:**3552-68.
14. **Bonafonte, M. A., C. Solano, B. Sesma, M. Alvarez, L. Montuenga, D. Garcia-Ros, and C. Gamazo.** 2000. The relationship between glycogen synthesis, biofilm formation and virulence in salmonella enteritidis. FEMS Microbiol Lett **191:**31-6.
15. **Botsford, J. L., and J. G. Harman.** 1992. Cyclic AMP in prokaryotes. Microbiol Rev **56:**100-22.
16. **Bowden, S. D., G. Rowley, J. C. Hinton, and A. Thompson.** 2009. Glucose and glycolysis are required for the successful infection of macrophages and mice by Salmonella enterica serovar typhimurium. Infect Immun **77:**3117-26.
17. **Bruckner, R., and F. Titgemeyer.** 2002. Carbon catabolite repression in bacteria: choice of the carbon source and autoregulatory limitation of sugar utilization. FEMS Microbiol Lett **209:**141-8.
18. **Burrowes, E., C. Baysse, C. Adams, and F. O'Gara.** 2006. Influence of the regulatory protein RsmA on cellular functions in Pseudomonas aeruginosa PAO1, as revealed by transcriptome analysis. Microbiology **152:**405-18.
19. **Carlin, N. I., and A. A. Lindberg.** 1986. Monoclonal antibodies specific for Shigella flexneri lipopolysaccharides: clones binding to type I and type III:6,7,8 antigens, group 6 antigen, and a core epitope. Infect Immun **53:**103-9.
20. **Carter, J. A., C. J. Blondel, M. Zaldivar, S. A. Alvarez, C. L. Marolda, M. A. Valvano, and I. Contreras.** 2007. O-antigen modal chain length in *Shigella flexneri* 2a is growth-regulated through RfaH-mediated transcriptional control of the wzy gene. Microbiology **153:**3499-507.
21. **Chang, D. E., D. J. Smalley, D. L. Tucker, M. P. Leatham, W. E. Norris, S. J. Stevenson, A. B. Anderson, J. E. Grissom, D. C. Laux, P. S. Cohen, and T. Conway.** 2004. Carbon nutrition of *Escherichia coli* in the mouse intestine. Proc Natl Acad Sci U S A **101:**7427-32.
22. **Chen, H. D., and G. Frankel.** 2005. Enteropathogenic Escherichia coli: unravelling pathogenesis. FEMS Microbiol Rev **29:**83-98.
23. **Chin, A. M., D. A. Feldheim, and M. H. Saier, Jr.** 1989. Altered transcriptional patterns affecting several metabolic pathways in strains of Salmonella typhimurium which overexpress the fructose regulon. J Bacteriol **171:**2424-34.
24. **Crasnier, M.** 1996. Cyclic AMP and catabolite repression. Res Microbiol **147:**479-82.

25. **D'Ari, R., A. Jaffe, P. Bouloc, and A. Robin.** 1988. Cyclic AMP and cell division in Escherichia coli. J Bacteriol **170:**65-70.
26. **D'Hauteville, H., S. Khan, D. J. Maskell, A. Kussak, A. Weintraub, J. Mathison, R. J. Ulevitch, N. Wuscher, C. Parsot, and P. J. Sansonetti.** 2002. Two msbB genes encoding maximal acylation of lipid A are required for invasive Shigella flexneri to mediate inflammatory rupture and destruction of the intestinal epithelium. J Immunol **168:**5240-51.
27. **Daskaleros, P. A.** 1988. Studies on Congo red binding and virulence in *Shigella* species. Dissertation. University of Texas at Austin, Austin, Texas.
28. **Daskaleros, P. A., and S. M. Payne.** 1987. Congo red binding phenotype is associated with hemin binding and increased infectivity of Shigella flexneri in the HeLa cell model. Infect Immun **55:**1393-8.
29. **Dorman, C. J., and M. E. Porter.** 1998. The *Shigella* virulence gene regulatory cascade: a paradigm of bacterial gene control mechanisms. Mol Microbiol **29:**677-84.
30. **Dubey, A. K., C. S. Baker, T. Romeo, and P. Babitzke.** 2005. RNA sequence and secondary structure participate in high-affinity CsrA-RNA interaction. Rna **11:**1579-87.
31. **Dubey, A. K., C. S. Baker, K. Suzuki, A. D. Jones, P. Pandit, T. Romeo, and P. Babitzke.** 2003. CsrA regulates translation of the *Escherichia coli* carbon starvation gene, *cstA*, by blocking ribosome access to the *cstA* transcript. J Bacteriol **185:**4450-60.
32. **Durand, J. M., B. Dagberg, B. E. Uhlin, and G. R. Bjork.** 2000. Transfer RNA modification, temperature and DNA superhelicity have a common target in the regulatory network of the virulence of Shigella flexneri: the expression of the virF gene. Mol Microbiol **35:**924-35.
33. **Epler, C. R., N. E. Dickenson, A. J. Olive, W. L. Picking, and W. D. Picking.** 2009. Liposomes recruit IpaC to the Shigella flexneri type III secretion apparatus needle as a final step in secretion induction. Infect Immun **77:**2754-61.
34. **Espina, M., A. J. Olive, R. Kenjale, D. S. Moore, S. F. Ausar, R. W. Kaminski, E. V. Oaks, C. R. Middaugh, W. D. Picking, and W. L. Picking.** 2006. IpaD localizes to the tip of the type III secretion system needle of Shigella flexneri. Infect Immun **74:**4391-400.
35. **Fabich, A. J., S. A. Jones, F. Z. Chowdhury, A. Cernosek, A. Anderson, D. Smalley, J. W. McHargue, G. A. Hightower, J. T. Smith, S. M. Autieri, M. P. Leatham, J. J. Lins, R. L. Allen, D. C. Laux, P. S. Cohen, and T. Conway.** 2008. Comparison of carbon nutrition for pathogenic and commensal Escherichia coli strains in the mouse intestine. Infect Immun **76:**1143-52.
36. **Falconi, M., B. Colonna, G. Prosseda, G. Micheli, and C. O. Gualerzi.** 1998. Thermoregulation of Shigella and Escherichia coli EIEC pathogenicity. A

temperature-dependent structural transition of DNA modulates accessibility of virF promoter to transcriptional repressor H-NS. EMBO J **17:**7033-43.

37. **Fields, J. A., and S. A. Thompson.** 2008. *Campylobacter jejuni* CsrA mediates oxidative stress responses, biofilm formation, and host cell invasion. J Bacteriol **190:**3411-6.
38. **Frirdich, E., and C. Whitfield.** 2005. Lipopolysaccharide inner core oligosaccharide structure and outer membrane stability in human pathogens belonging to the Enterobacteriaceae. J Endotoxin Res **11:**133-44.
39. **Goetz, M., A. Bubert, G. Wang, I. Chico-Calero, J. A. Vazquez-Boland, M. Beck, J. Slaghuis, A. A. Szalay, and W. Goebel.** 2001. Microinjection and growth of bacteria in the cytosol of mammalian host cells. Proc Natl Acad Sci U S A **98:**12221-6.
40. **Goldberg, M. B., and J. A. Theriot.** 1995. Shigella flexneri surface protein IcsA is sufficient to direct actin-based motility. Proc Natl Acad Sci U S A **92:**6572-6.
41. **Goldman, S. R., Y. Tu, and M. B. Goldberg.** 2008. Differential regulation by magnesium of the two MsbB paralogs of Shigella flexneri. J Bacteriol **190:**3526-37.
42. **Gosset, G., Z. Zhang, S. Nayyar, W. A. Cuevas, and M. H. Saier, Jr.** 2004. Transcriptome analysis of Crp-dependent catabolite control of gene expression in *Escherichia coli*. J Bacteriol **186:**3516-24.
43. **Gudapaty, S., K. Suzuki, X. Wang, P. Babitzke, and T. Romeo.** 2001. Regulatory interactions of Csr components: the RNA binding protein CsrA activates csrB transcription in *Escherichia coli*. J Bacteriol **183:**6017-27.
44. **Gutierrez, P., Y. Li, M. J. Osborne, E. Pomerantseva, Q. Liu, and K. Gehring.** 2005. Solution structure of the carbon storage regulator protein CsrA from Escherichia coli. J Bacteriol **187:**3496-501.
45. **Hale, T. L., E. V. Oaks, and S. B. Formal.** 1985. Identification and antigenic characterization of virulence-associated, plasmid-coded proteins of *Shigella* spp. and enteroinvasive *Escherichia coli*. Infect Immun **50:**620-9.
46. **Headley, V. L., and S. M. Payne.** 1990. Differential protein expression by Shigella flexneri in intracellular and extracellular environments. Proc Natl Acad Sci U S A **87:**4179-83.
47. **Heeb, S., and D. Haas.** 2001. Regulatory roles of the GacS/GacA two-component system in plant-associated and other gram-negative bacteria. Mol Plant Microbe Interact **14:**1351-63.
48. **Hellinga, H. W., and P. R. Evans.** 1985. Nucleotide sequence and high-level expression of the major *Escherichia coli* phosphofructokinase. Eur J Biochem **149:**363-73.
49. **Heroven, A. K., K. Bohme, M. Rohde, and P. Dersch.** 2008. A Csr-type regulatory system, including small non-coding RNAs, regulates the global

virulence regulator RovA of *Yersinia pseudotuberculosis* through RovM. Mol Microbiol **68:**1179-95.

50. **High, N., J. Mounier, M. C. Prevost, and P. J. Sansonetti.** 1992. IpaB of Shigella flexneri causes entry into epithelial cells and escape from the phagocytic vacuole. EMBO J **11:**1991-9.
51. **Hitchcock, P. J., and T. M. Brown.** 1983. Morphological heterogeneity among *Salmonella* lipopolysaccharide chemotypes in silver-stained polyacrylamide gels. J Bacteriol **154:**269-77.
52. **Hoch, J. A., and K. I. Varughese.** 2001. Keeping signals straight in phosphorelay signal transduction. J Bacteriol **183:**4941-9.
53. **Hong, M., Y. Gleason, E. E. Wyckoff, and S. M. Payne.** 1998. Identification of two *Shigella flexneri* chromosomal loci involved in intercellular spreading. Infect Immun **66:**4700-10.
54. **Hong, M., and S. M. Payne.** 1997. Effect of mutations in *Shigella flexneri* chromosomal and plasmid-encoded lipopolysaccharide genes on invasion and serum resistance. Mol Microbiol **24:**779-91.
55. **Ishige, K., S. Nagasawa, S.-i. Tokishita, and T. Mizuno.** 1994. A novel device of bacterial signal transducers. The EMBO Journal **13:**5195-5202.
56. **Jennison, A. V., and N. K. Verma.** 2004. *Shigella flexneri* infection: pathogenesis and vaccine development. FEMS Microbiol Rev **28:**43-58.
57. **Jonas, K., A. N. Edwards, R. Simm, T. Romeo, U. Romling, and O. Melefors.** 2008. The RNA binding protein CsrA controls c-di-GMP metabolism by directly regulating the expression of GGDEF proteins. Mol Microbiol.
58. **Jonas, K., and O. Melefors.** 2009. The Escherichia coli CsrB and CsrC small RNAs are strongly induced during growth in nutrient-poor medium. FEMS Microbiol Lett.
59. **Jonas, K., H. Tomenius, U. Romling, D. Georgellis, and O. Melefors.** 2006. Identification of YhdA as a regulator of the *Escherichia coli* carbon storage regulation system. FEMS Microbiol Lett **264:**232-7.
60. **Jones, S. A., M. Jorgensen, F. Z. Chowdhury, R. Rodgers, J. Hartline, M. P. Leatham, C. Struve, K. A. Krogfelt, P. S. Cohen, and T. Conway.** 2008. Glycogen and maltose utilization by *Escherichia coli* O157:H7 in the mouse intestine. Infect Immun **76:**2531-40.
61. **Joseph, B., and W. Goebel.** 2007. Life of *Listeria monocytogenes* in the host cells' cytosol. Microbes Infect **9:**1188-95.
62. **Joseph, B., K. Przybilla, C. Stuhler, K. Schauer, J. Slaghuis, T. M. Fuchs, and W. Goebel.** 2006. Identification of Listeria monocytogenes genes contributing to intracellular replication by expression profiling and mutant screening. J Bacteriol **188:**556-68.

63. **Kane, C. D., R. Schuch, W. A. Day, Jr., and A. T. Maurelli.** 2002. MxiE regulates intracellular expression of factors secreted by the *Shigella flexneri* 2a type III secretion system. J Bacteriol **184:**4409-19.
64. **Kaniuk, N. A., E. Vinogradov, J. Li, M. A. Monteiro, and C. Whitfield.** 2004. Chromosomal and plasmid-encoded enzymes are required for assembly of the R3-type core oligosaccharide in the lipopolysaccharide of Escherichia coli O157:H7. J Biol Chem **279:**31237-50.
65. **Kohler, H., S. P. Rodrigues, and B. A. McCormick.** 2002. *Shigella flexneri* Interactions with the Basolateral Membrane Domain of Polarized Model Intestinal Epithelium: Role of Lipopolysaccharide in Cell Invasion and in Activation of the Mitogen-Activated Protein Kinase ERK. Infect Immun **70:**1150-8.
66. **Lafont, F., G. Tran Van Nhieu, K. Hanada, P. Sansonetti, and F. G. van der Goot.** 2002. Initial steps of *Shigella* infection depend on the cholesterol/sphingolipid raft-mediated CD44-IpaB interaction. Embo J **21:**4449-57.
67. **Lan, R., and P. R. Reeves.** 2002. *Escherichia coli* in disguise: molecular origins of *Shigella*. Microbes Infect **4:**1125-32.
68. **Laux, D. C., P. S. Cohen, and T. Conway.** 2005. Role of the Mucus Layer in Bacterial Colonization of the Intestine, p. 199-212. *In* J. P. Nataro (ed.), Colonization of Mucosal Surfaces. ASM Press, Washington, D.C.
69. **Lawhon, S. D., J. G. Frye, M. Suyemoto, S. Porwollik, M. McClelland, and C. Altier.** 2003. Global regulation by CsrA in *Salmonella typhimurium*. Mol Microbiol **48:**1633-45.
70. **Lenz, D. H., M. B. Miller, J. Zhu, R. V. Kulkarni, and B. L. Bassler.** 2005. CsrA and three redundant small RNAs regulate quorum sensing in *Vibrio cholerae*. Mol Microbiol **58:**1186-202.
71. **Lostroh, C. P., and C. A. Lee.** 2001. The Salmonella pathogenicity island-1 type III secretion system. Microbes Infect **3:**1281-91.
72. **Lucchetti-Miganeh, C., E. Burrowes, C. Baysse, and G. Ermel.** 2008. The post-transcriptional regulator CsrA plays a central role in the adaptation of bacterial pathogens to different stages of infection in animal hosts. Microbiology **154:**16-29.
73. **Lucchini, S., H. Liu, Q. Jin, J. C. Hinton, and J. Yu.** 2005. Transcriptional adaptation of *Shigella flexneri* during infection of macrophages and epithelial cells: insights into the strategies of a cytosolic bacterial pathogen. Infect Immun **73:**88-102.
74. **Maurelli, A. T., B. Baudry, H. d'Hauteville, T. L. Hale, and P. J. Sansonetti.** 1985. Cloning of plasmid DNA sequences involved in invasion of HeLa cells by *Shigella flexneri*. Infect Immun **49:**164-71.

75. **Maurelli, A. T., B. Blackmon, and R. Curtiss, 3rd.** 1984. Temperature-dependent expression of virulence genes in Shigella species. Infect Immun **43:**195-201.
76. **Mavris, M., A. L. Page, R. Tournebize, B. Demers, P. Sansonetti, and C. Parsot.** 2002. Regulation of transcription by the activity of the Shigella flexneri type III secretion apparatus. Mol Microbiol **43:**1543-53.
77. **McMeechan, A., M. A. Lovell, T. A. Cogan, K. L. Marston, T. J. Humphrey, and P. A. Barrow.** 2005. Glycogen production by different Salmonella enterica serotypes: contribution of functional glgC to virulence, intestinal colonization and environmental survival. Microbiology **151:**3969-77.
78. **Mercante, J., A. N. Edwards, A. K. Dubey, P. Babitzke, and T. Romeo.** 2009. Molecular geometry of CsrA (RsmA) binding to RNA and its implications for regulated expression. J Mol Biol **392:**511-28.
79. **Mercante, J., K. Suzuki, X. Cheng, P. Babitzke, and T. Romeo.** 2006. Comprehensive alanine-scanning mutagenesis of *Escherichia coli* CsrA defines two subdomains of critical functional importance. J Biol Chem **281:**31832-42.
80. **Miranda, R. L., T. Conway, M. P. Leatham, D. E. Chang, W. E. Norris, J. H. Allen, S. J. Stevenson, D. C. Laux, and P. S. Cohen.** 2004. Glycolytic and gluconeogenic growth of Escherichia coli O157:H7 (EDL933) and E. coli K-12 (MG1655) in the mouse intestine. Infect Immun **72:**1666-76.
81. **Moller, T., T. Franch, P. Hojrup, D. R. Keene, H. P. Bachinger, R. G. Brennan, and P. Valentin-Hansen.** 2002. Hfq: a bacterial Sm-like protein that mediates RNA-RNA interaction. Mol Cell **9:**23-30.
82. **Molofsky, A. B., and M. S. Swanson.** 2003. Legionella pneumophila CsrA is a pivotal repressor of transmission traits and activator of replication. Mol Microbiol **50:**445-61.
83. **Morona, R., C. Daniels, and L. Van Den Bosch.** 2003. Genetic modulation of *Shigella flexneri* 2a lipopolysaccharide O antigen modal chain length reveals that it has been optimized for virulence. Microbiology **149:**925-39.
84. **Morrissey, J. H.** 1981. Silver stain for proteins in polyacrylamide gels: a modified procedure with enhanced uniform sensitivity. Anal Biochem **117:**307-10.
85. **Mounier, J., T. Vasselon, R. Hellio, M. Lesourd, and P. J. Sansonetti.** 1992. Shigella flexneri enters human colonic Caco-2 epithelial cells through the basolateral pole. Infect Immun **60:**237-48.
86. **Mulcahy, H., J. O'Callaghan, E. P. O'Grady, M. D. Macia, N. Borrell, C. Gomez, P. G. Casey, C. Hill, C. Adams, C. G. Gahan, A. Oliver, and F. O'Gara.** 2008. *Pseudomonas aeruginosa* RsmA plays an important role during murine infection by influencing colonization, virulence, persistence, and pulmonary inflammation. Infect Immun **76:**632-8.

87. **Murphy, E. R., and S. M. Payne.** 2007. RyhB, an iron-responsive small RNA molecule, regulates *Shigella dysenteriae* virulence. Infect Immun **75:**3470-7.
88. **Murray, E. L., and T. Conway.** 2005. Multiple regulators control expression of the Entner-Doudoroff aldolase (Eda) of *Escherichia coli*. J Bacteriol **187:**991-1000.
89. **Nakayama, S., and H. Watanabe.** 1998. Identification of cpxR as a positive regulator essential for expression of the Shigella sonnei virF gene. J Bacteriol **180:**3522-8.
90. **Nakayama, S., and H. Watanabe.** 1995. Involvement of cpxA, a sensor of a two-component regulatory system, in the pH-dependent regulation of expression of Shigella sonnei virF gene. J Bacteriol **177:**5062-9.
91. **Negre, D., C. Bonod-Bidaud, C. Geourjon, G. Deleage, A. J. Cozzone, and J. C. Cortay.** 1996. Definition of a consensus DNA-binding site for the Escherichia coli pleiotropic regulatory protein, FruR. Mol Microbiol **21:**257-66.
92. **Neidhardt, F. C., P. L. Bloch, and D. F. Smith.** 1974. Culture medium for enterobacteria. J Bacteriol **119:**736-47.
93. **Nikaido, H., and M. Vaara.** 1985. Molecular basis of bacterial outer membrane permeability. Microbiol Rev **49:**1-32.
94. **Niyogi, S. K.** 2005. Shigellosis. J Microbiol **43:**133-43.
95. **Ogawa, M., Y. Handa, H. Ashida, M. Suzuki, and C. Sasakawa.** 2008. The versatility of Shigella effectors. Nat Rev Microbiol **6:**11-6.
96. **Olive, A. J., R. Kenjale, M. Espina, D. S. Moore, W. L. Picking, and W. D. Picking.** 2007. Bile salts stimulate recruitment of IpaB to the *Shigella flexneri* surface, where it colocalizes with IpaD at the tip of the type III secretion needle. Infect Immun **75:**2626-9.
97. **Parsot, C., E. Ageron, C. Penno, M. Mavris, K. Jamoussi, H. d'Hauteville, P. Sansonetti, and B. Demers.** 2005. A secreted anti-activator, OspD1, and its chaperone, Spa15, are involved in the control of transcription by the type III secretion apparatus activity in Shigella flexneri. Mol Microbiol **56:**1627-35.
98. **Payne, S. M., and R. A. Finkelstein.** 1977. Detection and differentiation of iron-responsive avirulent mutants on Congo red agar. Infect Immun **18:**94-8.
99. **Peekhaus, N., and T. Conway.** 1998. What's for dinner?: Entner-Doudoroff metabolism in *Escherichia coli*. J Bacteriol **180:**3495-502.
100. **Pernestig, A. K., O. Melefors, and D. Georgellis.** 2001. Identification of UvrY as the cognate response regulator for the BarA sensor kinase in *Escherichia coli*. J Biol Chem **276:**225-31.
101. **Pessi, G., F. Williams, Z. Hindle, K. Heurlier, M. T. Holden, M. Camara, D. Haas, and P. Williams.** 2001. The global posttranscriptional regulator RsmA modulates production of virulence determinants and N-acylhomoserine lactones in *Pseudomonas aeruginosa*. J Bacteriol **183:**6676-83.

102. **Petersen, S., and G. M. Young.** 2002. Essential role for cyclic AMP and its receptor protein in *Yersinia enterocolitica* virulence. Infect Immun **70:**3665-72.
103. **Porter, M. E., and C. J. Dorman.** 1997. Differential regulation of the plasmid-encoded genes in the *Shigella flexneri* virulence regulon. Mol Gen Genet **256:**93-103.
104. **Porter, M. E., and C. J. Dorman.** 1997. Positive regulation of *Shigella flexneri* virulence genes by integration host factor. J Bacteriol **179:**6537-50.
105. **Preiss, J. (ed.).** 1987. Regulation of glycogen synthesis. ASM Press, Washington, DC.
106. **Qadri, F., S. A. Hossain, I. Ciznár, K. Haider, A. Ljungh, T. Wadstrom, and D. A. Sack.** 1988. Congo red binding and salt aggregation as indicators of virulence in *Shigella* species. J Clin Microbiol **26:**1343-8.
107. **Ramseier, T. M.** 1996. Cra and the control of carbon flux via metabolic pathways. Res Microbiol **147:**489-93.
108. **Ramseier, T. M., S. Bledig, V. Michotey, R. Feghali, and M. H. Saier, Jr.** 1995. The global regulatory protein FruR modulates the direction of carbon flow in Escherichia coli. Mol Microbiol **16:**1157-69.
109. **Romeo, T.** 1998. Global regulation by the small RNA-binding protein CsrA and the non-coding RNA molecule CsrB. Mol Microbiol **29:**1321-30.
110. **Romeo, T., M. Gong, M. Y. Liu, and A. M. Brun-Zinkernagel.** 1993. Identification and molecular characterization of *csrA*, a pleiotropic gene from *Escherichia coli* that affects glycogen biosynthesis, gluconeogenesis, cell size, and surface properties. J Bacteriol **175:**4744-55.
111. **Runyen-Janecky, L. J., and S. M. Payne.** 2002. Identification of chromosomal *Shigella flexneri* genes induced by the eukaryotic intracellular environment. Infect Immun **70:**4379-88.
112. **Sabnis, N. A., H. Yang, and T. Romeo.** 1995. Pleiotropic regulation of central carbohydrate metabolism in *Escherichia coli* via the gene *csrA*. J Biol Chem **270:**29096-104.
113. **Saier, M. H., Jr., and T. M. Ramseier.** 1996. The catabolite repressor/activator (Cra) protein of enteric bacteria. J Bacteriol **178:**3411-7.
114. **Saier, M. H., T. M. Ramseier, and J. Reizer.** 1987. Regulation of Carbon Utilization, p. 1325-1343. *In* F. C. Neidhardt, J. Ingram, and R. Curtiss (ed.), Escherichia coli and Salmonella Typhimurium:Cellular and Molecular Biology, vol. 1. ASM Press, Washington, D.C.
115. **Sakai, T., C. Sasakawa, and M. Yoshikawa.** 1988. Expression of four virulence antigens of Shigella flexneri is positively regulated at the transcriptional level by the 30 kiloDalton virF protein. Mol Microbiol **2:**589-97.
116. **Sambrook, J., and D. W. Russell.** 2001. Molecular cloning: a laboratory manual. Cold Spring Harbor Laboratory Press, Cold Spring Harbor, NY.

117. **Sandlin, R. C., M. B. Goldberg, and A. T. Maurelli.** 1996. Effect of O side-chain length and composition on the virulence of Shigella flexneri 2a. Mol Microbiol **22:**63-73.
118. **Sandlin, R. C., K. A. Lampel, S. P. Keasler, M. B. Goldberg, A. L. Stolzer, and A. T. Maurelli.** 1995. Avirulence of rough mutants of Shigella flexneri: requirement of O antigen for correct unipolar localization of IcsA in the bacterial outer membrane. Infect Immun **63:**229-37.
119. **Sasakawa, C., K. Kamata, T. Sakai, S. Makino, M. Yamada, N. Okada, and M. Yoshikawa.** 1988. Virulence-associated genetic regions comprising 31 kilobases of the 230-kilobase plasmid in *Shigella flexneri* 2a. J Bacteriol **170:**2480-4.
120. **Schroeder, G. N., and H. Hilbi.** 2008. Molecular pathogenesis of *Shigella* spp.: controlling host cell signaling, invasion, and death by type III secretion. Clin Microbiol Rev **21:**134-56.
121. **Simon, E. H., and I. Tessman.** 1963. Thymidine-Requiring Mutants of Phage T4. Proc Natl Acad Sci U S A **50:**526-32.
122. **Slauch, J. M., S. Garrett, D. E. Jackson, and T. J. Silhavy.** 1988. EnvZ functions through OmpR to control porin gene expression in *Escherichia coli* K-12. Journal of Bacteriology **170:**439-41.
123. **Smith, H.** 2000. Questions about the behaviour of bacterial pathogens in vivo. Philos Trans R Soc Lond B Biol Sci **355:**551-64.
124. **Stevenson, G., A. Kessler, and P. R. Reeves.** 1995. A plasmid-borne O-antigen chain length determinant and its relationship to other chain length determinants. FEMS Microbiol Lett **125:**23-30.
125. **Suzuki, K., P. Babitzke, S. R. Kushner, and T. Romeo.** 2006. Identification of a novel regulatory protein (CsrD) that targets the global regulatory RNAs CsrB and CsrC for degradation by RNase E. Genes Dev **20:**2605-17.
126. **Suzuki, K., X. Wang, T. Weilbacher, A. K. Pernestig, O. Melefors, D. Georgellis, P. Babitzke, and T. Romeo.** 2002. Regulatory circuitry of the CsrA/CsrB and BarA/UvrY systems of *Escherichia coli*. J Bacteriol **184:**5130-40.
127. **Sweeney, N. J., D. C. Laux, and P. S. Cohen.** 1996. Escherichia coli F-18 and E. coli K-12 eda mutants do not colonize the streptomycin-treated mouse large intestine. Infect Immun **64:**3504-11.
128. **Timmermans, J., and L. Van Melderen.** 2009. Conditional essentiality of the *csrA* gene in *Escherichia coli*. J Bacteriol **191:**1722-24.
129. **Tobe, T., S. Nagai, N. Okada, B. Adler, M. Yoshikawa, and C. Sasakawa.** 1991. Temperature-regulated expression of invasion genes in Shigella flexneri is controlled through the transcriptional activation of the virB gene on the large plasmid. Mol Microbiol **5:**887-93.

130. **Tobe, T., M. Yoshikawa, T. Mizuno, and C. Sasakawa.** 1993. Transcriptional control of the invasion regulatory gene virB of Shigella flexneri: activation by virF and repression by H-NS. J Bacteriol **175:**6142-9.
131. **Tobe, T., M. Yoshikawa, and C. Sasakawa.** 1995. Thermoregulation of virB transcription in *Shigella flexneri* by sensing of changes in local DNA superhelicity. J Bacteriol **177:**1094-7.
132. **Tran Van Nhieu, G., A. Ben-Ze'ev, and P. J. Sansonetti.** 1997. Modulation of bacterial entry into epithelial cells by association between vinculin and the Shigella IpaA invasin. Embo J **16:**2717-29.
133. **Tsai, C. M., and C. E. Frasch.** 1982. A sensitive silver stain for detecting lipopolysaccharides in polyacrylamide gels. Anal Biochem **119:**115-9.
134. **Van den Bosch, L., P. A. Manning, and R. Morona.** 1997. Regulation of O-antigen chain length is required for *Shigella flexneri* virulence. Mol Microbiol **23:**765-75.
135. **van Workum, M., S. J. van Dooren, N. Oldenburg, D. Molenaar, P. R. Jensen, J. L. Snoep, and H. V. Westerhoff.** 1996. DNA supercoiling depends on the phosphorylation potential in Escherichia coli. Mol Microbiol **20:**351-60.
136. **Varela, G., F. Schelotto, J. di Conza, and J. A. Ayala.** 2001. Analysis of the O-antigen chain length distribution during extracellular and intracellular growth of Shigella flexneri. Microb Pathog **31:**21-7.
137. **Vinopal, R. T., and D. G. Fraenkel.** 1974. Phenotypic suppression of phosphofructokinase mutations in Escherichia coli by constitutive expression of the glyoxylate shunt. J Bacteriol **118:**1090-100.
138. **Wang, R. F., and S. R. Kushner.** 1991. Construction of versatile low-copy-number vectors for cloning, sequencing and gene expression in *Escherichia coli*. Gene **100:**195-9.
139. **Wang, X., A. K. Dubey, K. Suzuki, C. S. Baker, P. Babitzke, and T. Romeo.** 2005. CsrA post-transcriptionally represses *pgaABCD*, responsible for synthesis of a biofilm polysaccharide adhesin of *Escherichia coli*. Mol Microbiol **56:**1648-63.
140. **Wanner, B. L.** 1992. Is cross regulation by phosphorylation of two-component response regulator proteins important in bacteria? J Bacteriol **174:**2053-8.
141. **Wassef, J. S., D. F. Keren, and J. L. Mailloux.** 1989. Role of M cells in initial antigen uptake and in ulcer formation in the rabbit intestinal loop model of shigellosis. Infect Immun **57:**858-63.
142. **Wei, B. L., A. M. Brun-Zinkernagel, J. W. Simecka, B. M. Pruss, P. Babitzke, and T. Romeo.** 2001. Positive regulation of motility and *flhDC* expression by the RNA-binding protein CsrA of *Escherichia coli*. Mol Microbiol **40:**245-56.
143. **Weilbacher, T., K. Suzuki, A. K. Dubey, X. Wang, S. Gudapaty, I. Morozov, C. S. Baker, D. Georgellis, P. Babitzke, and T. Romeo.** 2003. A novel sRNA

component of the carbon storage regulatory system of *Escherichia coli*. Mol Microbiol **48:**657-70.

144. **West, N. P., P. Sansonetti, J. Mounier, R. M. Exley, C. Parsot, S. Guadagnini, M. C. Prevost, A. Prochnicka-Chalufour, M. Delepierre, M. Tanguy, and C. M. Tang.** 2005. Optimization of virulence functions through glucosylation of *Shigella* LPS. Science **307:**1313-7.
145. **Yang, F., J. Yang, X. Zhang, L. Chen, Y. Jiang, Y. Yan, X. Tang, J. Wang, Z. Xiong, J. Dong, Y. Xue, Y. Zhu, X. Xu, L. Sun, S. Chen, H. Nie, J. Peng, J. Xu, Y. Wang, Z. Yuan, Y. Wen, Z. Yao, Y. Shen, B. Qiang, Y. Hou, J. Yu, and Q. Jin.** 2005. Genome dynamics and diversity of *Shigella* species, the etiologic agents of bacillary dysentery. Nucleic Acids Res **33:**6445-58.
146. **Yang, H., M. Y. Liu, and T. Romeo.** 1996. Coordinate genetic regulation of glycogen catabolism and biosynthesis in *Escherichia coli* via the CsrA gene product. J Bacteriol **178:**1012-7.
147. **Yethon, J. A., D. E. Heinrichs, M. A. Monteiro, M. B. Perry, and C. Whitfield.** 1998. Involvement of waaY, waaQ, and waaP in the modification of Escherichia coli lipopolysaccharide and their role in the formation of a stable outer membrane. J Biol Chem **273:**26310-6.
148. **Zheng, D., C. Constantinidou, J. L. Hobman, and S. D. Minchin.** 2004. Identification of the CRP regulon using in vitro and in vivo transcriptional profiling. Nucleic Acids Res **32:**5874-93.
149. **Zychlinsky, A., M. C. Prevost, and P. J. Sansonetti.** 1992. Shigella flexneri induces apoptosis in infected macrophages. Nature **358:**167-9.

Vita

Aja Lynne Gore was born in Knoxville, Tennessee on May 1, 1981. She began college at Texas A&M University, College Station in 1999 and graduated in 2002 with a B.S. in Microbiology. After graduation, Aja worked for Abbott Laboratories in Austin, Texas from January to August 2003. She began her studies at the University of Texas at Austin in August 2003.

PERMANENT ADDRESS:
20305 Merlin Falcon Trail
Pflugerville, Texas 78660

The dissertation was typed by the author.